TÉCNICO LISBOA

Minimal Solutions to the CKM Unitarity Problem with a Vector-like Quark Isosinglet

José Filipe Bastos

Thesis to obtain the Master of Science Degree in

Engineering Physics

Supervisor(s): Joaquim Inácio da Silva Marcos

Examination Committee

Chairperson: Mário João Martins Pimenta

Supervisor: Joaquim Inácio da Silva Marcos

Member of the Committee: Jorge Manuel Rodrigues Crispim Romão

January 2022

Acknowledgments

I would like to use this opportunity express my gratitude to my supervisor, Joaquim Silva Marcos, who guided me throughout this last year. During this period and under his guidance, I had the privilege of learning many invaluable aspects regarding the exciting field that is particle physics. His assistance was crucial in the elaboration of this work and I look forward to continue working with him.

I further thank Gustavo Castelo Branco and Margarida Rebelo of CFTP, as well as Francisco Botella from IFIC – Valencia for their collaboration and help. Their insights and advice were of extreme importance for the development of this work.

Finally, I would like to thank my parents and sisters for their never-ending support, encouragement and patience during these stressful and hectic times.

Resumo

Cálculos e resultados recentes apresentam fortes evidências de que a matriz CKM não é unitária, contradizendo o MP e sugerindo a existência de Nova Física (NF). Nesta tese, propomos uma extensão mínima do Modelo Padrão (MP) com um quark *vector-like* do tipo *up*, T, que fornece uma solução simples para o problema da unitaridade da matriz CKM (CKM-UP). Adotamos a parametrização Botella-Chau para a matriz de mistura 4×3, usando os três ângulos e fase habituais da matriz 3×3 do MP, mais três ângulos extra s_{14}, s_{24}, s_{34} e duas novas fases δ_{14}, δ_{24}.

Para alcançar uma solução mínima para o CKM-UP, supõe-se que a mistura de T com os quarks do MP é dominada por s_{14}. São obtidas características interessantes e um novo padrão de decaimentos do T, predominantemente para a primeira geração. Averiguou-se também se os limites pelos *Electroweak Precision Measurements* (EWPM) são excedidos.

Verifica-se que o parâmetro ε_K, sensível à violação de CP, desempenha um papel crucial em restringir este tipo de modelos. Impôs-se um limite (recentemente derivado) que restringe muito a NF de ε_K, e descobriu-se, no limite de dominância exata onde $s_{24}, s_{34} = 0$, que $\varepsilon_K^{\text{NP}}$ é demasiado elevado. No entanto, relaxando o limite de dominância exata, obtém-se uma região de parâmetro considerável, onde $\varepsilon_K^{\text{NP}}$ é compatível com a experiência, e as características do modelo previamente encontradas são preservadas. Outras quantidades importantes associadas aos EWPM são também estudadas. Em primeira aproximação, estes resultados são independentes de s_{34}, permitindo soluções dependentes apenas de três parâmetros de NF: s_{14}, s_{24} e $\delta' = \delta_{24} - \delta_{14}$.

Palavras-chave: Nova física, problema da unitariedade da matriz CKM, quarks *vector-like*, correntes neutras de mudança de sabor, *electroweak precision measurements*.

Abstract

Recent results and calculations provide strong evidence that the CKM matrix is not unitary, contradicting the Standard Model (SM) and suggesting New Physics (NP). In this thesis, we propose a minimal extension of the SM where an up-type vector-like quark isosinglet, denoted by T, is introduced, leading to a simple solution to the CKM unitarity problem (CKM-UP).

We adopt the Botella-Chau parametrization for the 4×3 quark mixing-matrix, containing the usual three angles and phase of the 3×3 SM-mixing, plus three extra angles s_{14}, s_{24}, s_{34} and two phases δ_{14}, δ_{24}. To fully achieve a minimal solution to the CKM-UP, we assume that the mixing of T with standard quarks is dominated by s_{14}. Interesting features and a novel pattern of T decays, predominantly to the first generation, are obtained. However, one has to make sure that the limits of Electroweak Precision Measurements (EWPM) from experiment, are not exceeded.

We have found that ε_K, sensitive to CP violation, plays a crucial role in constraining these type of models. Imposing a (recently derived) restrictive upper-bound on NP to ε_K, we find, in the limit of exact s_{14}-dominance where $s_{24}, s_{34} = 0$, that $\varepsilon_K^{\text{NP}}$ is too large. If, however, one relaxes this exact s_{14}-dominance limit, a significantly large parameter region is obtained, where $\varepsilon_K^{\text{NP}}$ is in agreement with experiment, maintaining previously encountered features. Other important EWPM associated quantities are also studied. To a good approximation, these results are independent of s_{34}, allowing for solutions solely using three NP parameters: s_{14},s_{24} and $\delta' = \delta_{24} - \delta_{14}$.

Keywords: New physics, CKM unitarity problem, vector-like quarks, flavour changing neutral currents, electroweak precision measurements.

Contents

List of Tables

List of Figures

List of Abbreviations

BC Botella-Chau

CC Charged current

CKM Cabibbo–Kobayashi–Maskawa

CKM-UP CKM unitarity problem

CP Charge conjugation parity symmetry

EW Electroweak

EWPM Electroweak precision measurements

FCNC Flavour changing neutral current

FLAG Flavour Lattice Averaging Group

GIM Glashow–Iliopoulos–Maiani

IL Inami-Lim

LD Long distance

LH Left-handed

LHC Large Hadron Collider

NC Neutral current

NNLO Next-to-next-to-leading order

NP New Physics

PDG Particle data group

QCD Quantum chromodynamics

QED Quantum electrodynamics

RG Renormalization group

RH Right-handed

SD Short distance

SM Standard Model

SSB Spontaneous symmetry breaking

VEV Vacuum expectation value

VIA Vacuum-insertion approximation

VLF Vector-like fermion

VLQ Vector-like quark

WB Weak basis

Chapter 1

Introduction

The Standard Model (SM) of particle physics is one of the most successful theories in all of physics as it manages, to provide an internally consistent and minimal framework that describes three fundamental interactions of Nature (electromagnetic, strong and weak interactions), unifying two of them (electroweak interaction), while including all known elementary particles. Moreover, it has several times predicted the existence of new particles and processes before they were eventually discovered.

However, it has become increasingly evident that the SM is incomplete and, thus, cannot be a final theory. Perhaps the most salient shortcoming of the SM is the non-inclusion of a description of gravity in the theory, but several other important examples exist, many of which resulting from direct incompatibilities with experimental results. Most notably, neutrino oscillation experiments [1–3] have shown that neutrinos are massive particles, which directly contradicts the underlying assumption present in the SM that they are massless particles. Moreover, this theory does not provide a satisfying justification for the observed matter-antimatter asymmetry in the universe, which leads to the currently open questions of baryogenesis and leptogenesis, and is also unable to explain the existence of dark matter.

Furthermore, the SM does not possess the predictive power one would expect from a final theory of particle physics, as it fails to make theoretical predictions for the coupling constants, masses and mixings of particles that we measure or explain the mass hierarchy observed between the different fermion generations. This is directly linked to the enormous amount of parameters that the theory leaves arbitrary and unrelated. For instance, in the quark sector, the 18 complex Yukawa couplings are arbitrary resulting in 36 free parameters which, as described by the SM, generate the 6 quark masses and the quark mixings which are functions of only 4 mixing parameters. Hence, this huge discrepancy between the number of free parameters and the number of observables, suggests that the SM has a great degree of redundancy. In addition to this, the SM gives no prediction to the number of particles in the theory or explain why there exist three sequential generations of fermions.

Despite all these issues, it is important to emphasise that the SM is indeed an extremely valuable and powerful theory and it is reasonable to assume that any complete theory of particle physics must stem from and be developed out of the SM framework. In fact, during the last decades, theoretical particle physicists have deeply invested their efforts on exploiting some of the unrestricted aspects of the

SM in order to develop potential extensions to this theory that may be able to improve it, i.e. that might circumvent some of its incompatibilities with experiments and increase its overall predictive power. For instance, the fact that the SM leaves the Yukawa sector unconstrained provides one with the freedom to propose flavour symmetries which, through the constraining of some of the free parameters of the theory, may offer explanations to the mass hierarchy of fermions or alternative ways of generating the lighter quark masses and mixings [4–7]. Also, the SM does not exclude the possibility of having new types of fermions or even extra Higgs doublets. These extensions and extra fields all lead to very exciting new results. Most prominently, the addition of Majorana neutrinos to the SM has provided a promising framework able to generate neutrino masses and explain results coming from neutrino oscillation experiments. These extensions with new fields enhance the charge conjugation parity (CP) violation of the SM [8–10], and thus might provide interesting solutions to the problem of matter-antimatter imbalance.

Some of these proposals for new physics (NP) beyond the SM may in the future be corroborated by the experimental detection of exotic particles or phenomena, while others will be excluded by stricter restrictions emerging from improvements to experimental precision. Moreover, new experiments and more refined theoretical calculations may identify anomalies, i.e. discrepancies between theoretical predictions and experimental results, motivating other new extensions and proposals for NP beyond the SM.

In this work, we explore an anomaly associated with the first row of the CKM matrix, the mixing matrix of the quark sector. Using more precise experimental determinations for form factors and radioactive corrections, recent new theoretical calculations seem to indicate that the 3×3 unitarity of this matrix in the SM might be violated, given that the normalisation of the first row currently seems to indicate that $|V_{ud}|^2 + |V_{us}|^2 + |V_{ub}|^2 < 1$ [11–18]. If confirmed, this would be a major result, providing evidence for NP beyond the SM. This problem is typically referred to as the CKM unitarity problem (CKM-UP), or Cabibbo angle anomaly. Although this anomaly can be explained using models not necessarily relying on the violation of CKM unitarity [19–23], some of the most elegant and simpler solutions rely on extensions of the SM quark sector with the introduction of a new type of quarks, the vector-like quarks (VLQs), which necessarily lead to deviations to CKM unitarity. Given that until now a unitary CKM has been so very successful in explaining a wide variety of phenomena, these deviations should be sufficiently suppressed. Conveniently, models with VLQs provide a natural mechanism for suppression of unwanted deviations, while leading to a rich phenomenology due to the large enhancement of the parameter space [24–27].

It has also been pointed out that one of the simplest extensions of the SM which can account for this NP, consist of the addition of either one down-type [28] or one up-type [29, 30] vector-like quark (VLQ) isosinglet. In both cases, the parameter space is very large, involving six mixing angles and three CP violating phases. This is the type of extension we will be interested in exploring here, particularly extensions with one up-type VLQ, which, as we shall demonstrate, appear to present a more natural solution to the CKM-UP. More concretely, the ultimate goal of this thesis is to look for a minimal solution to the CKM-UP i.e. a solution involving the least number of new fields and parameters added to the SM . To do this, we work in the framework of the SM extended with one up-type VLQ isosinglet, in

a minimal mixing limit case, and which we refer to as the s_{14}-dominance limit. This minimal solution not only addresses the CKM anomaly and obeys the stringent constraints coming from experiment and which arise from processes such as neutral meson mixings or kaon decays and others, but also, most important, maintains the main predictions of SM.

This thesis is organised as follows. In the next chapter we briefly revisit the SM, introducing notation and describing concepts directly related to the work: electroweak (EW) theory, interactions of quarks with the gauge and Higgs bosons and the CKM matrix. In chapter 3, we describe how extensions of the SM, implemented with the introduction of VLQs, may be able to successfully address the CKM unitarity problem in an elegant and simple manner. In addition, we explore how these frameworks affect the EW Lagrangian through the flavor changing neutral currents (FCNCs). We also verify how the modified theory compares with the SM. Then, in chapter 4 and making use of the results of the previous chapter, we explore how, within the framework of an extension of the SM with one up-type VLQ isosinglet, the modified EW theory affects the predictions for experimentally detectable phenomena and measurable physical quantities. Finally, in the last two chapters we introduce, within this context, a minimal solution to the CKM-UP: the s_{14}-dominance limit. We explore two versions of this limit and use the results from chapter 4 to assess their safety, i.e. whether they conform to current experimental data or not.

Chapter 2

A brief review of the Standard Model

The SM is a quantum field theory that describes the interactions of known elementary particles. Being a quantum field theory it combines a quantum description of Nature with a relativistic one, while treating fields as its fundamental entities. Therefore, particles observed experimentally are identified as being the excitations of these fields and all laws and physical quantities predicted by the theory are Lorentz invariant.

The SM is also a gauge theory based on the local symmetry group $SU(3)_C \times SU(2)_L \times U(1)_Y$, with the subscripts representing the colour charge, left-handed (LH) chirality and hypercharge, respectively. This group determines the possible interactions between particles and the number of gauge bosons. The focus of this work will be the electroweak (EW) theory which is the theory based on the local symmetry group $SU(2)_L \times U(1)_Y$.

Throughout this chapter we will present some of the main and most relevant concepts and features of the SM and its EW sector and we follow [31] and [32] closely.

2.1 Particle content of the Standard Model

The elementary particles included in the SM can be divided into fermion fields, gauge boson fields and the Higgs field. The SM fermions fields, which are spinors in Dirac space, are spin $1/2$ particles and can be further divided into quark and lepton fields. The former are represented by

$$\boldsymbol{Q'_L} = \begin{pmatrix} Q'_{1L} \\ Q'_{2L} \\ Q'_{3L} \end{pmatrix}, \quad \boldsymbol{q'} = \boldsymbol{q'_L} + \boldsymbol{q'_R} = \begin{pmatrix} q'_{1L} \\ q'_{2L} \\ q'_{3L} \end{pmatrix} + \begin{pmatrix} q'_{1R} \\ q'_{2R} \\ q'_{3R} \end{pmatrix}, \tag{2.1}$$

with $q'_i = \{u'_i, d'_i\}$ and

$$Q'_{iL} = \begin{pmatrix} u'_{iL} \\ d'_{iL} \end{pmatrix}. \tag{2.2}$$

There exist three copies of fields with essentially the same properties. Each copy, denoted by an

index $i = 1, 2, 3$, is referred to as a family/generation and consists of a doublet of $SU(2)_L$, Q_{iL}, and the singlets u_{iR} and d_{iR}, where u and d refer to the up and down-quark sectors, respectively. The quarks belonging to the up-sector have electric charge $Q = 2/3$, whereas the quarks belonging to the down sector have electric charge $Q = -1/3$. Note that the up-type ($q = u$) and down-type ($q = d$) left-handed (LH) quark fields of a given generation i, form the doublet of $SU(2)_L$. Currently, the three known families of quarks each including two quarks, one from each sector, constitute six different quark flavours. The indices L and R differentiate between the left and right-chiral components of these fields. In (2.1) we introduce a compact notation where $\boldsymbol{Q_L}$ (in bold) is a vector in family space containing all three quark doublets and similarly $\boldsymbol{q_{L,R}}$ contains the LH or RH components of all the quarks of a given sector.

Using a similar notation, the lepton fields can be represented by

$$\boldsymbol{L'_L} = \begin{pmatrix} L'_{1L} \\ L'_{2L} \\ L'_{3L} \end{pmatrix}, \quad \boldsymbol{\ell'} = \boldsymbol{\ell'_L} + \boldsymbol{\ell'_R} = \begin{pmatrix} \ell'_{1L} \\ \ell'_{2L} \\ \ell'_{3L} \end{pmatrix} + \begin{pmatrix} \ell'_{1R} \\ \ell'_{2R} \\ \ell'_{3R} \end{pmatrix}, \tag{2.3}$$

with

$$L'_{jL} = \begin{pmatrix} \nu'_{jL} \\ \ell'_{jL} \end{pmatrix}, \tag{2.4}$$

where now one has the $SU(2)_L$ lepton doublets, L_{jL}, formed by the LH components of the neutrino ν_j and charged lepton ℓ_{jL} fields. The RH components of the charged lepton fields are singlets of $SU(2)_L$ and there exists no RH component of the neutrino fields in the pure SM. For all of these fermion fields there exists a corresponding antiparticle which has the same mass but opposite physical charges.

The gauge boson fields are introduced to the theory through the covariant derivative

$$D^\mu = \partial^\mu - i \sum_{\mathcal{G}} g_{\mathcal{G}} \boldsymbol{A}^{\mathcal{G}}_\mu \cdot \boldsymbol{T}^{\mathcal{G}}, \tag{2.5}$$

where the index $\mathcal{G}$ spans the gauge groups of the theory, $\boldsymbol{T}^{\mathcal{G}} = (T^{\mathcal{G}}_1, ..., T^{\mathcal{G}}_n)$ correspond to the n generators of a given $SU(n)$ gauge group $\mathcal{G}$ in the fundamental representation and $\boldsymbol{A}^{\mathcal{G}}_\mu = (A^{\mathcal{G}}_{1\mu}, ..., A^{\mathcal{G}}_{n\mu})$ are the n gauge boson fields associated with this group. In turn, the covariant derivative itself is introduced as a modification to the ordinary derivative present in the Lagrangian containing the kinetic terms of a Dirac field,

$$\mathscr{L}^{\text{kin}} = i\overline{\psi}\gamma^\mu \partial_\mu \psi. \tag{2.6}$$

This modification is crucial to make the overall Lagrangian of the theory invariant under local gauge transformations, i.e. transformation such as

$$\psi \to \tilde{\psi} = U\left(\boldsymbol{\theta}(x_\mu)\right)\psi, \tag{2.7}$$

where

$$U(\boldsymbol{\theta}(x^\mu)) = e^{i\boldsymbol{\theta}(x^\mu)\cdot\boldsymbol{T}} \in SU(n) \tag{2.8}$$

are the unitary matrix representations of the gauge group $SU(n)$ and $\boldsymbol{\theta}(x^\mu)$ is an array of real parameters that depend on the space-time coordinates x^μ. Then, under these transformations, the gauge fields transform in such a way that

$$D_\mu\psi \to \tilde{D}_\mu\tilde{\psi} = U\left(\boldsymbol{\theta}(x^\mu)\right) D_\mu\psi, \tag{2.9}$$

i.e. the covariant derivatives of the fields transform in the same way as the fields, such that

$$\overline{\psi}\gamma^\mu D_\mu\psi = \overline{\tilde{\psi}}\gamma^\mu\tilde{D}_\mu\tilde{\psi}, \tag{2.10}$$

and local gauge invariance is achieved. It is then evident that the presence of the covariant derivative in the Lagrangian results in new interactions of the fermion fields, mediated by these gauge fields.

In the SM, with its $SU(3)_C \times SU(2)_L \times U(1)_Y$ gauge group, we have B^μ and $\boldsymbol{W}^\mu = (W_1^\mu, W_2^\mu, W_3^\mu)$ as the gauge bosons associated with the $U(1)_Y$ and $SU(2)_L$ gauge groups, respectively, while the gluon fields $\boldsymbol{G}^\mu = (G_1^\mu, ..., G_8^\mu)$ are associated with the $SU(3)_C$ gauge group. The Pauli matrices, $\tau_j/2$ $(j = 1, 2, 3)$, and the Gell-Mann matrices, $\lambda_a/2$ $(a = 1, ..., 8)$, divided by a factor of 2, correspond to the generators of $SU(2)_L$ and $SU(3)_C$ in the fundamental representation, respectively. The couplings to B^μ, W_j^μ and G_a^μ are quantified by the coupling constants g, g' and g_s, respectively.

The scalar content of the SM is contained in a single isospin doublet, the so-called Higgs doublet

$$\Phi = \begin{pmatrix} \phi^+ \\ \phi^0 \end{pmatrix}, \tag{2.11}$$

where ϕ^+ and ϕ^0 are, respectively, charged and complex scalar fields. With the Higgs mechanism, this doublet plays a central role in generating the masses of elementary particles. However, in this work we will not look into the details associated with this mechanism. Nonetheless, it is important to keep in mind that, for low energies, the ϕ^0 acquires a non-vanishing vacuum expectation value (VEV) $\langle\phi^0\rangle = v$ where $v \simeq 246$ GeV is the electroweak (EW) scale, leading to the vacuum sate

$$\langle\Phi\rangle = \frac{1}{\sqrt{2}}\begin{pmatrix} 0 \\ v \end{pmatrix} \tag{2.12}$$

for the Higgs doublet, which then results in the spontaneous symmetry breaking (SSB) of the EW gauge group, i.e.

$$SU(2)_L \times U(1)_Y \to U(1)_Q, \tag{2.13}$$

where $U(1)_Q$ is the unbroken gauge symmetry group of electromagnetic interactions, which conserves the electric charge $Q = I_3 + Y/2$, with the third component of weak isospin defined as $I_3 \equiv \tau_3/2$. It is nonetheless important to consider the excitations around the vacuum which can be parametrized as

$$\Phi = \frac{1}{\sqrt{2}} \exp\left(i \frac{\boldsymbol{\varphi} \cdot \boldsymbol{\tau}}{2v}\right) \begin{pmatrix} 0 \\ v + h \end{pmatrix}, \tag{2.14}$$

where h and $\boldsymbol{\varphi} = (\varphi_1, \varphi_2, \varphi_3)$ are scalar fields with vanishing VEVs. The field h is the (neutral) physical Higgs boson, while the $\boldsymbol{\varphi}$ are the unphysical Goldstone bosons, since they can be absorbed by an appropriate $SU(2)_L$ gauge transformation. In the rest of this work we shall adopt the unitary gauge where these unphysical fields disappear and the Lagrangian of the theory can be written solely in terms of physical fields. Thus, we will shall work with

$$\Phi = \frac{1}{\sqrt{2}} \begin{pmatrix} 0 \\ v + h \end{pmatrix}, \tag{2.15}$$

instead.

To conclude we present the EW gauge charges of the fermions and Higgs fields in table 2.1.

	I	I_3	Y	$Q = I_3 + Y/2$
$L_{iL} = \begin{pmatrix} \nu_{iL} \\ \ell_{iL} \end{pmatrix}$	$1/2$	$\begin{pmatrix} 1/2 \\ -1/2 \end{pmatrix}$	-1	$\begin{pmatrix} 0 \\ -1 \end{pmatrix}$
ℓ_{iR}	0	0	-2	-1
$Q_{iL} = \begin{pmatrix} u_{iL} \\ d_{iL} \end{pmatrix}$	$1/2$	$\begin{pmatrix} 1/2 \\ -1/2 \end{pmatrix}$	$1/3$	$\begin{pmatrix} 2/3 \\ -1/3 \end{pmatrix}$
u_{iR}	0	0	$4/3$	$2/3$
d_{iR}	0	0	$-2/3$	$-1/3$
$\Phi = \begin{pmatrix} \phi^+ \\ \phi^0 \end{pmatrix}$	1/2	$\begin{pmatrix} 1/2 \\ -1/2 \end{pmatrix}$	1	$\begin{pmatrix} 1 \\ 0 \end{pmatrix}$

Table 2.1: Eigenvalues of the weak isospin $I = \boldsymbol{\tau}/2$, of its third component $I_3 = \tau_3/2$, of the hypercharge Y, and of the electric charge Q for the fermion doublets and singlets as well as the Higgs doublet.

2.2 The Electroweak Lagrangian

The gauge-invariant and renormalizable Lagrangian of the the SM describes all interactions involving the known particles (with the exception of an eventually existing graviton and subsequent theory of quantum-gravity which are not the subject of this work). The SM can be divided in an EW theory which describes the electromagnetic and weak interactions of quarks, leptons, gauge bosons and the Higgs boson, and the theory of quantum chromodynamics (QCD), which describes the strong interactions involving quarks and gluons. As stated before, in this work we will focus primarily on the EW sector and in this section we shall explore some aspects of the Lagrangian describing it.

This Lagrangian can be divided in the following way

$$\mathscr{L}_{\text{EW}} = \mathscr{L}_g + \mathscr{L}_f + \mathscr{L}_{\text{Yuk}} + \mathscr{L}_\phi, \tag{2.16}$$

where $\mathscr{L}_g$ contains the kinetic and self-interaction terms of the gauge bosons, $\mathscr{L}_f$ contains the kinetic

terms of the fermion fields and the their interactions with the gauge bosons, $\mathscr{L}_{\text{Yuk}}$ describes the Yukawa interactions and $\mathscr{L}_\phi$ is the Higgs sector Lagrangian which describes the Higgs boson interactions with itself and the gauge bosons.

More concretely one has

$$\mathscr{L}_g = -\frac{1}{4}F_{\mu\nu}F^{\mu\nu} - \frac{1}{4}W^a_{\mu\nu}W^{\mu\nu}_a, \tag{2.17}$$

with

$$\begin{aligned} W^a_{\mu\nu} &= \partial_\mu W^a_\nu - \partial_\nu W^a_\mu + g\epsilon^{abc}W^b_\mu W^c_\nu, \\ F_{\mu\nu} &= \partial_\mu B_\nu - \partial_\nu B_\mu. \end{aligned} \tag{2.18}$$

For the fermion lagrangian one has

$$\mathscr{L}_f = i\overline{\boldsymbol{Q}}_{\boldsymbol{L}}\not{D}\boldsymbol{Q}_{\boldsymbol{L}} + i\overline{\boldsymbol{u}}_{\boldsymbol{R}}\not{D}\boldsymbol{u}_{\boldsymbol{R}} + i\overline{\boldsymbol{d}}_{\boldsymbol{R}}\not{D}\boldsymbol{d}_{\boldsymbol{R}} + i\overline{\boldsymbol{L}}_{\boldsymbol{L}}\not{D}\boldsymbol{L}_{\boldsymbol{L}} + i\overline{\boldsymbol{\ell}}_{\boldsymbol{R}}\not{D}\boldsymbol{\ell}_{\boldsymbol{R}}, \tag{2.19}$$

where

$$\not{D} \equiv \gamma_\mu D^\mu = \gamma_\mu\left(\partial^\mu - i\frac{g'}{2}YB^\mu - i\frac{g}{2}\boldsymbol{\tau}\cdot\boldsymbol{W}^{\boldsymbol{\mu}}\right), \tag{2.20}$$

is the covariant derivative for the EW sector. Therefore, one can write

$$\mathscr{L}_f = \mathscr{L}_f^{\text{kin}} + \mathscr{L}_f^{\text{int}}, \tag{2.21}$$

where

$$\mathscr{L}_f^{\text{kin}} = i\bar{\boldsymbol{u}}\not{\partial}\boldsymbol{u} + i\bar{\boldsymbol{d}}\not{\partial}\boldsymbol{d} + i\bar{\boldsymbol{\ell}}\not{\partial}\boldsymbol{\ell} + i\bar{\boldsymbol{\nu}}\not{\partial}\boldsymbol{\nu}, \tag{2.22}$$

contains the kinetic terms of all SM fermions, while $\mathscr{L}_f^{\text{int}}$ contains the interactions of these fermions with the gauge bosons. To write the latter piece in terms of the observed gauge bosons, the photon A_μ and the weak interaction neutral, Z_μ, and charged, $W^\pm_\mu$, gauge bosons, we do a rotation of Weinberg angle θ_W in the plane $\{W^\mu_3, B^\mu\}$,

$$\begin{pmatrix} A^\mu \\ Z^\mu \end{pmatrix} = \begin{pmatrix} c_W & -s_W \\ s_W & c_W \end{pmatrix}\begin{pmatrix} B^\mu \\ W^\mu_3 \end{pmatrix} \tag{2.23}$$

where

$$s_W \equiv \sin\theta_W \equiv \frac{g'}{\sqrt{g^2+g'^2}}, \qquad c_W \equiv \cos\theta_W \equiv \frac{g}{\sqrt{g^2+g'^2}}, \tag{2.24}$$

and we define

$$W^{\pm\mu} \equiv \frac{W_1^\mu \mp i W_2^\mu}{2}, \tag{2.25}$$

so that the Lagrangian describing gauge interactions of quarks is

$$\begin{aligned}\mathscr{L}_f^{\text{int}} = &-eA_\mu J^\mu_{\text{em}} - \frac{g}{2c_W}(\bar{\boldsymbol{u}}'_{\boldsymbol{L}} \not{Z} \boldsymbol{u}'_{\boldsymbol{L}} - \bar{\boldsymbol{d}}'_{\boldsymbol{L}} \not{Z} \boldsymbol{d}'_{\boldsymbol{L}} + \bar{\boldsymbol{\nu}}'_{\boldsymbol{L}} \not{Z} \boldsymbol{\nu}'_{\boldsymbol{L}} - \bar{\boldsymbol{\ell}}'_{\boldsymbol{L}} \not{Z} \boldsymbol{\ell}'_{\boldsymbol{L}} - 2s_W^2 J^\mu_{\text{em}} Z_\mu) \\ &- \frac{g}{\sqrt{2}}(\bar{\boldsymbol{u}}'_{\boldsymbol{L}} W^+ \boldsymbol{d}'_{\boldsymbol{L}} + \bar{\boldsymbol{d}}'_{\boldsymbol{L}} W^- \boldsymbol{u}'_{\boldsymbol{L}} + \bar{\boldsymbol{\nu}}'_{\boldsymbol{L}} W^+ \boldsymbol{\ell}'_{\boldsymbol{L}} + \bar{\boldsymbol{\ell}}'_{\boldsymbol{L}} W^- \boldsymbol{\nu}'_{\boldsymbol{L}}),\end{aligned} \tag{2.26}$$

where we introduced the electromagnetic current

$$\begin{aligned}J^\mu_{\text{em}} &= \frac{2}{3}(\bar{\boldsymbol{u}}'_{\boldsymbol{L}} \gamma^\mu \boldsymbol{u}'_{\boldsymbol{L}} + \bar{\boldsymbol{u}}'_{\boldsymbol{R}} \gamma^\mu \boldsymbol{u}'_{\boldsymbol{R}}) - \frac{1}{3}(\bar{\boldsymbol{d}}'_{\boldsymbol{L}} \gamma^\mu \boldsymbol{d}'_{\boldsymbol{L}} + \bar{\boldsymbol{d}}'_{\boldsymbol{R}} \gamma^\mu \boldsymbol{d}'_{\boldsymbol{R}}) - (\bar{\boldsymbol{\ell}}'_{\boldsymbol{L}} \gamma^\mu \boldsymbol{\ell}'_{\boldsymbol{L}} + \bar{\boldsymbol{\ell}}'_{\boldsymbol{R}} \gamma^\mu \boldsymbol{\ell}'_{\boldsymbol{R}}) \\ &= \frac{2}{3}\bar{\boldsymbol{u}}' \gamma^\mu \boldsymbol{u}' - \frac{1}{3}\bar{\boldsymbol{d}}' \gamma^\mu \boldsymbol{d}' - \bar{\boldsymbol{\ell}}' \gamma^\mu \boldsymbol{\ell}',\end{aligned} \tag{2.27}$$

and $e \equiv g \sin\theta_W$ is the elementary electric charge, which ensures that the QED results are recovered.

Then, the first two terms of (2.26) correspond to electromagnetic and weak neutral current (NC) Lagrangians, respectively, whereas the last corresponds to the charged current (CC) Lagrangian.

The Yukawa interactions are described by

$$-\mathscr{L}_{\text{Yuk}} = \overline{\boldsymbol{L}}'_{\boldsymbol{L}} \Phi Y^\ell \boldsymbol{\ell}'_{\boldsymbol{R}} + \overline{\boldsymbol{Q}}'_{\boldsymbol{L}} \tilde{\Phi} Y^u \boldsymbol{u}'_{\boldsymbol{R}} + \overline{\boldsymbol{Q}}'_{\boldsymbol{L}} \Phi Y^d \boldsymbol{d}'_{\boldsymbol{R}} + h.c., \tag{2.28}$$

where it should be noted that the Higgs doublet Φ and $\tilde{\Phi} = i\tau_2 \Phi^*$ are treated as numbers in family space. Also, $Y^{\ell,q}$ are 3×3 matrices with its components being the Yukawa couplings which (in general) are complex numbers. Unless there is no symmetry or mechanism which states otherwise, it is reasonable to expect that $|Y^{\ell,q}_{ij}| \sim 1$, although for the down quarks and the charged leptons, one has to change this to around $\mathcal{O}(10^{-2})$ (which, in our view, should require some justification in any concrete model).

Finally, regarding the Higgs sector one has

$$\mathscr{L}_\Phi = (D_\mu \Phi)^\dagger (D^\mu \Phi) - \mu^2 \Phi^\dagger \Phi - \lambda^2 \left(\Phi^\dagger \Phi\right)^2, \tag{2.29}$$

which will not play an active role throughout this work. It is however a very relevant part of the Lagrangian responsible for the SSB in the EW sector which generates the masses of the fermions and gauge bosons. In fact, the constant v introduced in (2.12) is obtained from the minimum of the potential part in this expression, which yields $v \equiv \sqrt{-\mu^2/\lambda}$.

In the next sections however, we will focus, more specifically, on the EW theory described by $\mathscr{L}_f$ in (2.19) and $\mathscr{L}_{\text{Yuk}}$ in (2.28), in particular, on the quark sector.

2.3 Quark masses and mixings

After SSB and using (2.15), the Yukawa interactions in (2.28) can be written as

$$\mathscr{L}_{\text{Yuk}} = \mathscr{L}_m + \mathscr{L}_h, \tag{2.30}$$

where $\mathscr{L}_m$ contains the mass terms of the SM fermions and $\mathscr{L}_h$ describes their interactions with the Higgs boson. After SSB, we obtain the mass terms for quarks

$$\mathscr{L}_m^q = -\overline{\boldsymbol{u}}'_{\boldsymbol{L}} m^u \boldsymbol{u}'_{\boldsymbol{R}} - \overline{\boldsymbol{d}}'_{\boldsymbol{L}} m^d \boldsymbol{d}'_{\boldsymbol{R}} + h.c, \tag{2.31}$$

where m^u and m^d are the up-quark and down-quark mass matrices, respectively, each one with entries given by

$$m_{ij}^q = \frac{v}{\sqrt{2}} Y_{ij}^q, \tag{2.32}$$

so that the EW scale imposes the mass scale for the SM quarks. In addition, the interactions with the Higgs boson are described by

$$\begin{aligned} \mathscr{L}_h^q &= -\overline{\boldsymbol{d}}'_{\boldsymbol{L}} Y^d \frac{h}{\sqrt{2}} \boldsymbol{d}'_{\boldsymbol{R}} - \overline{\boldsymbol{u}}'_{\boldsymbol{L}} Y^u \frac{h}{\sqrt{2}} \boldsymbol{u}'_{\boldsymbol{R}} + h.c. \\ &= -\overline{\boldsymbol{d}}'_{\boldsymbol{L}} m^d \frac{h}{v} \boldsymbol{d}'_{\boldsymbol{R}} - \overline{\boldsymbol{u}}'_{\boldsymbol{L}} m^u \frac{h}{v} \boldsymbol{u}'_{\boldsymbol{R}} + h.c. \end{aligned} \tag{2.33}$$

The fields with definite masses are those for which the mass matrices are diagonal, i.e. the mass matrix eigenstates. Then, exclusively using unitary matrices, since only those keep the terms in (2.19) invariant, one can relate the $\boldsymbol{q'}$ fields with their corresponding mass eigenstates $\boldsymbol{q}$, by $\boldsymbol{q}'_{\boldsymbol{L,R}} = V_{L,R}^q \boldsymbol{q}_{\boldsymbol{L,R}}$, or in terms of the six observed quark flavours

$$\begin{aligned} \boldsymbol{u}'_{\boldsymbol{L,R}} &= \begin{pmatrix} u'_1 \\ u'_2 \\ u'_3 \end{pmatrix}_{L,R} = V_{L,R}^u \begin{pmatrix} u \\ c \\ t \end{pmatrix}_{L,R} = \boldsymbol{u}_{\boldsymbol{L,R}}, \\ \boldsymbol{d}'_{\boldsymbol{L,R}} &= \begin{pmatrix} d'_1 \\ d'_2 \\ d'_3 \end{pmatrix}_{L,R} = V_{L,R}^d \begin{pmatrix} d \\ s \\ b \end{pmatrix}_{L,R} = \boldsymbol{d}_{\boldsymbol{L,R}}. \end{aligned} \tag{2.34}$$

and the mass terms can be written as

$$\mathscr{L}_m^q = -\overline{\boldsymbol{d}}_{\boldsymbol{L}} d_0^d \, \boldsymbol{d}_{\boldsymbol{R}} - \overline{\boldsymbol{u}}_{\boldsymbol{L}} d_0^u \, \boldsymbol{u}_{\boldsymbol{R}} + h.c, \tag{2.35}$$

with $d_0^q = V_L^{q\dagger} m^q V_R^q$ being the diagonal matrices that contain the definite masses of the respective sector's quark fields, i.e.

$$d_0^u = \begin{pmatrix} m_u & 0 & 0 \\ 0 & m_c & 0 \\ 0 & 0 & m_t \end{pmatrix}, \qquad d_0^d = \begin{pmatrix} m_d & 0 & 0 \\ 0 & m_s & 0 \\ 0 & 0 & m_b \end{pmatrix}. \tag{2.36}$$

Similarly the Lagrangian (2.33) can now be written as

$$\mathscr{L}_h^q = -\overline{\boldsymbol{d}}_{\boldsymbol{L}} \frac{h}{v} d_0^d \boldsymbol{d}_{\boldsymbol{R}} - \overline{\boldsymbol{u}}_{\boldsymbol{L}} \frac{h}{v} d_0^u \boldsymbol{u}_{\boldsymbol{R}} + h.c, \tag{2.37}$$

so that the interactions of quarks with the Higgs boson are flavour diagonal.

The unitarity of the transformation ensures that the electromagnetic and weak NCs keep their form, i.e.

$$\mathscr{L}_{\mathsf{NC}}^q = -eA_\mu J_{q,\mathsf{em}}^\mu - \frac{g}{2c_W} \left(\bar{\boldsymbol{u}}_{\boldsymbol{L}} \not{Z} \boldsymbol{u}_{\boldsymbol{L}} - \bar{\boldsymbol{d}}_{\boldsymbol{L}} \not{Z} \boldsymbol{d}_{\boldsymbol{L}} - 2 s_W^2 J_{q,\mathsf{em}}^\mu Z_\mu \right), \tag{2.38}$$

$$J_{q,\mathsf{em}}^\mu = \frac{2}{3} \bar{\boldsymbol{u}} \gamma^\mu \boldsymbol{u} - \frac{1}{3} \bar{\boldsymbol{d}} \gamma^\mu \boldsymbol{d}, \tag{2.39}$$

so that these transformations modify only the form of the charged currents into

$$\mathscr{L}_{\mathsf{CC}}^q = -\frac{g}{\sqrt{2}} \left(\bar{\boldsymbol{u}}_{\boldsymbol{L}} \not{W}^+ V_{\mathsf{CKM}} \boldsymbol{d}_{\boldsymbol{L}} + \bar{\boldsymbol{d}}_{\boldsymbol{L}} \not{W}^- V_{\mathsf{CKM}}^\dagger \boldsymbol{u}_{\boldsymbol{L}} \right), \tag{2.40}$$

where we find the Cabibbo-Kobayashi-Maskawa (CKM) matrix

$$V_{\mathsf{CKM}} \equiv V_L^{u\dagger} V_L^d \equiv \begin{pmatrix} V_{ud} & V_{us} & V_{ub} \\ V_{cd} & V_{cs} & V_{cb} \\ V_{td} & V_{ts} & V_{tb} \end{pmatrix}, \tag{2.41}$$

i.e. the 3×3 (charged current) unitary matrix with elements corresponding to the mixings of different quark flavours in the SM and in interactions mediated by the W bosons.

From (2.38-2.41) it is clear that, in the SM, (2.37), the electromagnetic as well as the weak NC are flavour conserving, while the CC are flavour changing in general.

Note that the matrices $V_R^{u,d}$ do not contribute to the physical CKM matrix and therefore they are physically meaningless, as the mixings and the masses correspond to all the information contained in the Yukawa couplings and, thus, in the mass matrices. In the next section we will focus on the SM CKM mixing matrix and its most important features.

2.4 The CKM matrix and CP violation

A general unitary matrix of dimension n can be parametrized by $n(n-1)/2$ angles and $n(n+1)/2$ phases. However, the CKM mixing matrix for n generations is parametrized by less phases [32]. In fact, using $2n$ arbitrary phases to rephase every quark field as

$$u_j \to e^{i\phi_j} u_j, \qquad d_k \to e^{i\phi_k} d_k, \tag{2.42}$$

with $j = \{u, c, t\}$, $k = \{d, s, b\}$, which simply corresponds to a physically inconsequential redefinition of these fields, such that

$$V_{jk} \to V_{jk} e^{i(\phi_k - \phi_j)}, \tag{2.43}$$

and the charged currents become

$$\begin{aligned} \mathscr{L}^q_{\mathsf{CC}} &\to -\frac{g}{\sqrt{2}} \sum_{j,k} \left(\bar{u}_{jL} \not{W}^+ e^{-i\phi_j} V_{jk}\, e^{i\phi_k} d_{kL} + h.c \right) \\ &= -\frac{g}{\sqrt{2}} e^{-i(\phi_u - \phi_d)} \sum_{j,k} \left(\bar{u}_{jL} \not{W}^+ e^{-i(\phi_j - \phi_u)} V_{jk} e^{i(\phi_k - \phi_d)} d_{kL} + h.c \right). \end{aligned} \tag{2.44}$$

This way, by factorizing one phase $e^{-i(\phi_u - \phi_d)}$, it becomes clear that there are $2n-1$ independent phases which can be used to eliminate some of the phases of V_{CKM}. Therefore, there exist

$$\frac{n(n+1)}{2} - (2n-1) = \frac{(n-1)(n-2)}{2} \tag{2.45}$$

phases that are not possible to eliminate. In combination with the $n(n-1)/2$ mixing angles, these $(n-1)(n-2)/2$ physical phases are all the parameters that are needed to fully construct the mixing matrix. In the $n=3$ case of the SM, there are three mixing angles θ_{12}, θ_{13} and θ_{23} and a single physical phase, which in the standard Particle Data Group (PDG) parametrization is named δ [33]. This parametrization of V_{CKM} is given by

$$\begin{aligned} V_{\mathsf{PDG}} &= \begin{pmatrix} 1 & 0 & 0 \\ 0 & c_{23} & s_{23} \\ 0 & -s_{23} & c_{23} \end{pmatrix} \begin{pmatrix} c_{13} & 0 & s_{13} e^{-i\delta} \\ 0 & 1 & 0 \\ -s_{13} e^{i\delta} & 0 & c_{13} \end{pmatrix} \begin{pmatrix} c_{12} & s_{12} & 0 \\ -s_{12} & c_{12} & 0 \\ 0 & 0 & 1 \end{pmatrix} \\ &= \begin{pmatrix} c_{12}c_{13} & s_{12}c_{13} & s_{13}e^{-i\delta} \\ -s_{12}c_{23} - c_{12}s_{23}s_{13}e^{i\delta} & c_{12}c_{23} - s_{12}s_{23}s_{13}e^{i\delta} & s_{23}c_{13} \\ s_{12}s_{23} - c_{12}c_{23}s_{13}e^{i\delta} & -c_{12}s_{23} - s_{12}c_{23}s_{13}e^{i\delta} & c_{23}c_{13} \end{pmatrix}, \end{aligned} \tag{2.46}$$

where $c_{ij} = \cos\theta_{ij}$, $s_{ij} = \sin\theta_{ij}$ and with $\theta_{ij} \in [0, \pi/2]$, $\delta \in [0, 2\pi]$. Other parametrizations of the SM mixing matrix that make use of the three mixing angles and the single physical phase will differ from this one by the placement of the phase, but all of them can be obtained from each other by rephasings of the quark fields which, as stated previously, have no physical implications. However, although these rephasings do not affect the magnitudes of the mixings, they can for sure modify their phases. Therefore, for each individual entry of V_{CKM} only their moduli $|V_{jk}|$ are physically meaningful. Nonetheless, there still exists physical meaning to be extracted from quantities associated with the physical phases of V_{CKM}, which are not modified with the rephasing of the quark fields, the so-called the rephasing invariants. Unsurprisingly, the moduli $|V_{jk}|$ are themselves rephasing invariant quantities, but less obvious examples are, for instance. the quartets

$$Q_{\alpha i \beta j} \equiv V_{\alpha i} V_{\beta j} V^*_{\alpha j} V^*_{\beta i}, \tag{2.47}$$

with $\alpha \neq \beta$ and $i \neq j$. These quantities have the property

$$Q_{\alpha i \beta j} = Q^*_{\alpha j \beta i} = Q_{\beta j \alpha i} = Q^*_{\beta i \alpha j} \tag{2.48}$$

and are clearly invariant under (2.42-2.43). Using these quantities one can relate the physical phase δ with quantities measurable experimentally. Some relevant examples are the rephasing invariant phases

$$\begin{aligned}
\alpha &\equiv \arg\left(-Q_{tdub}\right) = \arg\left(-\frac{V_{td}V^*_{tb}}{V_{cd}V^*_{cb}}\right), \\
\beta &\equiv \arg\left(-Q_{cdtb}\right) = \arg\left(-\frac{V_{cd}V^*_{cb}}{V_{td}V^*_{tb}}\right), \\
\gamma &\equiv \arg\left(-Q_{udcb}\right) = \arg\left(-\frac{V_{ud}V^*_{ub}}{V_{cd}V^*_{cb}}\right), \\
\chi &\equiv \arg\left(-Q_{cbts}\right) = \arg\left(-\frac{V_{cb}V^*_{cs}}{V_{tb}V^*_{ts}}\right), \\
\chi' &\equiv \arg\left(-Q_{uscd}\right) = \arg\left(-\frac{V_{us}V^*_{ud}}{V_{cs}V^*_{cd}}\right).
\end{aligned} \tag{2.49}$$

In general all nine entries of V_{CKM} can have phases which correspond to some function of the mixing angles and the physical phase. However, given that one can perform (at most) $2n-1=5$ independent rephasings of the quark fields, in the end only four of these phases are linearly independent. In fact, through rephasings of the quark fields one can achieve the form [34]

$$\arg\left(V_{\text{CKM}}\right) = \begin{pmatrix} 0 & \chi' & -\gamma \\ \pi & 0 & 0 \\ -\beta & \pi+\chi & 0 \end{pmatrix}, \tag{2.50}$$

so that the rephasing invariant phases β, γ, χ and χ' can together form a set of four linearly independent phases. This is similar to the fact that, from unitarity conditions such as

$$\begin{aligned}
|V_{jd}|^2 + |V_{js}|^2 + |V_{jt}|^2 = 1, \\
|V_{uk}|^2 + |V_{ck}|^2 + |V_{bk}|^2 = 1,
\end{aligned} \tag{2.51}$$

only four moduli $|V_{jk}|$ are linearly independent. Hence, with these four phases and, for instance, $|V_{us}|, |V_{cb}|, |V_{ub}|$ and $|V_{td}|$, one can reconstruct the full CKM matrix solely in terms of rephasing invariants.

Furthermore, the phases α, β and γ correspond to the internal angles of the unitarity triangle defined by the unitarity relation

$$V_{ud}V^*_{ub} + V_{cd}V^*_{cb} + V_{td}V^*_{tb} = 0 \tag{2.52}$$

which can be written in a more illustrative way as

$$1 = \left|\frac{V_{ud}V^*_{ub}}{V_{cd}V^*_{cb}}\right| e^{i\gamma} + \left|\frac{V_{td}V^*_{tb}}{V_{cd}V^*_{cb}}\right| e^{-i\beta}, \tag{2.53}$$

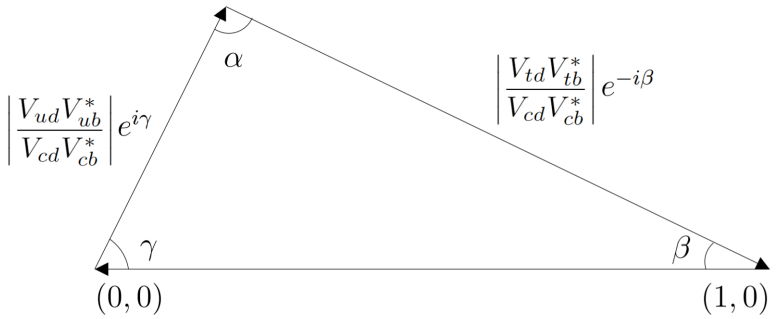

Figure 2.1: The "normalized" unitarity triangle obtained from (2.52) by dividing every side by $|V_{cd}V_{cb}^*|$.

as represented in figure 2.1. Therefore, one has

$$\alpha + \beta + \gamma = \pi + \mathsf{mod}(2\pi), \tag{2.54}$$

so that α can, in the SM, be given in terms of β and γ. The area of this triangle is given by

$$A_\Delta = \frac{|V_{cd}V_{cb}^*|\, h}{2} = \frac{|V_{cd}V_{cb}^* V_{ud}V_{ub}^*| \sin\gamma}{2} = \frac{|Q_{udcb}| \sin\gamma}{2} = \frac{|\mathsf{Im}\,(Q_{udcb})|}{2}, \tag{2.55}$$

where we not only used $h = |V_{ud}V_{ub}^*| \sin\gamma$ for the height of the unitarity triangle, but also used the relations in (2.48), as well as

$$-Q_{udcb} = |-Q_{udcb}|\, e^{i\gamma} = |Q_{udcb}|\,(\cos\gamma + i\sin\gamma) \tag{2.56}$$

which comes directly from the definition of γ in (2.49). The relation in (2.55) is usually written as

$$A_\Delta = \frac{J}{2}, \tag{2.57}$$

where we introduced another important example of a rephasing invariant, the CP invariant quantity, defined as

$$J \equiv |\mathsf{Im}\,(Q_{\alpha i\beta j})|\,. \tag{2.58}$$

This CP invariant quantity is not only rephasing invariant, but is also a quantity that is the same for all quartets in the SM. To understand this, we exploit once more the unitarity of V_{CKM},

$$\begin{aligned} &V_{\alpha i}V_{\alpha j}^* + V_{\beta i}V_{\beta j}^* + V_{\gamma i}V_{\gamma j}^* = 0 \\ \\ \implies\ &Q_{\alpha i\beta j} + |V_{\beta i}|^2 |V_{\beta j}|^2 = -Q_{\gamma k\beta j} \\ \\ \implies\ &\mathsf{Im}\,(Q_{\alpha i\beta j}) = -\mathsf{Im}\,(Q_{\gamma k\beta j})\,, \end{aligned} \tag{2.59}$$

with $i \neq j$. This result, along with the property in (2.48) leads to the conclusion that the imaginary parts of all nine SM quartets are the same up to a signal and therefore J is unique and all possible unitarity

quarks have the same area.

Now, using the parametrization in (2.46), one can show that

$$J = c_{12}s_{12}c_{23}s_{23}c_{13}^2 s_{13}\sin\delta, \tag{2.60}$$

which relates rephasing invariant quantities directly with the physical phase of V_{CKM}. In fact from this relation one can conclude that the CP invariant quantity J quantifies the violation of charge conjugation parity (CP) symmetry in the quark sector, which has to do with the way the charged-currents transform under these types of transformations. For instance, using the CP transformations of the fields [31]

$$\begin{aligned}
(\mathcal{CP})\,\bar{q}_{jL}(x^\mu)\,(\mathcal{CP})^\dagger &= -e^{-i\phi_j} q_\alpha^T(\tilde{x}^\mu) C^{-1}\gamma^0, \\
(\mathcal{CP})\,q_{kL}(x^\mu)\,(\mathcal{CP})^\dagger &= e^{i\phi_k}\gamma^0 C\bar{q}_{kL}^T(\tilde{x}^\mu), \\
(\mathcal{CP})\,W^{\pm\mu}(x^\mu)\,(\mathcal{CP})^\dagger &= -e^{i\phi_W} W_\mu^\mp(\tilde{x}^\mu),
\end{aligned} \tag{2.61}$$

where C is the charge conjugation operator, $\tilde{x}^\mu \equiv (t, -\vec{x})$ and ϕ_j, ϕ_k and ϕ_W are arbitrary phases, one can show that (omitting the references to space-time coordinates)

$$\begin{aligned}
(\mathcal{CP})\,\mathscr{L}_{\text{CC}}^q\,(\mathcal{CP})^\dagger &= \sum_{j,k} (\mathcal{CP}) \left(\bar{u}_{jL} V_{jk} \not{W}^+ d_{kL} + \bar{d}_{kL} V_{jk}^* \not{W}^- u_{jL}\right) (\mathcal{CP})^\dagger \\
&= \sum_{j,k} \left(\bar{d}_{kL} V_{jk} \not{W}^- u_{jL} e^{-i(\phi_W+\phi_j-\phi_k)} + \bar{u}_{jL} V_{jk}^* \not{W}^+ d_{kL} e^{i(\phi_W+\phi_j-\phi_k)}\right),
\end{aligned} \tag{2.62}$$

so that CP can only be a symmetry of the theory if

$$V_{jk} = V_{jk}^* e^{i(\phi_W+\phi_j-\phi_k)}. \tag{2.63}$$

By making the choice $\phi_W = 0$, the condition (2.63) can be written in matricial form as

$$V_{\text{CKM}} = K_u V_{\text{CKM}}^* K_d^{-1}, \tag{2.64}$$

where $K_{u,d}$ are diagonal matrices containing the phases associated with the CP transformations of up-type and down-type quark fields. This condition can only be fulfilled if the mixing matrix can be written as [32]

$$V_{\text{CKM}} = K_u^{\frac{1}{2}} \mathcal{O} K_d^{-\frac{1}{2}}, \tag{2.65}$$

where $\mathcal{O} = \mathcal{O}^* = \left(\mathcal{O}^T\right)^{-1}$ is a real orthonormal matrix. From the parametrization presented in (2.46) and the discussion that precedes it, it is clear that the SM mixing matrix cannot in general take this form, as there exists a single physical phase that cannot be factorised to achieve a parametrization with a single real orthonormal matrix depending on all mixing angles. Therefore, for CP to be a symmetry of the SM Lagrangian, one must have $\delta = 0$, or from (2.60) one must have $J = 0$. However, this is not the

case, as this invariant has been measured to be [33]

$$J = (3.18 \pm 0.15) \times 10^{-5} \tag{2.66}$$

and CP is indeed violated in the quark sector.

To conclude, we introduce an alternative but no less useful parametrization of the SM mixing matrix, the Wolfenstein parametrization [35] where the mixings are expanded in terms of the parameter $\lambda \simeq |V_{us}|$:

$$V_{\text{Wolf}} = \begin{pmatrix} 1-\lambda^2/2 & \lambda & A\lambda^3(\rho - i\eta) \\ -\lambda & 1-\lambda^2/2 & A\lambda^2 \\ A\lambda^3(1-\rho-i\eta) & -A\lambda^2 & 1 \end{pmatrix} + O(\lambda^4) \tag{2.67}$$

By comparing (2.46) with (2.67) one can easily check that

$$s_{12} \simeq \lambda, \qquad s_{13} \sim \lambda^3, \qquad s_{23} \sim \lambda^2, \tag{2.68}$$

which are relations which will be important in the final chapters of this work.

In the next chapter we will explore the modifications to the EW sector in extensions with VLQs and will introduce one of the main topics of this thesis the CKM unitarity problem.

Chapter 3

Extensions with VLQ isosinglets and the CKM unitarity problem

One of the most exciting developments in the current search for the new physics beyond the SM, is the possibility of adding vector-like fermions (VLFs) to the SM. VLFs and in particular vector-like quarks (VLQs) constitute one of the simplest additions to the SM, which consists of quark fields where the LH and RH chiral components transform in the same manner under the SM gauge group, i.e. contrary to what happens with SM fermions they are not chiral.

These types of extensions are also motivated by the fact that experimental data [36, 37] excludes the existence of a fourth chiral fermion family and they even appear naturally in some grand unified theories (GUTs), models with extra dimensions and others. The introduction of VLQs may also provide a solution to other important issues, such as the unification of the coupling constants as in the case of SUSY [38–40]. Another strong motivation for the study of VLQs is the fact that they provide the simplest solution of the strong CP problem without axions, as suggested by Barr and Nelson [41, 42].

In this work we will restrict our focus on the study of extensions of the SM with isosinglet VLQs, i.e. VLQs whose RH and LH chiral components are weak isospin singlets. The addition of these particles to the theory has very interesting phenomenological implications, such as the introduction of new sources of CP violation and the violation of CKM unitarity.

Another important aspect is the current search of the LHC for new heavy fermions, such as quarks with masses beyond the top quark and all sorts of decays as e.g. $T \to d\, W^+$, where T is a new up-type VLQ, the heavy-top.

In this chapter we show how the loss of CKM unitarity, inherent to VLQ extensions, is compatible with recent results for unitarity deviations of the SM mixing matrix, which represents another strong motivation for considering this type of extensions. Moreover, we shall explore how the introduction of VLQ isosinglets affects the EW theory studied before, in particular we show how this unitarity violation leads to the weak neutral currents no longer being flavor-diagonal, allowing for new types of interactions.

3.1 The CKM Unitarity Problem (CKM-UP)

The charged currents are controlled by the CKM matrix, which in the case of the SM is strictly unitary. Therefore, detection of deviations of unitarity should constitute compelling evidence of the existence of New Physics (NP) beyond the Standard Model [18, 28, 30].

The SM predicts for the first row of the CKM matrix

$$|V_{ud}|^2 + |V_{us}|^2 + |V_{ub}|^2 = 1, \tag{3.1}$$

which considering that $|V_{ub}|^2 \simeq 1.6 \times 10^{-5}$ can, to good approximation, be written as

$$|V_{ud}|^2 + |V_{us}|^2 = 1. \tag{3.2}$$

Given the current level of experimental precision and control of theoretical uncertainties, which has allowed $|V_{ud}|$ and $|V_{us}|$ to be determined with considerable precision, (3.2) has become the most promising test of CKM unitarity. It consists essentially in testing the Cabbibo mixing, i.e.

$$|V_{us}| = \sin\theta_c, \quad |V_{ud}| = \cos\theta_c, \quad |V_{us}/V_{ud}| = \tan\theta_c, \tag{3.3}$$

where θ_c refers to the Cabibbo mixing angle.

At energies much smaller than M_W, these two CKM matrix entries will enter the effective charged current interaction (see Appendix B) in

$$\mathcal{L}_{\text{eff}} = -\frac{4G_F}{\sqrt{2}}\overline{u}_L\left(V_{ud}\gamma_\mu d_L + V_{us}\gamma_\mu s_L\right)\left(\overline{e}_L\gamma^\mu\nu_e + \overline{\mu}_L\gamma^\mu\nu_\mu\right), \tag{3.4}$$

which describes leptonic decays of hadrons involving the valence quarks u, d and s. In fact, $|V_{us}|$ is calculated from experimental data on kaon decays, whereas results regarding neutron decay are most relevant for $|V_{ud}|$. The ratio $|V_{us}/V_{ud}|$ can be independently determined by comparing radiative decay rates of certain pion and kaon decays.

Using improved values for the form factors and radiative corrections associated to these processes Belfatto, Beradze and Berezhiani [28] calculated very precise independent results for each of the three quantities in (3.3),

$$|V_{us}| = 0.22333(60), \quad |V_{ud}| = 0.97370(14), \quad |V_{us}/V_{ud}| = 0.23130(50). \tag{3.5}$$

These results deviate from the condition (3.2) by more than 4σ, disfavouring the CKM unitarity at a 99.998% CL. In fact, the values in (3.5) are much more compatible with

$$|V_{ud}|^2 + |V_{us}|^2 = 1 - \Delta^2, \tag{3.6}$$

where at a 95% confidence level, one has

$$\Delta = 0.04 \pm 0.01. \tag{3.7}$$

This discrepancy between the SM and experimental data constitutes the CKM unitarity problem, which resolution will necessitate the introduction of some NP that can accommodate these new results. These considerations are further supported by recent results from FLAG [18].

The expression (3.6) suggests the need for an extra mixing, for instance a V_{14} with $|V_{14}| = \Delta$ which in turn allows for a new unitarity condition

$$|V_{ud}|^2 + |V_{us}|^2 + |V_{ub}|^2 + |V_{14}|^2 = 1. \tag{3.8}$$

This can be achieved through the introduction of a new vector-like quark to the theory, which will in turn lead to a larger mixing matrix with the 3×3 CKM matrix containing the mixings of the standard quarks being a non-unitary submatrix.

3.2 Electroweak theory with $SU(2)$ isosinglet quarks

Consider now the general case of the introduction to the theory of n_u up-type VLQ isosinglets $U'_i = U'_{iL} + U'_{iR}$ and n_d down-type quark isosinglets $D'_i = D'_{iL} + D'_{iR}$. Each one of these will correspond in flavour space to a component of one of the following vectors

$$\boldsymbol{U'} = \begin{pmatrix} U'_1 \\ U'_2 \\ ... \\ U'_{n_u} \end{pmatrix}, \qquad \boldsymbol{D'} = \begin{pmatrix} D'_1 \\ D'_2 \\ ... \\ D'_{n_d} \end{pmatrix}. \tag{3.9}$$

In this type of extensions, the EW Lagrangian becomes

$$\mathscr{L}_{\text{EW}} = \mathscr{L}_{\text{EW}}^{\text{SM}} + \mathscr{L}_f^{\text{VLQ}} + \mathscr{L}_{\text{Yuk}}^{\text{VLQ}} + \mathscr{L}_b^{\text{VLQ}}, \tag{3.10}$$

where $\mathscr{L}_{\text{EW}}^{\text{SM}}$ now refers to (2.16) and

$$\mathscr{L}_f^{\text{VLQ}} = i\overline{\boldsymbol{U}}' \not{D} \boldsymbol{U'} + i\overline{\boldsymbol{D}}' \not{D} \boldsymbol{D'}, \tag{3.11}$$

includes the kinetic terms of the VLQs and describes their interactions with the gauge bosons. These interactions will be the focus of the next section. Note that, since these new fields are isosinglets, one has

$$\begin{aligned} D_\mu \boldsymbol{U'} &= \partial_\mu \boldsymbol{U'} - ig' B_\mu Q \boldsymbol{U'} = \partial_\mu \boldsymbol{U'} - \tfrac{2ig'}{3} B_\mu \boldsymbol{U'}, \\ D_\mu \boldsymbol{D'} &= \partial_\mu \boldsymbol{D'} - ig' B_\mu Q \boldsymbol{D'} = \partial_\mu \boldsymbol{D'} + \tfrac{ig'}{3} B_\mu \boldsymbol{D'}, \end{aligned} \tag{3.12}$$

for their EW covariant derivatives.

The next term in (3.10),

$$-\mathscr{L}_{\text{Yuk}}^{\text{VLQ}} = \overline{\boldsymbol{Q}}'_{\boldsymbol{L}} \Phi Y^D \boldsymbol{D}'_{\boldsymbol{R}} + \overline{\boldsymbol{Q}}'_{\boldsymbol{L}} \tilde{\Phi} Y^U \boldsymbol{U}'_{\boldsymbol{R}} + h.c, \tag{3.13}$$

describes the Yukawa interactions involving these VLQs. Note that, in flavour space, Y^D and Y^U are matrices of size $3 \times n_d$ and $3 \times n_u$, respectively. Their entries correspond to extra Yukawa couplings where, unless there exists some special mechanisms such as a symmetry, one expects that $Y_{ij}^{U,D} \sim 1$. Also, after SSB, one can write

$$\mathscr{L}_{\text{Yuk}}^{\text{VLQ}} = \mathscr{L}_m^{\text{VLQ}} + \mathscr{L}_h^{\text{VLQ}}, \tag{3.14}$$

where

$$-\mathscr{L}_m^{\text{VLQ}} = \overline{\boldsymbol{d}}'_{\boldsymbol{L}} \omega^d \boldsymbol{D}'_{\boldsymbol{R}} + \overline{\boldsymbol{u}}'_{\boldsymbol{L}} \omega^u \boldsymbol{U}'_{\boldsymbol{R}} + h.c, \tag{3.15}$$

contains the mass terms arising from the Higgs mechanism that involve the new VLQ fields and the matrices ω^u and ω^d, of sizes $3 \times n_u$ and $3 \times n_d$, are given by

$$\omega^{u,d} = \frac{v}{\sqrt{2}} Y^{U,D}. \tag{3.16}$$

This piece is analogous to (2.31), but now the RH VLQs take the role of the RH components of the SM quarks. The remaining piece in (3.14) describes the interactions of the Higgs field that involve the VLQs fields and is given by

$$-\mathscr{L}_h^{\text{VLQ}} = \overline{\boldsymbol{d}}'_{\boldsymbol{L}} Y^D \frac{h}{\sqrt{2}} \boldsymbol{D}'_{\boldsymbol{R}} + \overline{\boldsymbol{u}}'_{\boldsymbol{L}} Y^U \frac{h}{\sqrt{2}} \boldsymbol{U}'_{\boldsymbol{R}} + h.c, \tag{3.17}$$

being analogous to the SM piece in (2.33).

Finally, the last term in (3.10) arises as a direct consequence of having LH isosinglet fields and therefore has no analogous in the SM. This piece contains the following bare mass terms

$$-\mathscr{L}_b^{\text{VLQ}} = \overline{\boldsymbol{D}}'_{\boldsymbol{L}} X^d \boldsymbol{d}'_{\boldsymbol{R}} + \overline{\boldsymbol{U}}'_{\boldsymbol{L}} X^u \boldsymbol{u}'_{\boldsymbol{R}} + \overline{\boldsymbol{D}}'_{\boldsymbol{L}} M^d \boldsymbol{D}'_{\boldsymbol{R}} + \overline{\boldsymbol{U}}'_{\boldsymbol{L}} M^u \boldsymbol{U}'_{\boldsymbol{R}} + h.c, \tag{3.18}$$

which are not generated from the Higgs mechanism. Here, X^d and X^u are $n_d \times 3$ and $n_u \times 3$ flavour matrices, whereas M^d and M^u are $n_d \times n_d$ and $n_u \times n_u$, respectively.

3.2.1 The emergence of FCNCs at tree-level

From the Lagrangian describing the interactions of quarks with gauge bosons we derive the electromagnetic current involving all quarks, which from (3.11) and (3.12) now gets a contribution from the VLQs, modifying (2.39) to

$$J_{q,\text{em}}^{\mu} = \frac{2}{3}\left(\overline{\boldsymbol{u}}' \gamma^\mu \boldsymbol{u}' + \overline{\boldsymbol{U}}' \gamma^\mu \boldsymbol{U}'\right) - \frac{1}{3}\left(\overline{\boldsymbol{d}}' \gamma^\mu \boldsymbol{d}' + \overline{\boldsymbol{D}}' \gamma^\mu \boldsymbol{D}'\right). \tag{3.19}$$

This form motivates the introduction of the following vectors

$$\mathcal{U}' \equiv \begin{pmatrix} \boldsymbol{u'} \\ \boldsymbol{U'} \end{pmatrix}, \qquad \mathcal{D}' \equiv \begin{pmatrix} \boldsymbol{d'} \\ \boldsymbol{D'} \end{pmatrix}, \tag{3.20}$$

respectively of dimension $(3+n_u)$ and $(3+n_d)$, and for (3.21) we obtain

$$J^{\mu}_{q,\mathsf{em}} = \frac{2}{3}\overline{\mathcal{U}'}\gamma^{\mu}\mathcal{U}' - \frac{1}{3}\overline{\mathcal{D}}'\gamma^{\mu}\mathcal{D}', \tag{3.21}$$

analogous to the SM form in (2.39).

Considering the mass terms in (2.31) and (3.15) and the bare mass terms in (3.18), one may write all mass terms of the theory as

$$-\mathscr{L}^{q}_{M} = \overline{\mathcal{U}}'_{\boldsymbol{L}}\mathcal{M}^{u}\mathcal{U}'_{\boldsymbol{R}} + \overline{\mathcal{D}}'_{\boldsymbol{L}}\mathcal{M}^{d}\mathcal{D}'_{\boldsymbol{R}} + h.c, \tag{3.22}$$

where the two new quark mass matrices

$$\mathcal{M}^{u,d} = \begin{pmatrix} m^{u,d} & \omega^{u,d} \\ X^{u,d} & M^{u,d} \end{pmatrix}, \tag{3.23}$$

represented here in block form, are matrices of size $(3+n_u)\times(3+n_u)$ and $(3+n_d)\times(3+n_d)$, respectively.

One can relate the mass eigenstates with the fields in (3.20) through

$$\begin{aligned} \mathcal{U}'_{\boldsymbol{L,R}} = \mathcal{V}^{u}_{L,R}\mathcal{U}_{\boldsymbol{L,R}} \equiv \begin{pmatrix} A^{u}_{L,R} \\ B^{u}_{L,R} \end{pmatrix} \begin{pmatrix} \boldsymbol{u_{L,R}} \\ \boldsymbol{U_{L,R}} \end{pmatrix}, \\ \mathcal{D}'_{\boldsymbol{L,R}} = \mathcal{V}^{d}_{L,R}\mathcal{D}_{\boldsymbol{L,R}} \equiv \begin{pmatrix} A^{d}_{L,R} \\ B^{d}_{L,R} \end{pmatrix} \begin{pmatrix} \boldsymbol{d_{L,R}} \\ \boldsymbol{D_{L,R}} \end{pmatrix}, \end{aligned} \tag{3.24}$$

so that (3.22) is transformed into

$$-\mathscr{L}^{q}_{M} = \overline{\mathcal{U}}_{\boldsymbol{L}}\mathscr{D}^{u}\mathcal{U}_{\boldsymbol{R}} + \overline{\mathcal{D}}_{\boldsymbol{L}}\mathscr{D}^{d}\mathcal{D}_{\boldsymbol{R}} + h.c, \tag{3.25}$$

where the diagonal matrices $\mathscr{D}^{u,d}$, generically given by

$$\mathscr{D} = \mathcal{V}^{\dagger}_{L}\mathcal{M}\mathcal{V}_{R}, \tag{3.26}$$

contain the masses of all the $3+n_{u,d}$ quarks of each sector. The matrices $\mathcal{V}^{u}_{L,R}$ and $\mathcal{V}^{d}_{L,R}$ of size $(3+n_u)\times(3+n_u)$ and $(3+n_d)\times(3+n_d)$, respectively, are unitary in order to keep the kinetic terms of quarks invariant, i.e.

$$\begin{aligned} \mathscr{L}^{\mathsf{kin}}_{q} &= i\overline{\boldsymbol{u}}'\partial\!\!\!/\boldsymbol{u}' + i\overline{\boldsymbol{U}}'\partial\!\!\!/\boldsymbol{U}' + i\overline{\boldsymbol{d}}'\partial\!\!\!/\boldsymbol{d}' + i\overline{\boldsymbol{D}}'\partial\!\!\!/\boldsymbol{D}' \\ &= i\overline{\mathcal{U}}'\partial\!\!\!/\mathcal{U}' + i\overline{\mathcal{D}}'\partial\!\!\!/\mathcal{D}' = i\overline{\mathcal{U}}\partial\!\!\!/\mathcal{U} + i\overline{\mathcal{D}}\partial\!\!\!/\mathcal{D}. \end{aligned} \tag{3.27}$$

The blocks $A^{u,d}_{L,R}$ correspond to the first three rows of $\mathcal{V}^{u,d}_{L,R}$, whereas $B^{u,d}_{L,R}$ correspond to the last $n_{u,d}$ rows. These blocks are not unitary, in fact the unitarity of $\mathcal{V}^{u}_{L,R}$ and $\mathcal{V}^{d}_{L,R}$ leads to

$$\begin{aligned} \mathcal{V}^\dagger\mathcal{V} &= A^\dagger A + B^\dagger B = \mathbb{1}_{(3+n)}, \\ \mathcal{V}\mathcal{V}^\dagger &= \begin{pmatrix} AA^\dagger & AB^\dagger \\ BA^\dagger & BB^\dagger \end{pmatrix} = \begin{pmatrix} \mathbb{1}_3 & 0_{3\times n} \\ 0_{n\times 3} & \mathbb{1}_n \end{pmatrix}, \end{aligned} \tag{3.28}$$

where the indices u, d and L, R are omitted for simplicity.

Using these relations, the analogous to the CCs in (2.40) can be written in terms of the mass eigenstates as

$$\mathscr{L}^q_{\mathsf{CC}} = -\frac{g}{\sqrt{2}}\left(\overline{\boldsymbol{u}'}_L \not{W}^+ \boldsymbol{d'_L} + h.c.\right) = -\frac{g}{\sqrt{2}}\left(\overline{\mathcal{U}}_{\boldsymbol{L}} \not{W}^+ (A^{u\dagger}_L A^d_L)\mathcal{D}_{\boldsymbol{L}} + \overline{\mathcal{D}}_{\boldsymbol{L}} \not{W}^-_\mu (A^{d\dagger}_L A^u_L)\mathcal{U}_{\boldsymbol{L}}\right), \tag{3.29}$$

so that the new mixing matrix of this model with VLQs is now

$$\mathcal{V}_{\mathsf{CKM}} \equiv A^{u\dagger}_L A^d_L = \mathcal{V}^{u\dagger}_L K_0 \mathcal{V}^d_L, \qquad K_0 = \begin{pmatrix} \mathbb{1}_3 & 0_{3\times n_d} \\ 0_{n_u\times 3} & 0_{n_u\times n_d} \end{pmatrix}, \tag{3.30}$$

which is a $(3+n_u)\times(3+n_d)$ matrix and no longer unitary.

The electromagnetic current remains invariant, i.e.

$$J^\mu_{q,\mathsf{em}} = \frac{2}{3}\overline{\mathcal{U}}'\gamma^\mu\mathcal{U}' - \frac{1}{3}\overline{\mathcal{D}}'\gamma^\mu\mathcal{D}' = \frac{2}{3}\overline{\mathcal{U}}\gamma^\mu\mathcal{U} - \frac{1}{3}\overline{\mathcal{D}}\gamma^\mu\mathcal{D}, \tag{3.31}$$

and therefore, no new exotic process in QED involving VLQs and SM quarks are present. On the other hand, the neutral current Lagrangian in (2.38) gets modified to

$$\mathscr{L}^q_{\mathsf{NC}} = -eA_\mu J^\mu_{q,\mathsf{em}} - \frac{g}{2c_W}\left(\overline{\mathcal{U}}_{\boldsymbol{L}} \not{Z} (A^{u\dagger}_L A^u_L)\mathcal{U}_{\boldsymbol{L}} - \overline{\mathcal{D}}_{\boldsymbol{L}} \not{Z} (A^{d\dagger}_L A^d_L)\mathcal{D}_{\boldsymbol{L}} - 2s^2_W J^\mu_{q,\mathsf{em}} Z_\mu\right). \tag{3.32}$$

so that the weak NC are no longer diagonal in flavour space, but instead are in general controlled by non-diagonal and non-unitary matrices

$$\begin{aligned} F^u &= A^{u\dagger}_L A^u_L = A^{u\dagger}_L A^d_L A^{d\dagger}_L A^u_L = \mathcal{V}_{\mathsf{CKM}}\mathcal{V}^\dagger_{\mathsf{CKM}}, \\ F^d &= A^{d\dagger}_L A^d_L = A^{d\dagger}_L A^u_L A^{u\dagger}_L A^d_L = \mathcal{V}^\dagger_{\mathsf{CKM}}\mathcal{V}_{\mathsf{CKM}}. \end{aligned} \tag{3.33}$$

Collecting all these expressions, the full Lagrangian describing the interactions of gauge-bosons with all quarks in the EW sector can now be expressed as

$$\mathscr{L}^{\mathsf{int}}_q = -eA_\mu J^\mu - \frac{g}{2c_W}\left(\overline{\mathcal{U}}_{\boldsymbol{L}} \not{Z} F^u \mathcal{U}_{\boldsymbol{L}} - \overline{\mathcal{D}}_{\boldsymbol{L}} \not{Z} F^d \mathcal{D}_{\boldsymbol{L}} - 2s^2_W J^\mu_{em} Z_\mu\right) - \frac{g}{\sqrt{2}}\left(\overline{\mathcal{U}}_{\boldsymbol{L}} \not{W}^+ \mathcal{V}_{\mathsf{CKM}}\mathcal{D}_{\boldsymbol{L}} + h.c\right). \tag{3.34}$$

Note that since $\mathcal{V}_{\mathsf{CKM}}$ is now a larger matrix with extra mixings, new vertices involving the W-boson are

introduced in the theory. However, the quintessential implication of introducing VLQs is the emergence of flavour changing neutral currents (FCNCs) at tree-level.

In the SM, processes involving FCNCs are allowed but only at loop-level and are highly suppressed by the entries of the CKM matrix and the GIM mechanism. In extensions with VLQs, the FCNCs mediated by the Z-boson are now controlled by the non-diagonal matrices $F^{u,d}$, so that, for example, the coupling of the up and charm quarks to the Z-boson will be non-vanishing, which means that a vertex such as the one in figure 3.1 is now allowed.

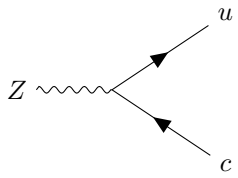

Figure 3.1: One of the new vertices associated to the Z-mediated FCNCs that emerge in extensions with VLQs.

Tree-level FCNCs can also arise in interactions of quarks with the Higgs field. Using (2.33) and (3.17), one has

$$-\mathscr{L}_h^q = \overline{\boldsymbol{u}}'_{\boldsymbol{L}} \frac{h}{\sqrt{2}} \mathcal{Y}^u \mathcal{U}'_{\boldsymbol{R}} + \overline{\boldsymbol{d}}'_{\boldsymbol{L}} \frac{h}{\sqrt{2}} \mathcal{Y}^d \mathcal{D}'_{\boldsymbol{R}} + h.c, \tag{3.35}$$

where we have defined the matrix $\mathcal{Y}^{u,d} \equiv \left(Y^{u,d},\ Y^{U,D}\right)$. In terms of the mass eigenstates, one has

$$-\mathscr{L}_h^q = \overline{\mathcal{U}}_{\boldsymbol{L}} \frac{h}{\sqrt{2}} \left(A_L^{u\dagger} \mathcal{Y}^u \mathcal{V}_R^u\right) \mathcal{U}_{\boldsymbol{R}} + \overline{\mathcal{D}}_{\boldsymbol{L}} \frac{h}{\sqrt{2}} \left(A_L^{d\dagger} \mathcal{Y}^d \mathcal{V}_R^d\right) \mathcal{D}_{\boldsymbol{R}} + h.c, \tag{3.36}$$

so that these couplings are no longer flavour diagonal. In fact, from the diagonalisation of the mass matrix for each sector, one has

$$\mathcal{M} = \begin{pmatrix} \frac{v}{\sqrt{2}} \mathcal{Y} \\ \mathcal{B} \end{pmatrix} = \mathcal{V}_L \mathscr{D} \mathcal{V}_R^\dagger = \begin{pmatrix} A_L \\ B_L \end{pmatrix} \mathscr{D} \mathcal{V}_R^\dagger \implies \mathcal{Y} = \frac{\sqrt{2}}{v} A_L \mathscr{D} \mathcal{V}_R^\dagger \tag{3.37}$$

where $\mathcal{B}^{u,d} \equiv \left(X^{u,d},\ M^{u,d}\right)$ contains the couplings coming from bare mass terms. Thus,

$$-\mathscr{L}_h^q = \overline{\mathcal{U}}_{\boldsymbol{L}} \frac{h}{v} F^u \mathscr{D}^u \mathcal{U}_{\boldsymbol{R}} + \overline{\mathcal{D}}_{\boldsymbol{L}} \frac{h}{v} F^d \mathscr{D}^d \mathcal{D}_{\boldsymbol{R}} + h.c, \tag{3.38}$$

leading to manifestly non-diagonal couplings and, therefore, to the emergence of Higgs-meadiated FCNCs, which similarly to Z-boson mediated FCNCs, are controlled by $F^{u,d}$. This means that e.g. the vertex in figure 3.2 is now allowed.

The emergence of these FCNCs leads to new very important phenomenological effects, which will be studied in detail in chapter 4.

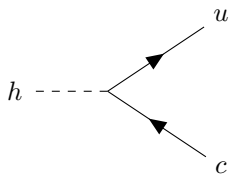

Figure 3.2: One of the new vertices associated to the Higgs-mediated FCNCs that emerge in extensions with VLQs.

3.2.2 New Mass Scale and Suppression of the FCNCs

As mentioned before, processes involving FCNCs in the SM are extremely suppressed. In this regard, the tree-level FCNCs generated in extensions with VLQs could potentially pose problems. We show here that this is not necessarily the case, provided that these new VLQs have masses considerably larger than the EW scale.

To illustrate this statement, consider for each sector the relation

$$\mathcal{H} \equiv \mathcal{M}\mathcal{M}^\dagger = \mathcal{V}_L \mathscr{D}^2 \mathcal{V}_L^\dagger, \tag{3.39}$$

coming from (3.26), as well as

$$\mathcal{V}_L = \begin{pmatrix} K & R \\ S & T \end{pmatrix}, \qquad \mathscr{D} = \begin{pmatrix} d_0 & 0 \\ 0 & D_0 \end{pmatrix}, \tag{3.40}$$

where d_0 and D_0 are the diagonal matrices containing the masses of the SM quarks and VLQs, respectively, K is a 3×3 matrix while T is $n \times n$ and R and S^T are $3 \times n$ matrices. Now, by using (3.23), the relation in (3.39) can be expressed as

$$\begin{gathered} (mm^\dagger + \omega\omega^\dagger)K + (mX^\dagger + \omega M^\dagger)S = Kd_0^2, \\ (mm^\dagger + \omega\omega^\dagger)R + (mX^\dagger + \omega M^\dagger)T = RD_0^2, \\ (Xm^\dagger + M\omega^\dagger)K + (XX^\dagger + MM^\dagger)S = Sd_0^2, \\ (Xm^\dagger + M\omega^\dagger)R + (XX^\dagger + MM^\dagger)T = TD_0^2. \end{gathered} \tag{3.41}$$

Assuming a new mass scale $v' \gg v$ for the VLQs, to which the entries of M, X and D_0 are proportional to, and given that the entries of the unitary matrices $\mathcal{V}_L^{u,d}$ are of order 1, one has from the second relation of (3.41)

$$R \approx \frac{(mX^\dagger + \omega M^\dagger)T}{D_0^2} \sim \frac{v}{v'} \ll 1. \tag{3.42}$$

Similarly, from the third relation of (3.41) one has

$$S \approx \left(XX^\dagger + MM^\dagger\right)^{-1}(Xm^\dagger + M\omega^\dagger)K \sim \frac{v}{v'} \ll 1, \tag{3.43}$$

so that for large v' the entries of R and S are naturally suppressed. Inserting (3.43) in the first relation of (3.41) one obtains

$$mm^\dagger + \omega\omega^\dagger + (mX^\dagger + \omega M^\dagger)\left(XX^\dagger + MM^\dagger\right)^{-1}(Xm^\dagger + M\omega^\dagger) \approx Kd_0^2K^{-1}, \tag{3.44}$$

The LHS of (3.44) can be interpreted as the effective 3×3 matrix of the lightest quarks

$$H_{\text{eff}} \equiv mm^\dagger + \omega\omega^\dagger + (mX^\dagger + \omega M^\dagger)\left(XX^\dagger + MM^\dagger\right)^{-1}(Xm^\dagger + M\omega^\dagger), \tag{3.45}$$

which, analogous to H in the SM, contains essentially all information about the mixing and masses of three standard generations of quarks. From the unitarity of $\mathcal{V}_L$ one also has

$$K^\dagger K = \mathbb{1}_3 - S^\dagger S, \qquad KK^\dagger = \mathbb{1}_3 - RR^\dagger, \tag{3.46}$$

which coupled with (3.42) and (3.43), shows that K is indeed a unitary matrix in approximation, for $v' \gg v$.

Using (3.30) and (3.40) one finds

$$\mathcal{V}_{\text{CKM}} = \begin{pmatrix} K_u^\dagger K_d & K_u^\dagger R_d \\ R_u^\dagger K_d & R_u^\dagger R_d \end{pmatrix}, \tag{3.47}$$

so that the 3×3 upper-left block now plays the role of the mixing matrix of the three lightest generations. From (3.42) it is clear that the entries outside this block are naturally suppressed, so that the CC mixings of VLQ with each other and with SM quarks may be expected to be small.

From (3.47) and using (3.33) and (3.46), the matrices controlling the FCNCs can be expressed as

$$F = \begin{pmatrix} K^\dagger K & K^\dagger R \\ R^\dagger K & R^\dagger R \end{pmatrix} = \begin{pmatrix} \mathbb{1}_3 - S^\dagger S & K^\dagger R \\ R^\dagger K & R^\dagger R \end{pmatrix}, \tag{3.48}$$

so that the FCNCs involving the SM quarks are in principle suppressed by the ratio $(v/v')^2$. The remaining entries of $F^{u,d}$ will also be small for large v' and therefore the effects of FCNCs involving directly the new VLQs may be suppressed too. Thus, sufficiently suppressed tree-level FCNCs may be achieved in extension with VLQs, provided that their masses are large. Note that, currently, the minimal bound for the mass of an isosinglet quark is already of the order of around the TeV, a couple times larger than the EW scale.

3.3 Solving the CKM unitarity problem with an up-type VLQ isosinglet

As mentioned before the introduction of VLQs to the SM may be able to solve the CKM-UP. In principle, one could introduce any number of VLQs to the two quark sectors, but as we show here, the introduction of a single VLQ is already very promising.

The introduction of a down-type isosinglet, a heavy-bottom B, will result in a 3×4 mixing matrix

$$\mathcal{V}_{\text{CKM}} = \begin{pmatrix} V_{ud} & V_{us} & V_{ub} & V_{uB} \\ V_{cd} & V_{cs} & V_{cb} & V_{cB} \\ V_{td} & V_{ts} & V_{tb} & V_{tB} \end{pmatrix}, \tag{3.49}$$

and the unitarity problem found for the first row of the CKM matrix in the SM, as stated in (3.6), can be solved by simply having $|V_{uB}| = \Delta$.

If instead one exclusively introduces an up-type isosinglet, a heavy-top T, to the theory then the new mixing matrix will be a 4×3 matrix of the form

$$\mathcal{V}_{\text{CKM}} = \begin{pmatrix} V_{ud} & V_{us} & V_{ub} \\ V_{cd} & V_{cs} & V_{cb} \\ V_{td} & V_{ts} & V_{tb} \\ V_{Td} & V_{Ts} & V_{Tb} \end{pmatrix}, \tag{3.50}$$

with three orthonormal columns but no longer orthonormal rows. Thus, the first row of CKM no longer respects the unitary condition, but (3.6) can still be verified for the first row of

$$\mathcal{V}^{u\dagger} = \begin{pmatrix} V_{ud} & V_{us} & V_{ub} & V_{14} \\ V_{cd} & V_{cs} & V_{cb} & V_{24} \\ V_{td} & V_{ts} & V_{tb} & V_{34} \\ V_{Td} & V_{Ts} & V_{Tb} & V_{44} \end{pmatrix}, \tag{3.51}$$

the unitarity matrix which diagonalises $\mathcal{H}^u = \mathcal{M}^u \mathcal{M}^{u\dagger}$ in the WB where the 3×3 down sector mass matrix is diagonal, and which, from (3.30), relates to $\mathcal{V}_{\text{CKM}}$. More concretely one has

$$\mathcal{V}_{\text{CKM}} = \mathcal{V}_L^{u\dagger} K_0 V_L^d = \mathcal{V}_L^{u\dagger} \tilde{\mathcal{V}}_L^d K_0 \equiv \mathcal{V}^{u\dagger} K_0, \qquad K_0^T = \begin{pmatrix} 1 & 0 & 0 & 0 \\ 0 & 1 & 0 & 0 \\ 0 & 0 & 1 & 0 \end{pmatrix}, \tag{3.52}$$

where V_L^d is a general 3×3 transformation that relates the LH flavor states with the LH mass eigenstates, whereas

$$\tilde{\mathcal{V}}_L^d = \begin{pmatrix} & & & 0 \\ & V_L^d & & 0 \\ & & & 0 \\ 0 & 0 & 0 & 1 \end{pmatrix}. \tag{3.53}$$

The CKM unitarity problem may then be solved by having $|V_{14}| = \Delta$.

Thus, a minimal solution to the CKM problem may be achieved with the introduction of either a heavy-top or a heavy-bottom to the SM. A solution with a heavy-bottom, however, will run into other difficulties. To understand this, consider, an extension with only a heavy-bottom. The matrix which diagonalises $\mathcal{H}_d = \mathcal{M}_d \mathcal{M}_d^\dagger$ in the WB where the 3×3 mass matrix of the up sector is diagonal is

$$\mathcal{V}^d = \begin{pmatrix} V_{ud} & V_{us} & V_{ub} & V_{uB} \\ V_{cd} & V_{cs} & V_{cb} & V_{cB} \\ V_{td} & V_{ts} & V_{tb} & V_{tB} \\ V_{41} & V_{42} & V_{43} & V_{44} \end{pmatrix}, \tag{3.54}$$

where analogously to (3.52), one has

$$\mathcal{V}_{\text{CKM}} = V_L^{u\dagger} K_0 \mathcal{V}_L^d = K_0 \tilde{\mathcal{V}}_L^{u\dagger} \mathcal{V}_L^d \equiv K_0 \mathcal{V}^d, \qquad K_0 = \begin{pmatrix} 1 & 0 & 0 & 0 \\ 0 & 1 & 0 & 0 \\ 0 & 0 & 1 & 0 \end{pmatrix}, \tag{3.55}$$

so that the down-sector mass matrix in a suitable basis may be given by

$$\mathcal{M}^d = \mathcal{V}^d \mathscr{D} = \begin{pmatrix} m_d V_{ud} & m_s V_{us} & m_b V_{ub} & m_B V_{uB} \\ m_d V_{cd} & m_s V_{cs} & m_b V_{cb} & m_B V_{cB} \\ m_d V_{td} & m_s V_{ts} & m_b V_{tb} & m_B V_{tB} \\ m_d V_{41} & m_s V_{42} & m_b V_{43} & m_B V_{44} \end{pmatrix}. \tag{3.56}$$

Hence, in this WB one has $|\mathcal{M}^d_{14}| = m_B |V_{uB}|$, which for a heavy-bottom of mass $m_B \sim 1$ TeV yields $|\mathcal{M}^d_{14}| \sim 40$ GeV for $|V_{uB}| \approx 0.04$. However, one should recall that all the entries in the first three rows originate from the Higgs mechanism and are all proportional to the EW scale and Yukawa couplings of the same order. Therefore, having $|\mathcal{M}^d_{14}|$ much larger than $|\mathcal{M}^d_{33}| \simeq m_b$, where $m_b(m_b) \simeq 4.18$ GeV [33], seems somewhat unnatural.

The same is not the case if instead a heavy-top with $m_T \sim 1$ TeV is added to the SM, because in this case one has

$$\mathcal{M}^u = \mathcal{V}^u \mathscr{D} = \begin{pmatrix} m_u V_{ud}^* & m_c V_{cd}^* & m_t V_{td}^* & m_T V_{Td}^* \\ m_u V_{us}^* & m_c V_{cs}^* & m_t V_{ts}^* & m_T V_{Ts}^* \\ m_u V_{ub}^* & m_c V_{cb}^* & m_t V_{tb}^* & m_T V_{Tb}^* \\ m_u V_{14}^* & m_c V_{24}^* & m_t V_{34}^* & m_T V_{44}^* \end{pmatrix}, \tag{3.57}$$

with $|\mathcal{M}^u_{33}| \simeq m_t \simeq 172.9$ GeV and even with $m_T \sim 4$ TeV one can still have $|\mathcal{M}^u_{33}| \gtrsim |\mathcal{M}^u_{14}|$ TeV[1]. Therefore, an extension with a heavy-top is a much more natural way of solving the CKM-UP and this will be the focus of the next chapters. We also point to the results of [30] where it is shown that the possibility of having only an heavy-bottom to added the SM is close to being excluded.

In the next chapter, we will be focused on studying the phenomenological implications of adding an heavy-top to the SM on processes such as neutral mixings or kaon decays.

[1] This is assuming $|V_{Td}| \sim |V_{14}|$ which is typically the case.

Chapter 4

Phenomenological effects of mixing with a heavy-top

In the previous chapter we showed that a minimal extension of the SM with an up-type VLQ isosinglet may constitute an elegant way of solving the CKM-UP. However, it was also demonstrated that, in general, extensions with VLQ isosinglets generate new interactions associated with FCNCs. In principle, these interactions can introduce new contributions to processes such as neutral meson mixings or rare meson decays, and which are constrained by current experimental data.

In this chapter we will study in detail the NP contributions to some of these processes that arise when a heavy-top is added to the SM and explore some of the constraints that are currently imposed by experimental results on the most relevant quantities associated with such processes. We will be particularly interested in studying neutral meson mixings and kaon decays, which typically impose important constraints on these types of extensions. At the end we shall quickly look at the possible decay channels of the new heavy-top.

One point that is very important to keep in mind is that in this particular case there are only FCNCs involving up-type quarks. Here, $\mathcal{V}_{\text{CKM}}$ will be a non-unitary 4×3 matrix (see (3.50)) and the matrices controlling the FCNCs are

$$\begin{aligned} F^u &= \mathcal{V}_{\text{CKM}}\mathcal{V}_{\text{CKM}}^\dagger = \mathcal{V}_L^{u\dagger} K_0 K_0^T \mathcal{V}_L^u, \\ F^d &= \mathcal{V}_{\text{CKM}}^\dagger \mathcal{V}_{\text{CKM}} = V_L^{d\dagger} V_L^d = \mathbb{1}_3, \end{aligned} \tag{4.1}$$

where

$$K_0^T = \begin{pmatrix} 1 & 0 & 0 & 0 \\ 0 & 1 & 0 & 0 \\ 0 & 0 & 1 & 0 \end{pmatrix}, \tag{4.2}$$

and V_L^d and $\mathcal{V}_L^u$ are, respectively, the 3×3 and 4×4 unitary matrices that diagonalize $H_d = m_d m_d^\dagger$ and $\mathcal{H}_u = \mathcal{M}_u \mathcal{M}_u^\dagger$.

Furthermore, throughout this chapter we will focus specifically on parametrization of $\mathcal{V}_{\text{CKM}}$ where the quantity

$$\lambda_u^K \equiv V_{us}^* V_{ud}, \tag{4.3}$$

is real. This is because with this choice, the expression for several of the most important quantities become easier to calculate than in the general case.

4.1 $K^0 - \overline{K}^0$ mixing

As stated above, the sole introduction of an up-type VLQ will lead to the emergence of FCNCs exclusively in the up-quark sector, which in turn will generate different types of NP contributions depending on the meson system. In this and the following subsection the mixing of neutral mesons $N^0 - \overline{N}^0$ composed by down-type valence quarks, $N = K, B_{d,s}$, is explored.

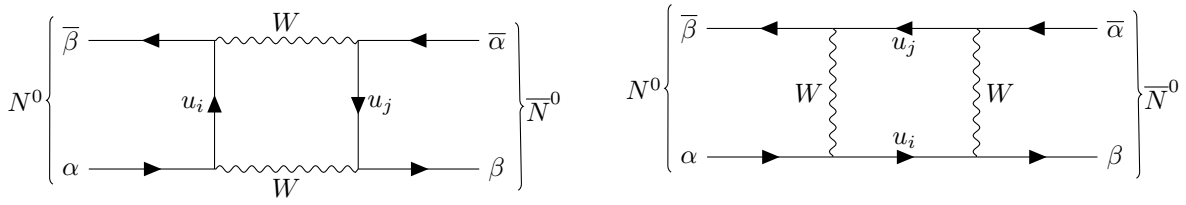

Figure 4.1: Leading contributions to $K^0 - \overline{K}^0$ and $B_{d,s}^0 - \overline{B}_{d,s}^0$ mixing, $u_{i,j} = u, c, t$.

In the SM these processes have box diagram as their leading order contributions. These are represented in figure 4.1 and in the limit of vanishing external quark masses are described by the effective Lagrangian [30, 31, 43]

$$\mathscr{L}_{\text{eff}}^N = -\frac{G_F^2 M_W^2}{4\pi^2} \sum_{i,j=u,c,t} \lambda_i^N \lambda_j^N S_0(x_i, x_j)(\overline{\beta}_L \gamma^\mu \alpha_L)(\overline{\beta}_L \gamma_\mu \alpha_L), \tag{4.4}$$

where α and β are the valence quarks that define the neutral meson N^0 and λ_i^N are CKM factors defined as

$$\lambda_i^N \equiv V_{i\beta}^* V_{i\alpha}. \tag{4.5}$$

Here we have introduced the gauge-invariant Inami-Lim (IL) box functions $S_0(x_i, x_j)$ with $x_i \equiv (m_i/M_W)^2$ (see Appendix A). The IL functions [44] encapsulate the complicated dependence of a process involving loops on the internal quark masses. The physical constants G_F and M_W are the Fermi constant and the mass of the W-boson, respectively.

With an extra particle, i.e. the heavy-top T, (4.4) is modified into

$$\mathscr{L}_{\text{eff}}^N = -\frac{G_F^2 M_W^2}{4\pi^2} \sum_{i,j=c,t,T} \lambda_i^N \lambda_j^N S_0(x_i, x_j)(\overline{\beta}_L \gamma^\mu \alpha_L)(\overline{\beta}_L \gamma_\mu \alpha_L) + h.c., \tag{4.6}$$

which corresponds to a very simple generalisation of the SM piece with the VLQ, now also allowed to run inside the loops in figure 4.1. Note that all contributions associated with the up quark were discarded which can be justified by the fact that $x_u \simeq 0$ to a very good approximation and that, by exploiting the orthonormality of the first two columns of the mixing matrix, one has

$$\lambda_u^N + \lambda_c^N + \lambda_t^N + \lambda_T^N = 0, \tag{4.7}$$

and thus, by writing it in terms of the three remaining factors, the factor λ_u^N can be eliminated.

For the moment we will focus on the neutral kaon mixing. Two relevant quantities associated with this neutral meson system are the mass difference $\Delta m_K = m_{K_L} - m_{K_S}$ and the CP violation parameter ε_K. Both of these are related to M_{12}^K, the off-diagonal element of the neutral kaon matrix, which can be computed from

$$M_{12}^K = -\frac{1}{2m_K} \langle K^0 | \, \mathscr{L}_{\text{eff}}^K \, | \overline{K}^0 \rangle \, . \tag{4.8}$$

Following [31, 45], using the vacuum-insertion approximation (VIA) and the phase choice $\mathcal{CP} \, |K^0\rangle = - |\overline{K}^0\rangle$, one has

$$\langle K^0 | \, (\bar{s}_L \gamma^\mu d_L)(\bar{s}_L \gamma_\mu d_L) \, | \overline{K}^0 \rangle = \frac{2}{3} f_K^2 m_K^2, \tag{4.9}$$

where m_K is the mass of the kaon and f_K is its decay constant. In the end, if QCD corrections are included one obtains

$$M_{12}^K = \frac{G_F^2 M_W^2}{12\pi^2} f_K^2 m_K B_K \mathcal{S}_K, \tag{4.10}$$

where B_K is the bag parameter which is a factor estimated from lattice QCD calculations and that accounts for QCD corrections to the VIA, whereas

$$\mathcal{S}_K = \sum_{i,j=c,t,T} \eta_{ij}^K \lambda_i^K \lambda_j^K S_0(x_i, x_j), \tag{4.11}$$

contains the dependence on the mixing and internal quark masses, but where now other QCD correction factors η_{ij}^K of $\mathcal{O}(1)$ are also included. These quantities account for high energy QCD effects and renormalisation group (RG) evolution to lower scales. Note that this form is valid for scales below the charm threshold $\mu_c = \mathcal{O}(m_c)$ [46].

It should be stressed that (4.10) corresponds exclusively to the short-distance (SD) contribution to $K^0 - \overline{K}^0$ associated with the leading box diagram contributions in 4.1 and which can be computed using perturbative QCD. Here, we have overlooked the long-distance (LD) contributions which are harder to compute as they correspond to having intermediate meson states in the $K^0 - \overline{K}^0$ transition instead of up-type quarks and the W bosons and cannot be computed perturbatively.

With this in mind, the mass difference can now be written as

$$\Delta m_K \simeq 2|M_{12}^K| + (\Delta m_K)_{\mathsf{LD}}, \tag{4.12}$$

where $(\Delta m_K)_{\mathsf{LD}}$ refers to the long-distance contributions which are expected to significantly affect the value of Δm_K. Presently, we only have a formula for the short-distance piece for this observable,

$$(\Delta m_K)_{\mathsf{SD}} \simeq 2\left|M_{12}^K\right| = \frac{G_F^2 M_W^2 m_K f_K^2 B_K \left|\mathcal{S}_K\right|}{6\pi^2}. \tag{4.13}$$

On the other hand, the parameter ε_K which quantifies indirect CP violation in the $K_L \to \pi\pi$ decay, is dominated by the short-distance piece and can be related to M_{12}^K through [47]

$$|\varepsilon_K| \simeq \frac{\kappa_\varepsilon}{\sqrt{2}\Delta m_K} |\mathsf{Im}\left(M_{12}^K\right)|, \tag{4.14}$$

for the adopted parametrization where λ_u^K is real. Given the difficulty of computing $(\Delta m_K)_{\mathsf{LD}}$, we shall use the experimental value of Δm_K, $\Delta m_K^{\mathsf{exp}} = (3.484 \pm 0.006) \times 10^{-12}$ MeV [33], in the numerical calculations of ε_K.

Expressions for the NP contributions to $(\Delta m_K)_{\mathsf{SD}}$ and ε_K can now be obtained by writing the sum (4.11) as

$$\mathcal{S}_K = \mathcal{S}_K^{\mathsf{SM}} + \mathcal{S}_K^{\mathsf{NP}}, \tag{4.15}$$

where

$$\begin{aligned} \mathcal{S}_K^{\mathsf{SM}} &= \eta_{cc}^K \left(\lambda_c^K\right)^2 S_0(x_c) + 2\eta_{ct}^K \lambda_c^K \lambda_t^K S_0(x_c, x_t) + \eta_{tt}^K \left(\lambda_t^K\right)^2 S_0(x_t), \\ \mathcal{S}_K^{\mathsf{NP}} &= 2\eta_{cT}^K \lambda_c^K \lambda_T^K S_0(x_c, x_T) + 2\eta_{tT}^K \lambda_c^K \lambda_T^K S_0(x_t, x_T) + \eta_{TT}^K \left(\lambda_T^K\right)^2 S_0(x_T), \end{aligned} \tag{4.16}$$

leading to[1]

$$\left(\Delta m_K^{\mathsf{NP}}\right)_{\mathsf{SD}} \approx \frac{G_F^2 M_W^2 m_K f_K^2 B_K \left|\mathcal{S}_K^{\mathsf{NP}}\right|}{6\pi^2}, \tag{4.17}$$

$$|\varepsilon_K^{\mathsf{NP}}| = \frac{G_F^2 M_W^2 m_K f_K^2 B_K \kappa_\varepsilon}{12\sqrt{2}\pi^2 \Delta m_K} |\mathsf{Im}\left(\mathcal{S}_K^{\mathsf{NP}}\right)|. \tag{4.18}$$

These expressions can be used to constraint our model with a heavy-top. To consider such a model safe with regard to the neutral kaon system we establish the following criteria

$$\left(\Delta m_K^{\mathsf{NP}}\right)_{\mathsf{SD}} \lesssim \Delta m_K^{\mathsf{exp}} = (3.484 \pm 0.006) \times 10^{-12}\ \mathsf{MeV}, \tag{4.19}$$

$$|\varepsilon_K^{\mathsf{NP}}| \lesssim \delta\varepsilon_K \equiv 2.48 \times 10^{-4}, \tag{4.20}$$

where we will use $\delta\varepsilon_K$ to refer to the upper-bound for $|\varepsilon_K^{\mathsf{NP}}|$.

[1] Given that $|\mathcal{S}_K^{\mathsf{SM}} + \mathcal{S}_K^{\mathsf{NP}}| \leq |\mathcal{S}_K^{\mathsf{SM}}| + |\mathcal{S}_K^{\mathsf{NP}}|$, (4.17) represents an approximate upper bound for $\left(\Delta m_K^{\mathsf{NP}}\right)_{\mathsf{SD}}$, not an exact formula.

For $\left(\Delta m_K^{\text{NP}}\right)_{\text{SD}}$ we require simply that it is lower than the experimental value, given the theoretical uncertainty still associated with the SM prediction and its LD piece. Henceforth, we will drop the SD label so that, unless mentioned explicitly, Δm_K and Δm_K^{NP} will refer to short-distance contributions.

On the other hand, the condition for $|\varepsilon_K^{\text{NP}}|$ is much more stringent. This strongly contrasts with the typical constraint utilised in these types of models [29, 30],

$$|\varepsilon_K^{\text{NP}}| \lesssim |\varepsilon_K^{\text{exp}}|. \tag{4.21}$$

To establish this new upper-bound, we make use of the experimental value $|\varepsilon_K^{\text{exp}}| = (2.228 \pm 0.011) \times 10^{-3}$ [33] and the SM prediction $|\varepsilon_K^{\text{SM}}| = (2.16 \pm 0.18) \times 10^{-3}$. This SM prediction, presented in a recent paper by Brod, Gorbahn and Stamou [48] is obtained by circumventing the large uncertainties associated to the charm-quark contribution and is very similar to the experimental value[2]. Therefore, we no longer find it reasonable to maintain (4.21), which now appears to be a too permissible upper-bound, and adopt (4.20) instead.

We now briefly explain the reasoning behind this upper-bound: the NP contribution in a model like this should verify

$$\left|\varepsilon_K^{\text{NP}}\right| \leq \left|\varepsilon_K^{\text{exp}} - \varepsilon_K^{\text{SM}}\right|, \tag{4.22}$$

but since

$$\left|\varepsilon_K^{\text{exp}} - \varepsilon_K^{\text{SM}}\right| \geq \left|\varepsilon_K^{\text{exp}}\right| - \left|\varepsilon_K^{\text{SM}}\right|, \tag{4.23}$$

we choose to set the conservative constraint

$$\left|\varepsilon_K^{\text{NP}}\right| \lesssim \left|\varepsilon_K^{\text{exp}}\right| - \left|\varepsilon_K^{\text{SM}}\right|, \tag{4.24}$$

where at 1σ one expects

$$\left|\varepsilon_K^{\text{exp}}\right| - \left|\varepsilon_K^{\text{SM}}\right| \lesssim [2.228 - 2.16 + 0.18] \times 10^{-3} = 2.48 \times 10^{-4} \equiv \delta\varepsilon_K. \tag{4.25}$$

From (4.24) and (4.25) one obtains the condition (4.20). Therefore, as a consequence of now having $\left|\varepsilon_K^{\text{SM}}\right| \approx \left|\varepsilon_K^{\text{exp}}\right|$, this upper-bound for $\left|\varepsilon_K^{\text{exp}}\right|$ is quite small, being only around 10% of the experimental value. This is a very important result that should now set new and much more stringent conditions to this type of extensions. This condition will also play an important role in the following chapters.

4.2 $B_{d,s}^0 - \overline{B}_{d,s}^0$ mixings

Similar considerations as in the K^0 system apply to the B_q^0 systems ($q = d, s$), but in this case given that $\lambda_c^{B_q} \sim \lambda_t^{B_q}$ and

[2]Note that, although this prediction is obtained in the context of manifest CKM unitarity, this result is still relevant to our work, given that we assume small unitarity deviations.

$$S_0(x_c), S_0(x_c, x_t) \ll S_0(x_t), \tag{4.26}$$

one obtains the simpler expression

$$\mathcal{S}_{B_q}^{\mathsf{SM}} = \eta_{tt}^{B_q} \left(\lambda_t^{B_q}\right)^2 S_0(x_t). \tag{4.27}$$

A similar simplification can also be made for $\mathcal{S}_{B_q}^{\mathsf{NP}}$ by using

$$S_0(x_c, x_T) \ll S_0(x_t, x_T), S_0(x_T), \tag{4.28}$$

so that

$$\mathcal{S}_{B_q}^{\mathsf{NP}} = 2\eta_{tT}^{B_q} \lambda_t^{B_q} \lambda_T^{B_q} S_0(x_t, x_T) + \eta_{TT}^{B_q} \left(\lambda_T^{B_q}\right)^2 S_0(x_T). \tag{4.29}$$

In the end, in a similar fashion as before in the kaon system, one has

$$\Delta m_{B_q}^{\mathsf{SM}} \approx \frac{G_F^2 M_W^2 m_{B_q} f_{B_q}^2 B_{B_q} \left|\mathcal{S}_{B_q}^{\mathsf{SM}}\right|}{6\pi^2}, \tag{4.30}$$

$$\Delta m_{B_q}^{\mathsf{NP}} \approx \frac{G_F^2 M_W^2 m_{B_q} f_{B_q}^2 B_{B_q} \left|\mathcal{S}_{B_q}^{\mathsf{NP}}\right|}{6\pi^2}, \tag{4.31}$$

but now the references to the short-distance contributions are dropped because these dominate the experimental values of Δm_{B_q} completely, while the long-distance contributions are negligible [31]. In fact, using the current PDG best-fit values for the moduli of the CKM matrix without imposing unitarity [33], i.e. using

$$\begin{aligned} |V_{td}| &\simeq (8.0 \pm 0.3) \times 10^{-3}, \\ |V_{ts}| &\simeq (38.8 \pm 1.1) \times 10^{-3}, \\ |V_{tb}| &\simeq 1.013 \pm 0.030, \end{aligned} \tag{4.32}$$

one can roughly estimate

$$\begin{aligned} \Delta m_{B_d}^{\mathsf{SM}} &\approx (3.06 \pm 0.29) \times 10^{-10}\ \mathsf{MeV}, \\ \Delta m_{B_s}^{\mathsf{SM}} &\approx (1.07 \pm 0.09) \times 10^{-8}\ \mathsf{MeV}, \end{aligned} \tag{4.33}$$

by using (4.27) and (4.30). These estimates show how the short-distance SM predictions essentially saturate the experimental values (see table A.1 in Appendix A), leaving also very little room for NP. We will then require that the NP contribution originating from an extension with a heavy-top verify

$$\delta m_{B_q} \equiv \frac{\Delta m_{B_q}^{\mathsf{NP}}}{\Delta m_{B_q}^{\mathsf{SM}}} = \left| \frac{\mathcal{S}_{B_q}^{\mathsf{NP}}}{\mathcal{S}_{B_q}^{\mathsf{SM}}} \right| \lesssim 0.1, \tag{4.34}$$

i.e. they should be at most of the same order of magnitude as the uncertainties in the estimates (4.33).

4.3 $D^0 - \overline{D}^0$ mixing

Similarly to the meson systems studied above, the leading order short-distance contribution to the $D^0 - \overline{D}^0$ mixing in the SM are given by box diagrams such as the ones in figure 4.1, now with down-type internal quarks and up-type external quarks. These will be generated by dipenguin[3] diagrams and the experimental value of Δm_D is also essentially given by long-distance contributions [31].

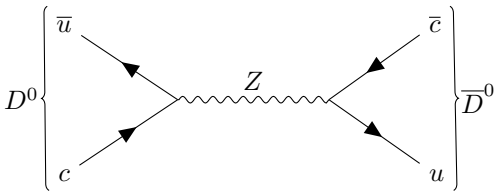

Figure 4.2: NP contribution to $D^0 - \overline{D}^0$ mixing via Z-mediated FCNC.

Nonetheless, the leading NP contribution will be dominated by the tree level diagram in figure 4.2, described by

$$\mathscr{L}_D^{\mathsf{NP}} = -\frac{G_F}{\sqrt{2}} (F_{12}^u)^2 (\overline{u}_L \gamma^\mu c_L)(\overline{u}_L \gamma_\mu c_L), \tag{4.35}$$

which arises as a direct consequence of the FCNCs that now exist in up-quark sector. Note that at tree-level and in the limit of vanishing external masses there is no contribution coming from the FCNCs involving the Higgs boson.

Therefore, one can quantify the NP contribution with the mixing parameter [49, 50]

$$x_D^{\mathsf{NP}} \equiv \frac{\Delta m_D^{\mathsf{NP}}}{\Gamma_D} \simeq \frac{\sqrt{2} G_F}{3\Gamma_D} r(m_c, M_Z) B_D f_D^2 m_D \left| F_{12}^u \right|^2, \tag{4.36}$$

where a factor $r(m_c, M_Z) \approx 0.778$ (see Appendix A), which accounts for RG effects, was introduced. In order to consider a model with a heavy-top safe with regard to this meson system, we will require that the NP contribution does not exceed the experimental value, i.e. [51]

$$x_D^{\mathsf{NP}} \leq x_D^{\mathsf{exp}} = 0.39^{+0.11}_{-0.12}\%. \tag{4.37}$$

[3]Penguin diagrams are one loop corrections to tree level such as the one in 4.2 where one of the vertices is replaced by an "effective vertex" containing the loop (see figures 4.3 and 4.4). Dipenguin diagrams are two-loop diagrams where both vertices are replaced by such "effective vertices". The dipenguin diagrams which are significant in some neutral meson mixings are gluon-mediated (see figure 17.4 of [31]).

4.4 Rare kaon decays

In this section we will be studying the rare kaon decays $K_L \to \pi^0 \overline{\nu}\nu$ and $K^+ \to \pi^+ \overline{\nu}\nu$, which are two golden modes for testing the SM given that their LD contributions are negligible [31, 43]. One should keep in mind that

$$K_L \approx \frac{K^0 + \overline{K}^0}{\sqrt{2}}, \tag{4.38}$$

so that, for the two decays we will be studying, one has in terms of quarks

$$\begin{aligned} K^0 \to \pi^0 \overline{\nu}\nu &: \overline{s} \to \overline{d}\nu\overline{\nu}, \\ \overline{K}^0 \to \pi^0 \overline{\nu}\nu &: s \to d\nu\overline{\nu}, \\ K^+ \to \pi^+ \overline{\nu}\nu &: \overline{s} \to \overline{d}\nu\overline{\nu}. \end{aligned} \tag{4.39}$$

Therefore, both of these decays are described by essentially the same diagrams (see figure 4.3). We will now discuss the effects of introducing a heavy-top to each decay individually.

4.4.1 $K_L \to \pi^0 \overline{\nu}\nu$

Firstly, we consider the rare decay $K_L \to \pi^0 \overline{\nu}\nu$, which in the SM has branching ratio, i.e. the fraction of K_L decays that correspond to this specific decay channel, proportional to [31]

$$k^0_{\mathsf{SM}} \simeq \left| \mathsf{Im}\lambda_c^K X_0(x_c) + \mathsf{Im}\lambda_t^K X_0(x_t) \right|^2, \tag{4.40}$$

for parametrizations where λ_u^K is real. Here, we introduced a new gauge independent IL function $X_0(x_i)$ (see Appendix A).

The charm quark contribution can be neglected given that $X_0(x_c) \ll X_0(x_t)$ and $\mathsf{Im}\lambda_c^K = -\mathsf{Im}\lambda_t^K$. Hence, with the addition of the heavy-top, the branching ratio is proportional to

$$k^0 = \left| \mathsf{Im}\lambda_t^K X_0(x_t) + \mathsf{Im}\lambda_T^K X_0(x_T) + \mathsf{Im}A_{ds} \right|^2, \tag{4.41}$$

so that

$$\frac{\mathsf{Br}(K_L \to \pi^0 \overline{\nu}\nu)}{\mathsf{Br}(K_L \to \pi^0 \overline{\nu}\nu)_{\mathsf{SM}}} = \frac{k^0}{k^0_{\mathsf{SM}}} = \left| \frac{\mathsf{Im}\lambda_t^K X_0(x_t) + \mathsf{Im}\lambda_T^K X_0(x_T) + \mathsf{Im}A_{ds}}{\mathsf{Im}\lambda_t^K X_0(x_t)} \right|^2. \tag{4.42}$$

The second term in (4.41) corresponds to the expected generalisation of the terms in (4.40) after an extra quark is introduced. The last term arises as a consequence of the fact that this new quark is a VLQ isosinglet and it accounts for the decoupling behaviour that arises with its addition. The gauge-invariant factor A_{ds} is given by [52–55]

$$A_{ds} = \sum_{ij} V_{id} \left(F^u - \mathbb{1}\right)_{ij} V_{js}^* N(x_i, x_j), \tag{4.43}$$

where

$$N(x_i, x_j) = \frac{x_i x_j}{8} \left(\frac{\log x_i - \log x_j}{x_i - x_j} \right), \tag{4.44}$$

$$N(x_i, x_i) \equiv \lim_{x_j \to x_i} N(x_i, x_j) = \frac{x_i}{8}. \tag{4.45}$$

To understand the need for this correction, it is instructive to analyse the diagrams that contribute to this process, which are presented in figures 4.3. It is from summing all these contributions that the expression for $X_0(x_i)$ is obtained. However, one should note that in these calculations, which are typically made in the 't Hooft-Feynman gauge, diagrams involving the $\phi^\pm$ Goldstone bosons are also considered [31, 44]. Therefore, in this gauge all contributions come from the diagrams in figure 4.3 and all the diagrams where one or more $W^\pm$ gauge bosons are replaced by Goldstone bosons $\phi^\pm$. Also in this particular gauge, the combination of all box diagrams is associated with the IL function $B_0(x_i)$, whereas the combination of all weak penguin diagrams is associated with $C_0(x_i)$ (see Appendix A). In another gauge, the functions corresponding to these diagrams would be different, i.e. they are gauge dependent, but the combination [44, 56]

$$X_0(x_i) \equiv C_0(x_i) - 4B_0(x_i) \tag{4.46}$$

is gauge independent, and as it is, this happens to be the function on which the Lagrangian describing this process depends in a similar fashion as (4.4) depends on the gauge-invariant IL function $S_0(x_i, x_j)$.

All the diagrams in figure 4.3 will have expressions that share the same form, both in the SM and in extensions with a heavy-top, now with $u_i = u, c, t, T$, except for the penguin-diagram associated with the loop in figure 4.3(b.4), where the internal up-quark line couples to the Z-gauge boson and therefore $C_0(x_i)$ (and hence $X_0(x_i)$) should be modified by the presence of FCNCs. These modifications are taken care by the addition of the A_{ds} factor.

As suggested by (3.48), the NC mixing of the heavy-top with the SM up-type quarks will be suppressed as a consequence of its large mass, meaning that typically $F^u_{4i} \ll 1$. The same is expected for the NC couplings between different SM up-type quarks. In the decoupling limit, where the heavy-top does not mix with the SM quarks, one has

$$F_u - \mathbb{1}_4 \to \begin{pmatrix} 0_{3\times3} & 0_{3\times1} \\ 0_{1\times3} & -1 \end{pmatrix}. \tag{4.47}$$

Thus, in a more realistic scenario with very suppressed, but non-zero mixing with the SM quarks, i.e. when approaching the decoupling limit, one can expect to have

$$A_{ds} \simeq -\lambda_T^K \frac{x_T}{8}, \tag{4.48}$$

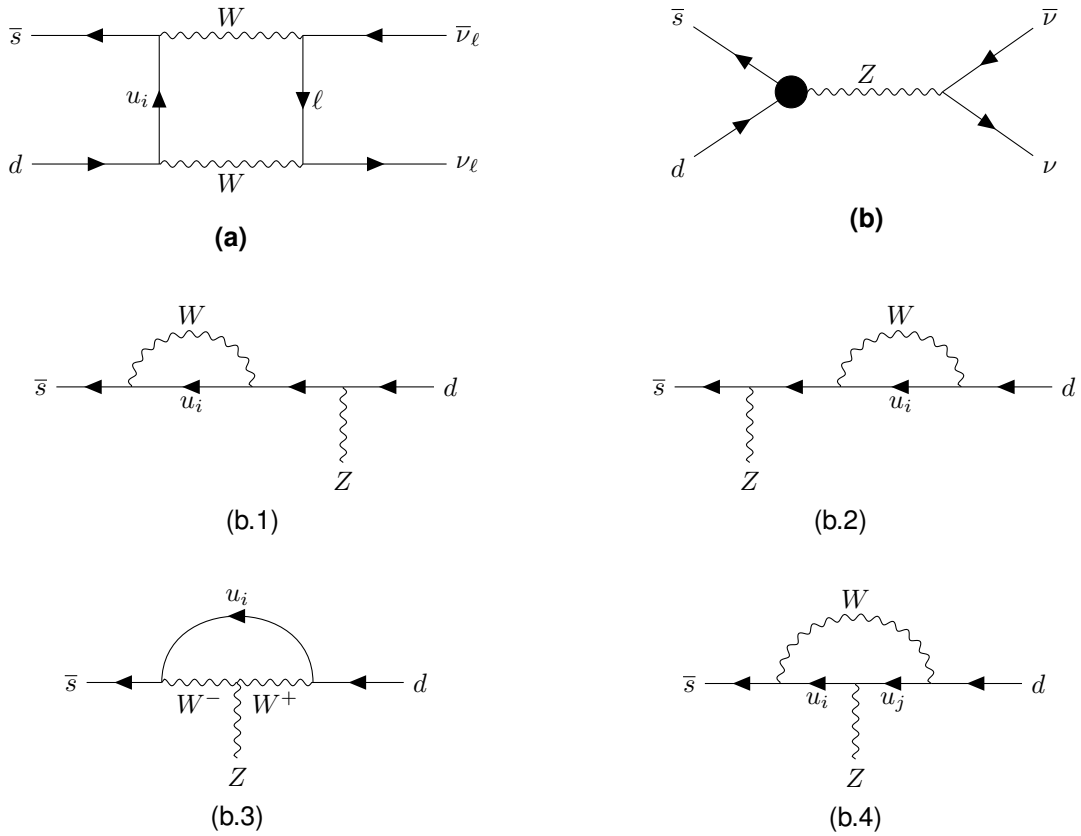

Figure 4.3: Diagrams for $\overline{s}d \to \nu\overline{\nu}$, which are relevant to the $K_L \to \pi^0\overline{\nu}\nu$ and $K^+ \to \pi^+\overline{\nu}\nu$ decays in the unitary gauge. For the box diagrams in **(a)**, one has $\ell = e, \mu, \tau$. The diagrams represented by **(b)** correspond to penguin-diagram contributions. The blob in black refers to the possible loops represented in the diagrams b.1-4. For all these diagrams one has $u_{i,j} = u, c, t, T$.

so that, in this limit, (4.41) can be written as

$$k^0 = \left| \mathrm{Im}\lambda_t^K X_0(x_t) + \mathrm{Im}\lambda_T^K \tilde{X}_0(x_T) \right|^2 , \tag{4.49}$$

where we defined an "effective" Inami-Lim function

$$\tilde{X}_0(x_T) \equiv X_0(x_T) - \frac{x_T}{8} = \frac{3}{8}\frac{x_T}{x_T - 1}\left(1 + \frac{x_T - 2}{x_T - 1}\log x_T\right), \tag{4.50}$$

for the heavy-top piece. Therefore, in this limit the NP piece has a logarithmic behaviour in x_T. In these types of analyses the factor A_{ds} is often overlooked, but in its absence this piece would be linear in x_T and dangerously large NP contributions could be achieved for $m_T \sim 1$ TeV or even lower.

The current upper-bound, coming from the KOTO experiment, for the branching ratio of this decay is at around $\mathrm{Br}(K_L \to \pi^0\overline{\nu}\nu) \lesssim 3 \times 10^{-9}$ (90% CL), whereas the SM prediction is much smaller being $\mathrm{Br}(K_L \to \pi^0\overline{\nu}\nu)_{\mathrm{SM}} \approx 3 \times 10^{-11}$ [33]. This upper-bound may potentially be lowered in future experiments and $\mathrm{Br}(K_L \to \pi^0\overline{\nu}\nu)_{\mathrm{exp}} \sim \mathrm{Br}(K_L \to \pi^0\overline{\nu}\nu)_{\mathrm{SM}}$ may be achieved, but for now the possibility of very large NP contributions cannot be ruled out. Thus, at the moment this process does not set stringent constraints on the type of extension we are studying, but it can be interesting to evaluate whether such

an extension can bridge the gap between the SM prediction and the experimental upper-bound or not.

4.4.2 $K^+ \to \pi^+ \overline{\nu}\nu$

In the SM and in a parametrization where λ_u^K is real, the branching ratio of the decay $K^+ \to \pi^+ \overline{\nu}\nu$ is proportional to [31]

$$k_{\text{SM}}^+ \simeq \left| \lambda_c^K X_0^{\text{NNL}}(x_c) + \lambda_t^K X_0(x_t) \right|^2, \tag{4.51}$$

whereas in an extension with a heavy-top it is proportional to

$$k^+ \simeq \left| \lambda_c^K X_0^{\text{NNL}}(x_c) + \lambda_t^K X_0(x_t) + \lambda_T^K X_0(x_T) + A_{ds} \right|^2, \tag{4.52}$$

so that

$$\frac{\text{Br}(K^+ \to \pi^+ \overline{\nu}\nu)}{\text{Br}(K^+ \to \pi^+ \overline{\nu}\nu)_{\text{SM}}} = \frac{k^+}{k_{\text{SM}}^+} = \left| \frac{\lambda_c^K X_0^{\text{NNL}}(x_c) + \lambda_t^K X_0(x_t) + \lambda_T^K X_0(x_T) + A_{ds}}{\lambda_c^K X^{\text{NNL}}(x_c) + \lambda_t^K X_0(x_t)} \right|^2. \tag{4.53}$$

Here, the charm contribution cannot be overlooked because even though $X^{\text{NNL}}(x_c) \ll X_0(x_t)$, one now has $\lambda_c^K \gg \lambda_t^K$. Also, note that instead of simply using $X_0(x_c)$ as the charm contribution we use $X^{\text{NNL}}(x_c) \simeq 1.04 \times 10^{-3}$ by following [57], which is the charm contribution at next-to-next-to-leading order (NNLO). This correction is important because, as mentioned above, the Inami-Lim function $X_0(x_i)$ is obtained from combining the contributions of penguin and box diagrams to neutrino decays of mesons and the expression for $X_0(x_i)$ in Appendix A is obtained by taking the limit of vanishing masses for the leptons involved in the box diagrams in 4.3(a), so that this function involves solely the mass of the internal up-type quark. This is a good approximation for the top and heavy-top contributions given that $m_t, m_T \gg m_\tau$, however for the charm quark one has $m_c < m_\tau$ and (A.8) is no longer valid. Hence, it should be replaced by

$$X^{\text{NNL}}(x_c) = X_{\text{SD}}^{\text{NNL}}(x_c) + \delta X(x_c), \tag{4.54}$$

where $\delta X(x_c)$ refers to the long-distance contribution. The short-distance piece is, at NNLO, given by

$$X_{\text{SD}}^{\text{NNL}}(x_c) = \frac{2}{3} X_e^{\text{NNL}}(x_c) + \frac{1}{3} X_\tau^{\text{NNL}}(x_c), \tag{4.55}$$

so that the contributions involving the lepton τ and the remaining lighter leptons are considered separately.

Currently, measurements of this decay yield $\text{Br}(K^+ \to \pi^+ \overline{\nu}\nu)_{\text{exp}} = \left(10.6^{+4.0}_{-3.4} \pm 0.9\right) \times 10^{-11}$, whereas the SM prediction is $\text{Br}(K^+ \to \pi^+ \overline{\nu}\nu)_{\text{SM}} = (8.4 \pm 1.0) \times 10^{-11}$ [58]. These results allow one to establish the following rough 1σ and 2σ ranges[4] for the ratio in (4.53)

[4] These ranges were calculated using the usual formulas for uncertainty propagation, with $\sigma_{\text{SM}} = 1 \times 10^{-12}$ and $\sigma_{\text{exp}} = 4.1 \times 10^{-12} = \sqrt{4.0^2 + 0.9^2} \times 10^{-12}$ for the standard deviations of the SM prediction and experimental values, respectively.

$$0.75 \lesssim \left(\frac{\text{Br}(K^+\to\pi^+\overline{\nu}\nu)}{\text{Br}(K^+\to\pi^+\overline{\nu}\nu)_{\text{SM}}}\right)_{1\sigma} \lesssim 1.77,$$
$$0.24 \lesssim \left(\frac{\text{Br}(K^+\to\pi^+\overline{\nu}\nu)}{\text{Br}(K^+\to\pi^+\overline{\nu}\nu)_{\text{SM}}}\right)_{2\sigma} \lesssim 2.28, \tag{4.56}$$

which are large as a result of the considerable experimental uncertainty associated with this branching ratio. Nonetheless, through the expression (4.53), the conditions in (4.56) can set relevant constraints on the mass of the heavy-top and its mixings with SM quarks.

4.5 CP violation parameter ε'/ε

The parameter ε'/ε measures direct CP violation in $K_L \to \pi\pi$ decays. The SM contribution can be described by the simplified expression [59]

$$\left(\frac{\varepsilon'}{\varepsilon}\right)_{\text{SM}} = F(x_t)\text{Im}\lambda_t^K, \tag{4.57}$$

where $F(x_t)$ corresponds to the following linear combinations of Inami-Lim functions

$$F(x_t) = P_0 + P_X X_0(x_t) + P_Y Y_0(x_t) + P_Z Z_0(x_t) + P_E E_0(x_t), \tag{4.58}$$

where the expressions for these functions and the values of the constants P_0, P_X, P_Y, P_Z and P_E are presented in Appendix A. To understand the origin of this expression, consider the diagrams that contribute to this process at loop level and are relevant to the construction of the IL functions in (4.58). These are displayed in figure 4.4. Note once more that in the 't Hooft-Feynman gauge where it is useful to carry out the calculations for these diagrams, one has to also consider the diagrams where one or more gauge bosons $W^\pm$ are replaced by Goldstone bosons $\phi^\pm$ [31, 44]. In this gauge, for each type of diagram their amplitude will depend on one of the functions in (A.11-A.19): the box-diagram depends on $B_0(x_i)$ and the Z-mediated penguins depend on $C_0(x_i)$ as mentioned in the previous subsection, but now we have additionally the electromagnetic penguins depending on $D_0(x_i)$ and the gluonic penguins depending on $E_0(x_i)$. As mentioned earlier, in general, the expressions for $B_0(x_i)$ and $C_0(x_i)$ are gauge-dependent, but the same is also true for $D_0(x_i)$, whereas E_0 is gauge independent [56]. As done before for $X_0(x_i)$, it useful to combine these three functions in a gauge-invariant way, resulting on two additional functions[5]

$$Y_0(x_i) \equiv C_0(x_i) - B_0(x_i),$$
$$Z_0(x_i) \equiv C_0(x_i) + \tfrac{1}{4}D_0(x_i), \tag{4.59}$$

which were introduced along with $E_0(x_i)$ in (4.58). The function $F(x_i)$ is therefore a linear combination of all the gauge-independent functions which are relevant to this process.

When a heavy-top quark is introduced, this parameter acquires a NP contribution which can be

[5]This gauge independent definition of $Y_0(x_i)$ appears to be incompatible with the gauge independent expression for $X_0(x_i)$ in (4.46). This issue is addressed in Appendix A, where it is shown that this is not the case.

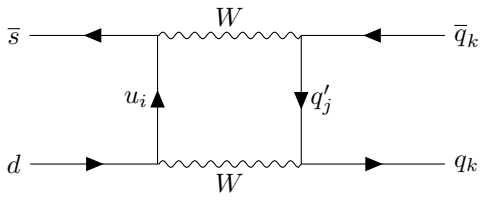

(a)

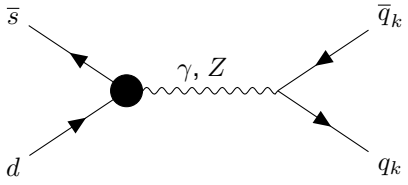

(b)

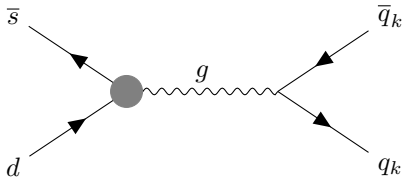

(c)

Figure 4.4: Diagrams that contribute to the decay $K_L \to \pi\pi$ at loop level in the unitary gauge. For the box diagrams in **(a)** one has $d_j = d, s, b$ and q'_j corresponds to a quark belonging to the opposite sector to that of $q_k = u, d$. The diagrams represented by **(b)** correspond to the EW-penguin contributions, whereas **(c)** represents the gluonic-penguin contributions. The blob in black refers to the loops represented in figures 4.3(b.1-4), whereas the blob in grey refers only to the loops in figures 4.3(b.1,2,4). For the loops of electromagnetic and gluonic-penguins, the Z bosons in these loops are replaced by a photon γ or a gluon g. For all diagrams one has $u_i = u, c, t, T$.

approximated by [43, 52]

$$\left(\frac{\varepsilon'}{\varepsilon}\right)_{\text{NP}} \simeq F(x_T)\text{Im}\lambda_T^K + (P_X + P_Y + P_Z)A_{ds}, \tag{4.60}$$

where, as before, the first term is a simple generalisation of the SM piece which is expected from the introduction of a new quark and the last one accounts for the fact that this new quark is an isosinglet. Note that the factor A_{ds} is only introduced as a correction to the contributions associated with $X_0(x_t), Y_0(x_t)$ and $Z_0(x_t)$, because these contributions depend on $C_0(x_i)$ and, thus, in this type of extension, will be affected by the emerging weak FCNCs. When using (4.60) we assume that the factors P_0, P_X, P_Y, P_Z and P_E are the same for the heavy-top contribution, i.e. we assume these factors are constant or at least do not change significantly when changing the argument of $F(x_i)$ from $x_i = x_t$ to $x_i = x_T$, similarly to what is done in [43].

When approaching the decoupling limit one would have

$$\left(\frac{\varepsilon'}{\varepsilon}\right)_{\text{NP}} \simeq \tilde{F}(x_T)\text{Im}\lambda_T^K, \tag{4.61}$$

where the ”effective” function

$$\tilde{F}(x_T) \equiv F(x_T) - \frac{x_T}{8}\left(P_X + P_Y + P_Z\right) \tag{4.62}$$

also evolves approximately as a logarithmic function of x_T.

Finally, one can establish a rough 1σ range for the NP contribution [60]

$$-4 \times 10^{-4} \lesssim \left(\frac{\varepsilon'}{\varepsilon}\right)_{\mathsf{NP}} \lesssim 10 \times 10^{-4}, \tag{4.63}$$

and a model with a heavy-top can be considered safe if (4.60) verifies (4.63).

4.6 The heavy-top decay channels

Following [61], the partial decay widths for the different $T \to q_i B$, where $B = Z, h, W^{\pm}$ and $q_i = u_i, d_i$ represents the up/down-type SM quark of generation i, can, in the limit of $m_T^2 \gg M_B^2, m_{q_i}^2$, be written as

$$\Gamma(T \to u_i Z) \simeq \frac{m_T^2}{32\pi v^2}\left|F_{4i}^u\right|^2, \tag{4.64}$$

$$\Gamma(T \to u_i h) \simeq \frac{m_T^2}{32\pi v^2}\left|F_{4i}^u\right|^2, \tag{4.65}$$

$$\Gamma(T \to d_i W) \simeq \frac{m_T^2}{16\pi v^2}\left|V_{Td_i}\right|^2. \tag{4.66}$$

It is relevant to study these quantities because typically, searches for heavy quarks are done based on a set of assumptions made for these partial decay widths and it is from the results of these searches that we currently obtain lower-bounds for heavy quark masses. Usually, it is assumed that

$$\begin{gathered}\mathsf{Br}(T \to u_i Z) + \mathsf{Br}(T \to u_i h) + \mathsf{Br}(T \to d_i W) \simeq 1. \\ \Gamma(T \to u_i Z) : \Gamma(T \to u_i h) : \Gamma(T \to d_i W) \simeq 1 : 1 : 2,\end{gathered} \tag{4.67}$$

where

$$\mathsf{Br}(T \to q_i B) \equiv \frac{\Gamma(T \to q_i B)}{\sum_{j,q,B}\Gamma(T \to q_j B)}. \tag{4.68}$$

The second assumption is well supported by (4.64-4.66), because, considering the form of $\mathcal{V}_{\mathsf{CKM}}$ and F^u in (3.47) and (3.48) with $K_d \simeq \mathbb{1}_3$, one has $|F_{4i}^u| \approx |V_{Td_i}|$, so that, for every generation of SM quarks

$$\Gamma(T \to u_i Z) \simeq \Gamma(T \to u_i h) \simeq 2\Gamma(T \to d_i W). \tag{4.69}$$

However, the first assumption is not really justified, as the total decay width may be more evenly distributed among all generations. What also remains unjustified but appears to have become common

wisdom, is the usual assumption of having the first relation apply to the third generation, i.e. it is assumed that T decays predominantly to $u_i = t$ and $d_i = b$, leading to lower-bounds such as the $m_T = 1.01$ TeV [62] and $m_T = 1.31$ TeV [63] coming from the CMS and ATLAS experiments, respectively.

In the following chapters we will apply all results derived throughout this chapter to a very particular type of extension of the SM with an heavy-top: the minimal solutions to the CKM-UP.

Chapter 5

The s_{14}-dominance hypothesis: a minimal solution to the CKM-UP with a heavy-top

5.1 The Botella-Chau parametrization and the salient features of s_{14}-dominance limit

Consider again the SM with the minimal addition of one VLQ resulting in a heavy-top quark T. In this framework, and in the WB where the 3×3 down sector mass matrix is diagonal, i.e. $M_d =$ diag(m_d, m_s, m_b), the mixing matrix is given by

$$\mathcal{V}_{\text{CKM}} = \mathcal{V}^\dagger K_0, \tag{5.1}$$

where, with the Botella-Chau (BC) parameterization [64], $\mathcal{V}^\dagger$ can be written as

$$\mathcal{V}^\dagger = \mathcal{O}_{34}\,\mathcal{U}_{24}\,\mathcal{U}_{14}\,\mathcal{V}_{\text{PDG}}$$

$$= \begin{pmatrix} 1 & 0 & 0 & 0 \\ 0 & 1 & 0 & 0 \\ 0 & 0 & c_{34} & s_{34} \\ 0 & 0 & -s_{34} & c_{34} \end{pmatrix} \begin{pmatrix} 1 & 0 & 0 & 0 \\ 0 & c_{24} & 0 & s_{24}e^{-i\delta_{24}} \\ 0 & 0 & 1 & 0 \\ 0 & -s_{24}e^{i\delta_{24}} & 0 & c_{24} \end{pmatrix} \begin{pmatrix} c_{14} & 0 & 0 & s_{14}e^{-i\delta_{14}} \\ 0 & 1 & 0 & 0 \\ 0 & 0 & 1 & 0 \\ -s_{14}e^{i\delta_{14}} & 0 & 0 & c_{14} \end{pmatrix} \cdot \tag{5.2}$$

$$\cdot \begin{pmatrix} 1 & 0 & 0 & 0 \\ 0 & c_{23} & s_{23} & 0 \\ 0 & -s_{23} & c_{23} & 0 \\ 0 & 0 & 0 & 1 \end{pmatrix} \begin{pmatrix} c_{13} & 0 & s_{13}e^{-i\delta} & 0 \\ 0 & 1 & 0 & 0 \\ -s_{13}e^{i\delta} & 0 & c_{13} & 0 \\ 0 & 0 & 0 & 1 \end{pmatrix} \begin{pmatrix} c_{12} & s_{12} & 0 & 0 \\ -s_{12} & c_{12} & 0 & 0 \\ 0 & 0 & 1 & 0 \\ 0 & 0 & 0 & 1 \end{pmatrix}$$

with $c_{ij} = \cos\theta_{ij}$ and $s_{ij} = \sin\theta_{ij}$, and $\theta_{ij} \in [0, \pi/2]$, $\delta_{ij} \in [0, 2\pi]$. The two new phases δ_{14} and δ_{24} will in general correspond to new sources of CP violation. The matrix $\mathcal{V}_{\text{PDG}}$ depends exclusively on SM parameters and corresponds to the product in the last line of (5.2) and is the 4×4 generalization of V_{PDG}, the standard PDG [33] parameterization for the CKM matrix in the SM model introduced in (2.46), i.e.

$$\mathcal{V}_{\text{PDG}} = \begin{pmatrix} & & & 0 \\ & V_{\text{PDG}} & & 0 \\ & & & 0 \\ 0 & 0 & 0 & 1 \end{pmatrix}. \tag{5.3}$$

Note that the BC parametrization is such that

$$|V_{ud}|^2 + |V_{us}|^2 + |V_{ub}|^2 = 1 - s_{14}^2 \tag{5.4}$$

making it evident that, in this context, a solution for the observed 3×3 CKM-UP implies that the angle $s_{14} = \Delta$ is non-zero.

From (5.1) and (5.2), it is very straightforward to conclude that in this parametrization one has

$$\begin{aligned} V_{ud} &= \mathcal{V}_{11}^\dagger = c_{12}c_{13}c_{14}, \\ V_{us} &= \mathcal{V}_{12}^\dagger = s_{12}c_{13}c_{14}, \end{aligned} \tag{5.5}$$

and therefore, on concludes that the CKM factor

$$\lambda_u^K = V_{us}^* V_{ud} = s_{12}c_{12}c_{13}^2c_{14}^2 \tag{5.6}$$

is real in this parametrization, and thus that the results from last chapter conveniently hold in the BC parametrization. Henceforth, we shall adopt this parametrization.

Furthermore, one obtains for the matrix that controls the FCNCs

$$
\begin{aligned}
F^u &= \begin{pmatrix} 1-|\mathcal{V}_{41}|^2 & -\mathcal{V}_{41}^*\mathcal{V}_{42} & -\mathcal{V}_{41}^*\mathcal{V}_{43} & -\mathcal{V}_{41}^*\mathcal{V}_{44} \\ -\mathcal{V}_{42}^*\mathcal{V}_{41} & 1-|\mathcal{V}_{42}|^2 & -\mathcal{V}_{42}^*\mathcal{V}_{43} & -\mathcal{V}_{42}^*\mathcal{V}_{44} \\ -\mathcal{V}_{43}^*\mathcal{V}_{41} & -\mathcal{V}_{43}^*\mathcal{V}_{42} & 1-|\mathcal{V}_{43}|^2 & -\mathcal{V}_{43}^*\mathcal{V}_{44} \\ -\mathcal{V}_{44}^*\mathcal{V}_{41} & -\mathcal{V}_{44}^*\mathcal{V}_{42} & -\mathcal{V}_{44}^*\mathcal{V}_{43} & 1-|\mathcal{V}_{44}|^2 \end{pmatrix} \\
&= \begin{pmatrix} c_{14}^2 & -c_{14}s_{14}s_{24}e^{i\delta'} & -c_{14}s_{14}c_{24}s_{34}e^{-i\delta_{14}} & -c_{14}s_{14}c_{24}c_{34}e^{-i\delta_{14}} \\ -c_{14}s_{14}s_{24}e^{-i\delta'} & 1-c_{14}^2s_{24}^2 & -c_{14}^2c_{24}s_{24}s_{34}e^{-i\delta_{24}} & -c_{14}^2c_{24}s_{24}c_{34}e^{-i\delta_{24}} \\ -c_{14}s_{14}c_{24}s_{34}e^{i\delta_{14}} & -c_{14}^2c_{24}s_{24}s_{34}e^{i\delta_{24}} & 1-c_{14}^2c_{24}^2s_{34}^2 & -c_{14}^2c_{24}^2c_{34}s_{34} \\ -c_{14}s_{14}c_{24}c_{34}e^{i\delta_{14}} & -c_{14}^2c_{24}s_{24}c_{34}e^{i\delta_{24}} & -c_{14}^2c_{24}^2c_{34}s_{34} & 1-c_{14}^2c_{24}^2c_{34}^2 \end{pmatrix},
\end{aligned}
\tag{5.7}
$$

where, for reasons which will become clear in the following subsections, we define the difference between the two new mixing phases as

$$
\delta' \equiv \delta_{24} - \delta_{14}. \tag{5.8}
$$

Now, in an attempt to fully achieve a minimal solution of the CKM-UP, we impose the s_{14}-dominance limit for the mixing, by taking

$$
s_{14} = \Delta \sim \lambda^2, \quad s_{24} = s_{34} = 0, \tag{5.9}
$$

where $\lambda \simeq |V_{us}|$ is one of the parameters used in the Wolfenstein parametrization of the CKM matrix, introduced in (2.67), and one should recall (3.7). With this prescription (5.2) takes the very manageable form

$$
\mathcal{V}^\dagger = \begin{pmatrix} c_{12}c_{13}c_{14} & s_{12}c_{13}c_{14} & s_{13}c_{14}e^{-i\delta} & s_{14} \\ -s_{12}c_{23} - e^{i\delta}c_{12}s_{13}s_{23} & c_{12}c_{23} - e^{i\delta}s_{12}s_{13}s_{23} & c_{13}s_{23} & 0 \\ s_{12}s_{23} - e^{i\delta}c_{12}s_{13}c_{23} & -c_{12}s_{23} - e^{i\delta}s_{12}s_{13}c_{23} & c_{13}c_{23} & 0 \\ -c_{12}c_{13}s_{14} & -s_{12}c_{13}s_{14} & -s_{13}s_{14}e^{-i\delta} & c_{14} \end{pmatrix}, \tag{5.10}
$$

and with (5.1), the mixing matrix is given by

$$
\mathcal{V}_{\text{CKM}} = \begin{pmatrix} c_{12}c_{13}c_{14} & s_{12}c_{13}c_{14} & s_{13}c_{14}e^{-i\delta} \\ -s_{12}c_{23} - e^{i\delta}c_{12}s_{13}s_{23} & c_{12}c_{23} - e^{i\delta}s_{12}s_{13}s_{23} & c_{13}s_{23} \\ s_{12}s_{23} - e^{i\delta}c_{12}s_{13}c_{23} & -c_{12}s_{23} - e^{i\delta}s_{12}s_{13}c_{23} & c_{13}c_{23} \\ -c_{12}c_{13}s_{14} & -s_{12}c_{13}s_{14} & -s_{13}s_{14}e^{-i\delta} \end{pmatrix}. \tag{5.11}
$$

Note that the two new CP violating phases can be eliminated through rephasings of the quark fields, so that in this limit we are effectively only adding a parameter to the SM mixing, the angle θ_{14}. The first row of $\mathcal{V}_{\text{CKM}}$ is only slightly modified by a factor of $c_{14} \simeq 1$, whereas the second and third rows remain intact. On the other hand, the new forth row of $\mathcal{V}_{\text{CKM}}$ is suppressed by a factor of s_{14}. This row is associated to three new couplings, generating at tree level the three decays represented in figure 5.1.

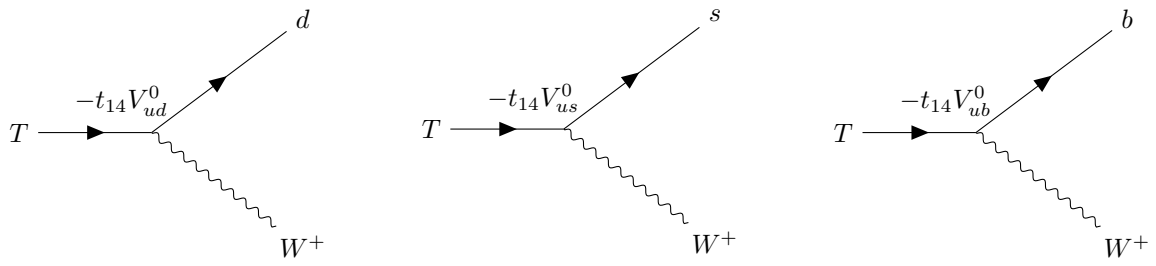

Figure 5.1: Decays of the type $T \to d_i\ W^+$ in the framework of s_{14}-dominance. Here $V^0_{\alpha\beta}$ refers to the SM mixings and $t_{ij} = \tan\theta_{ij}$.

The matrix controlling the FCNCs in (5.7), now reduces to the much simpler form

$$F^u = \mathcal{V}_{\text{CKM}}\mathcal{V}^\dagger_{\text{CKM}} = \begin{pmatrix} c^2_{14} & 0 & 0 & -c_{14}s_{14} \\ 0 & 1 & 0 & 0 \\ 0 & 0 & 1 & 0 \\ -c_{14}s_{14} & 0 & 0 & s^2_{14} \end{pmatrix}, \tag{5.12}$$

and in this case, at tree level only two new decays involving FCNCs arise: $T \to u\ Z$ and $T \to u\ h$ which are represented in figure 5.2.

Figure 5.2: Decays of the type $T \to u_i\ Z$ and $T \to u_i\ h$ in the framework of s_{14}-dominance. The only decays allowed are the ones involving the u quark.

Here, immediately one can identify some of the most salient features of the s_{14}-dominance limit as being the dominant coupling of T with up and down quarks, the significantly smaller coupling of T with the bottom quark and the vanishing of the coupling of T with the charm and top quarks. These large couplings of the very massive heavy-top to the lighter first generation, instead of the much heavier third generation is opposed to the usual "wisdom", making this a particularly intriguing and exciting limit to study.

Moreover, the simple forms of (5.11) and (5.12) allow one to make some quick predictions regarding neutral meson mixings. For instance, as illustrated in figures 5.3 and 5.4 one can expect the NP contributions to $B^0_{d,s} - \overline{B}^0_{d,s}$ to be very suppressed, so that these processes will be dominated by the SM contributions. In addition, the fact that $F^u_{12} = 0$ means there will exist no NP contribution to $D^0 - \overline{D}^0$ mixing at tree level.

Another, no less, important feature is the fact that the CKM factor

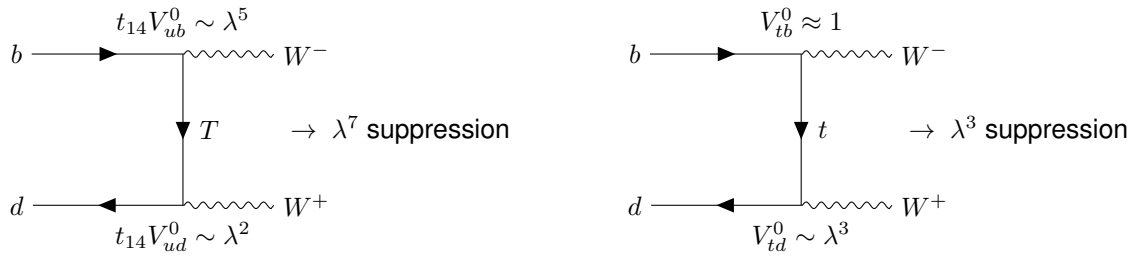

Figure 5.3: A quick analysis of the CKM factors involved in the box diagrams that contribute to $\Delta m^{\text{SM}}_{B_d}$ and $\Delta m^{\text{NP}}_{B_d}$, suggests that the NP contribution is extremely suppressed in the s_{14}-dominance limit. Here $V^0_{\alpha\beta}$ refers to the SM mixings and $t_{ij} = \tan\theta_{ij}$.

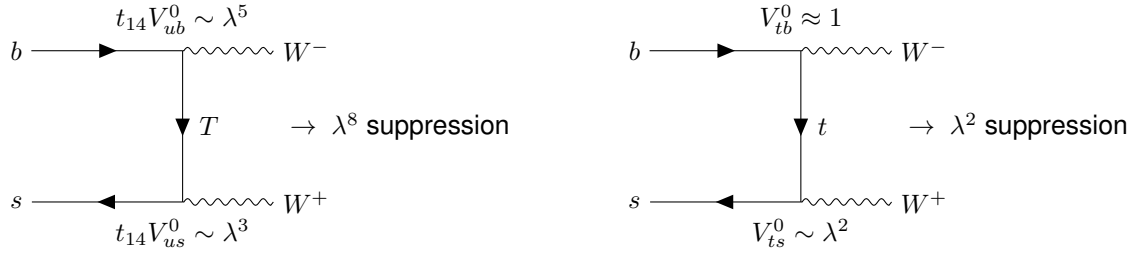

Figure 5.4: Analogous figure to figure 5.3 but now regarding the B^0_s system.

$$\lambda^K_T = \lambda^K_u t^2_{14} \tag{5.13}$$

is real, which imposes vanishing NP contributions to ε'/ε and to the branching ratio of the $K_L \to \pi^0\overline{\nu}\nu$ decay[1].

For other processes, especially the mixing of neutral kaons, the situation is more complex and a more detailed analysis is required. We will focus on this in the next subsection.

5.2 Detailed Phenomenological Analysis

Here, we present a more rigorous analysis, in the limit of s_{14}-dominance, for the processes studied in chapter 4 that have non-vanishing NP contribution. We start by further exploring the implications of this limit on the heavy-top decays and by checking the predicted suppression of the NP contributions to the $B^0_{d,s} - \overline{B}^0_{d,s}$ mixings. Then we shall turn to the not yet discussed neutral kaon mixing and the $K^+ \to \pi^+\overline{\nu}\nu$ decay.

Given that in this limit the first three rows of CKM essentially remain intact, one can simply work with values compatible with the PDG to achieve the experimentally predicted magnitudes for the CKM entries, the rephasing invariant phases and the CP violation invariant (see section 5.3). Thus, hereafter, we will use

[1] To be more precise, this is only true if one also has $\text{Im}A_{ds} = 0$, which is not exactly true, but is an extremely good approximation in this limit (see (5.29))

$$\theta_{12} \simeq 0.2264, \quad \theta_{13} \simeq 0.0037, \quad \theta_{23} \simeq 0.0405, \quad \delta \simeq 1.215, \tag{5.14}$$

throughout the following sections and the next chapter.

Hence, in the s_{14}-dominance minimal limit, the only two free parameters will be the new mixing angle s_{14} and the heavy-top mass m_T. In the case of the mixing angle in order to tackle the CKM-UP one assumes that $s_{14} = \Delta \in [0.03, 0.05]$, as suggested in (5.9). For the heavy-top mass we are interested in searching for regions that may be accessible in upcoming generations of accelerators and therefore we shall restrict ourselves to the study of regions where $m_T \leq 2.5$ TeV. This is in agreement with the rough upper-bound presented in [30] for models with an heavy-top where $|V_{14}| \simeq 0.04$.

With this in mind, we will now analyse the phenomenological consequences of mixing with the heavy-top in the s_{14}-dominance limit, with the aim of finding a region in (s_{14}, m_T) space where the model passes the tests posed by the mentioned EWPMs related quantities.

5.2.1 The heavy-top decay channels

From 4.6, the partial decay widths for the different heavy-top decays are given by

$$\Gamma(T \to u\, Z) \simeq \Gamma(T \to u\, h) \simeq \frac{m_T^2}{32\pi v^2} \left|F_{41}^u\right|^2 \simeq \frac{m_T^2}{32\pi v^2} c_{14}^2 s_{14}^2, \tag{5.15}$$

$$\Gamma(T \to c\, Z) = \Gamma(T \to t\, Z) = \Gamma(T \to c\, h) = \Gamma(T \to t\, h) = 0, \tag{5.16}$$

$$\Gamma(T \to d\, W^+) \simeq \frac{2m_T^2}{32\pi v^2} \left|V_{Td}\right|^2 \simeq \frac{2m_T^2}{32\pi v^2} c_{12}^2 c_{13}^2 s_{14}^2, \tag{5.17}$$

$$\Gamma(T \to s\, W^+) \simeq \frac{2m_T^2}{32\pi v^2} \left|V_{Ts}\right|^2 \simeq \frac{2m_T^2}{32\pi v^2} s_{12}^2 c_{13}^2 s_{14}^2, \tag{5.18}$$

$$\Gamma(T \to b\, W^+) \simeq \frac{2m_T^2}{32\pi v^2} \left|V_{Tb}\right|^2 \simeq \frac{2m_T^2}{32\pi v^2} s_{13}^2 s_{14}^2, \tag{5.19}$$

so that one has

$$\Gamma(T \to d\, W^+) \simeq 2\Gamma(T \to u\, Z) \simeq 2\Gamma(T \to u\, h), \tag{5.20}$$

as well as

$$\mathsf{Br}\left(T \to d\, W^+\right) + \mathsf{Br}\left(T \to u\, Z\right) + \mathsf{Br}\left(T \to u\, h\right) \simeq 1, \tag{5.21}$$

$$\mathsf{Br}\left(T \to s\, W^+\right) + \mathsf{Br}\left(T \to c\, Z\right) + \mathsf{Br}\left(T \to c\, h\right) \simeq s_{12}^2 \ll 1, \tag{5.22}$$

$$\text{Br}\left(T \to b\, W^+\right) + \text{Br}\left(T \to t\, Z\right) + \text{Br}\left(T \to t\, h\right) \simeq s_{13}^2 \ll 1. \tag{5.23}$$

which is strikingly different from the most typical assumptions in searches for pair production of VLQs. As described in 4.6, usually the lower-bounds for the heavy-top mass are larger than 1 TeV and they are obtained in these searches by assuming the sum in (5.23) to be equal to one, but in the s_{14}-dominance limit this assumption must be dropped. From the fact that the dominant decays involve only the lighter first generation and the fact that $\Gamma(T \to u\, Z) : \Gamma(T \to u\, h) : \Gamma(T \to d\, W^+) = 1 : 1 : 2$, one can set a lower-bound for m_T as low as $m_T = 0.685$ TeV [65].

This result, coupled with the prescription $m_T \leq 2.5$ TeV, then allows one to establish $m_T \in [0.685, 2.5]$ TeV as a narrower region of interest for the heavy-top mass, which we shall use throughout the rest of this work.

5.2.2 NP contributions to neutral meson mixings

To check how small the NP contribution to $B^0_{d,s}$ mixing are when compared to the SM it is useful to analyse the ratio

$$\delta m_{B_i} \equiv \frac{\Delta m_{B_i}^{\text{NP}}}{\Delta m_{B_i}^{\text{SM}}} \simeq \left| \frac{2 S_{tT} \lambda_t^{B_i} \lambda_T^{B_i} + S_{TT} (\lambda_T^{B_i})^2}{S_{tt} (\lambda_t^{B_i})^2} \right|, \tag{5.24}$$

where the expressions in 4.2 were used, as well as the notation $S_{ij} \equiv S_0(x_i, x_j)$. As represented in figures 5.3 and 5.4, the CKM factors relevant in (5.26) verify in this limit,

$$|\lambda_T^{B_d} / \lambda_t^{B_d}| \sim \lambda^4, \qquad |\lambda_T^{B_s} / \lambda_t^{B_s}| \sim \lambda^6, \tag{5.25}$$

so that the last term on the numerator of (5.26) can be effectively discarded. One then has

$$\delta m_{B_i} \simeq \left| \frac{2 S_{tT} \lambda_T^{B_i}}{S_{tt} \lambda_t^{B_i}} \right|, \tag{5.26}$$

which, from (5.25) and the fact that $S_{tT} \lesssim 3.5 S_t$ for $m_T \in [0.685, 2.5]$, leads us to the same conclusion as before: the NP contributions to $B^0_{d,s}$ oscillations are extremely suppressed in the s_{14}-dominance limit. For instance, for $m_T \leq 2.5$ TeV and $s_{14} \lesssim 0.05$ one has $\delta m_{B_d} \lesssim 0.72\%$ and $\delta m_{B_s} \lesssim 0.04\%$, so that the criteria we defined in (4.34) is clearly fulfilled and this limit can indeed be considered safe with regards to $B^0_{d,s}$ oscillations.

In the case of the kaon system the analysis becomes more complicated, mainly because as shown in 4.1 more terms are relevant in the NP piece. In fact, one now has

$$\Delta m_K^{\text{NP}} \simeq \frac{G_F^2 M_W^2 m_K f_K^2 B_K}{6\pi^2} \left| 2 S_{cT} \eta_{cT}^K \lambda_c^K \lambda_T^K + 2 S_{tT} \eta_{tT}^K \lambda_t^K \lambda_T^K + S_{TT} \eta_{TT}^K (\lambda_T^K)^2 \right|. \tag{5.27}$$

In figure 5.5 expression (5.27) is plotted for (5.14) and for three values of s_{14} within our range of interest. From this figure one can readily conclude that, differently from the mass differences associated to neutral B-meson oscillations, the NP contributions to neutral kaon mixing are much larger, and even

though the criteria

$$\Delta m_K^{\text{NP}} \lesssim \Delta m_K^{\text{exp}} = (3.484 \pm 0.006) \times 10^{-12} \text{ MeV}, \tag{5.28}$$

we established in (4.19) seems to be less restrictive than (4.34), there are still values of s_{14} and m_T within the regions of interest for which this condition is not fulfilled, more specifically for $s_{14} \gtrsim 0.045$ and $m_T \gtrsim 2$ TeV. Nonetheless, overall there is a fairly large region where this limit can be considered safe.

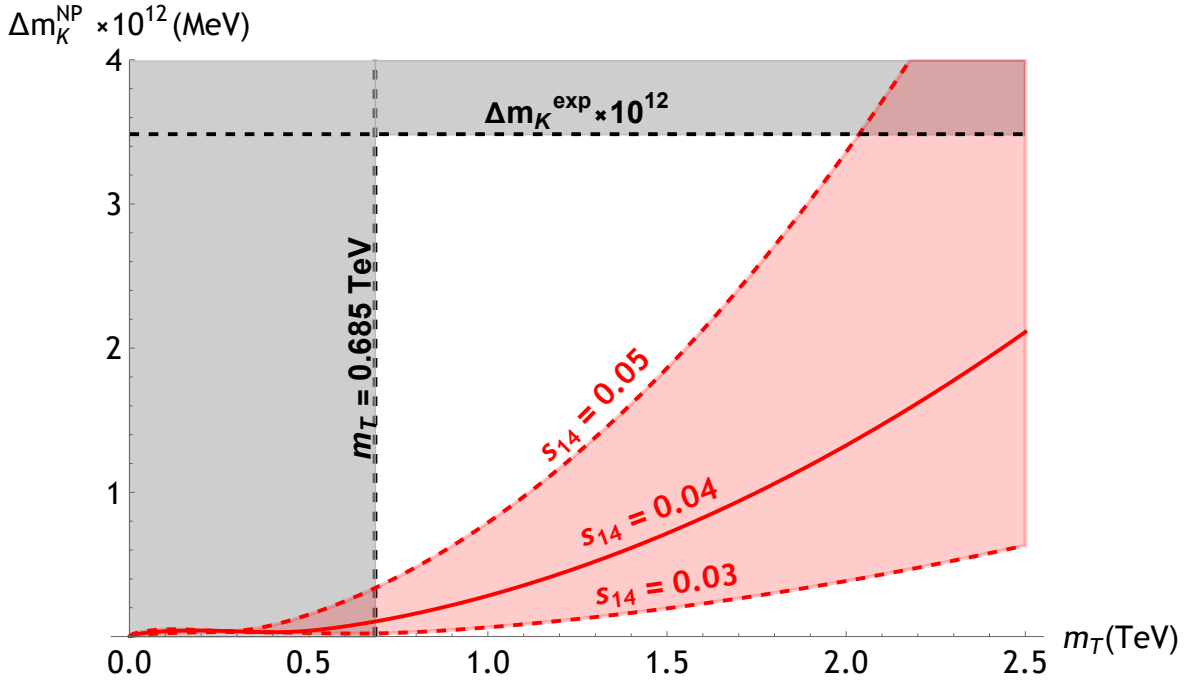

Figure 5.5: Evolution of Δm_K^{NP} with the mass of the heavy-top, for $s_{14} = \{0.03, 0.04, 0.05\}$ and $m_T \leq 2.5$ TeV. The region in red corresponds to the range of interest $s_{14} \in [0.03, 0.05]$, whereas the grey regions correspond to the regions excluded by imposing $m_T \geq 0.685$ TeV and by the criteria (5.28).

It is relevant to point out that the apparent unbounded behaviour of Δm_K^{NP} with increasing m_T is simply an artefact of fixing $s_{14} = \Delta$ in order to solve the CKM-UP. Without this constraint one would have $|V_{Td}|, |V_{Ts}|, |V_{Tb}| \sim v/v'$ (see 3.2.2) becoming smaller with increasing $m_T \sim v'$. Therefore, one would have $\lambda_T^N \sim v'^{-2}$ as well as $S_{cT}, S_{tT} \sim \log m_T^2 \sim \log\left(v'^2\right)$ and $S_{TT} \sim m_T^2 \sim v'^2$, so that the NP contributions to neutral meson mixings are expected to be naturally suppressed with increasing m_T. When fixing $|V_{Td}| \simeq s_{14} = \Delta$ in order to study the possible ranges of m_T that allow the CKM-UP to be solved while having $\Delta m_K^{\text{NP}} \lesssim \Delta m_K^{\text{exp}}$, the mixings can no longer counterbalance the growth of the IL functions with increasing m_T and one obtains the behaviour displayed in figure 5.5. Nonetheless, it should be noted that while imposing $|V_{Td_i}| \simeq \Delta \sim v/v'$, we are also imposing $m_T \sim v' \lesssim 6$ TeV as an implicit upper-bound for the heavy-top mass.

5.2.3 The $K^+ \to \pi^+ \overline{\nu}\nu$ decay

To study the NP contribution to this decay it is relevant to first compute the factor A_{ds} defined in (4.43). In this minimal limit, given the simple form of (5.12), it is obvious that

$$A_{ds} \simeq -\lambda_T \frac{x_T}{8}, \tag{5.29}$$

by using $c_{14}^2 \simeq 1$. This is the same expression as the one encountered in (4.48) for the approximate decoupling limit. Then, in this limit, the ratio in (4.53) can be written as

$$\frac{\text{Br}\,(K^+ \to \pi^+ \overline{\nu}\nu)}{\text{Br}\,(K^+ \to \pi^+ \overline{\nu}\nu)_{\text{SM}}} \simeq \left| 1 + \frac{\lambda_T^K \tilde{X}_0(x_T)}{\lambda_c^K X_0^{\text{NNL}}(x_c) + \lambda_t^K X_0(x_t)} \right|^2 , \tag{5.30}$$

where one should recall from (4.50) that

$$\tilde{X}_0(x_T) \equiv \frac{x_T}{8(x_T-1)} \left(3 + \frac{3x_T - 6}{x_T - 1} \log x_T \right) . \tag{5.31}$$

In figure 5.6 we present plots of the ratio in (5.30) as a function of m_T for various values of s_{14}. From these plots it seems that larger values of s_{14} and m_T are favoured and it is clear that even the rough 2σ range (4.56) imposes important constraints on our model, especially on the lower-bounds for s_{14} and m_T. These types of constraints are very distinct to the ones found for Δm_K, in the sense that they exclude different regions of the (s_{14}, m_T) parameter space, as they tend to exclude both smaller values of s_{14} and m_T. However, some values of s_{14} around $s_{14} \simeq 0.03$ might still be allowed.

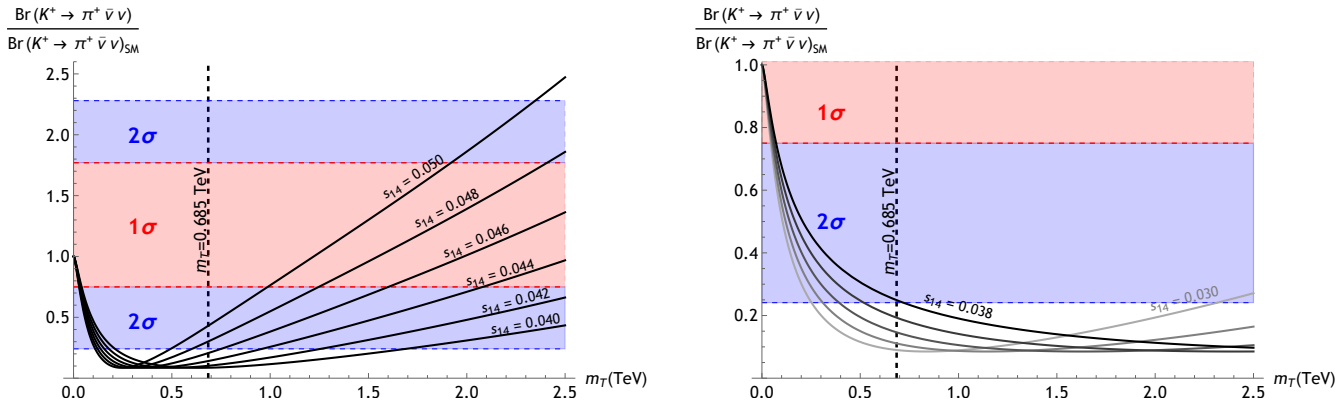

Figure 5.6: Plot of (5.30) as a function of m_T for various values of $s_{14} \in [0.04, 0.05]$ (on the left) and $s_{14} \in [0.03, 0.04[$ (on the right) using (5.14). On both panels, the curves span values of s_{14} in steps of 2×10^{-3}. The coloured regions refer to the 1σ and 2σ ranges in (4.56).

5.2.4 The ε_K problem

For the CP violation parameter ε_K, using (4.18) and (5.11), one easily find the expression

$$|\varepsilon_K^{\text{NP}}| = \frac{G_F^2 M_W^2 m_K f_K^2 B_K \kappa_\varepsilon}{12\sqrt{2}\pi^2 \Delta m_K} |\mathcal{F}| , \tag{5.32}$$

where

$$\mathcal{F} = (\eta_{tT}^K S_{tT} - \eta_{cT}^K S_{cT}) c_{12} c_{13}^2 c_{23} s_{12} s_{13} s_{23} s_{14}^2 \sin\delta, \tag{5.33}$$

which is dominated by the term involving the top-quark contribution.

In figure 5.7, the heavy-top mass dependence of expression (5.32) is plotted using (5.14), for three values of s_{14}. From this plot one can conclude that $|\varepsilon_K^{\text{NP}}| < \delta\varepsilon_K$ is only achieved in experimentally ruled out regions for m_T and is completely incompatible with $s_{14} \in [0.03, 0.05]$. Thus, we conclude that the parameter region of exact s_{14}-dominance, where we strictly have that $s_{24} = s_{34} = 0$, is not safe with regard to the parameter ε_K. It is important to emphasise that, although this limit would not be compatible with the usual upper-bound (4.21), the new much more restrictive upper bound $|\varepsilon_K^{\text{NP}}| \lesssim \delta\varepsilon_K$ makes this incompatibility significantly worse.

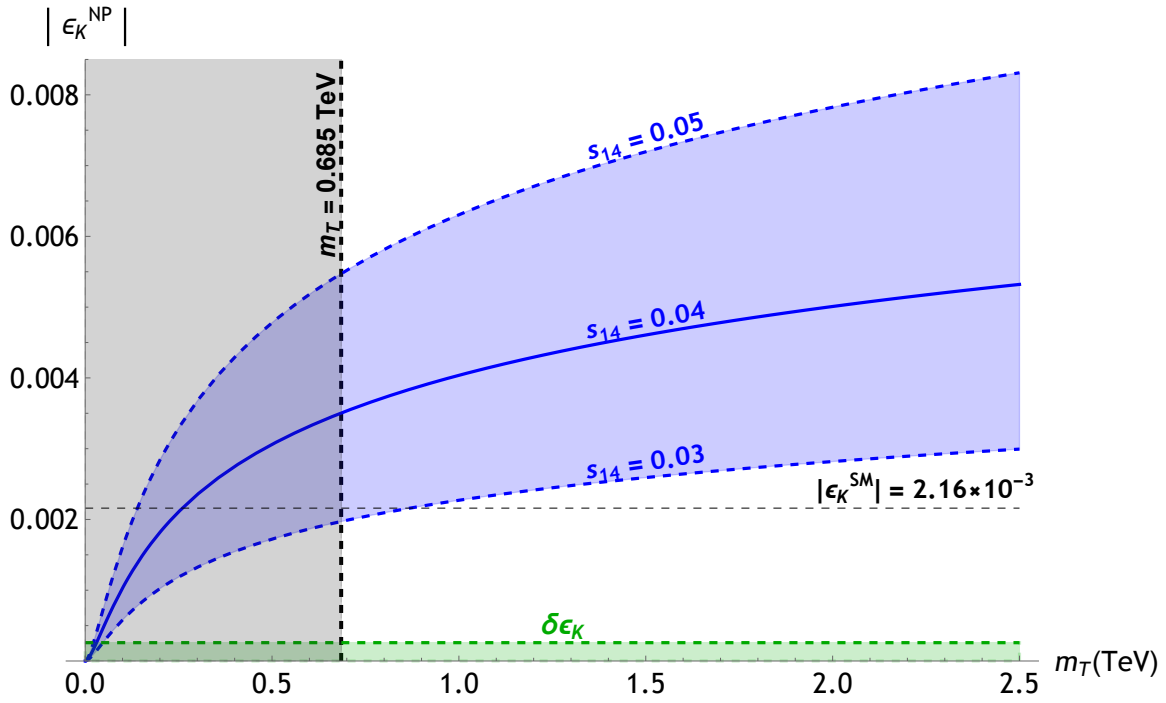

Figure 5.7: $|\varepsilon_k^{\text{NP}}|$ as a function of m_T in the framework of strict s_{14}-dominance, for $s_{14} = \{0.03, 0.04, 0.05\}$ and $m_T \leq 2.5$ TeV. The region in blue corresponds to the range of interest $s_{14} \in [0.03, 0.05]$, whereas the grey region refers to values of m_T below the lower-bound, $m_T = 0.685$ TeV. The horizontal black dashed line corresponds to $|\varepsilon_K^{\text{NP}}| = |\varepsilon_K^{\text{SM}}|$. In green we represent the region $|\varepsilon_K^{\text{NP}}| < \delta\varepsilon_K = 2.48 \times 10^{-4}$ inside of which we consider the model to be safe.

This is inherently connected to the fact that λ_T^K is real in this limit. Generally, one would have

$$\varepsilon_K^{\text{NP}} \propto \text{Im}\left(\lambda_t^K \lambda_T^K + (\lambda_T^K)^2\right) = \text{Re}\lambda_T^K \text{Im}\lambda_t^K + \text{Im}\lambda_T^K \text{Re}\lambda_t^K + 2\text{Im}\lambda_T^K \text{Re}\lambda_T^K, \tag{5.34}$$

where the smaller charm contribution was neglected. In this strict s_{14}-dominance, i.e. where $s_{24}, s_{34} = 0$, only the first term survives as $\text{Im}\lambda_T^K = 0$. This, coupled with the fact that $\text{Re}\lambda_T^K$ consists of a single term, allows one to achieve the very simple form in (5.32) and (5.33). Therefore, the region of parameters where $|\varepsilon_K^{\text{NP}}| \lesssim \delta\varepsilon_K$ is extremely tiny and corresponds to values of s_{14} and m_T that are currently excluded.

However, in a general case with $s_{24}, s_{34} \neq 0$ the remaining terms in (5.34) do not vanish and both $\text{Re}\lambda_T^K$ and $\text{Im}\lambda_T^K$ are composed by several terms, leading to an expression for $|\varepsilon_K^{\text{NP}}|$ that is much more complex. Also, since we now include not only these two new mixing angles, but also two new CP violating phases, the parameter space becomes much larger and one might reasonably hypothesise

that all these terms can, through choices of these new four parameters, combine in a large number of different ways that allow $|\varepsilon_K^{\text{NP}}| < \delta\varepsilon_K$ to be achieved for $m_T \in [0.685, 2.5]$ TeV and $s_{14} \in [0.03, 0.05]$. The allowed region of the parameter space should therefore be much larger.

Meanwhile, as we have demonstrated, the s_{14}-dominance limit is extremely interesting because it allows for a minimal solution to the CKM-UP in which, with the exception of ε_K, Δm_K and Br $(K^+ \to \pi^+ \overline{\nu}\nu)$, many of the most relevant observables associated to the electroweak precision measurements (EWPM) will automatically receive very small or even no NP contribution. For Δm_K and Br $(K^+ \to \pi^+ \overline{\nu}\nu)$, however, there is still a significant range for m_T and s_{14} where we might consider this limit safe. Thus, we find that ε_K is the only observable studied in chapter 4 that is truly out of range. This is however not surprising, as we consider such a compact and strict limit.

Two important questions arise:

- How much does one need to deviate from the strict s_{14}-dominance limit ($s_{24}, s_{34} = 0$) in order to achieve $|\varepsilon_K^{\text{NP}}| < \delta\varepsilon_K$ inside the range of interest for the masses m_T?
- What are the phenomenological implications of this deviation? Can the main features of s_{14}-dominance still be preserved?

These questions will be the focus of the next chapter.

5.3 Numerical Example I: Absolute s_{14}-dominance

For the moment, and as a final illustration, not only of the problem with this minimal solution, but also of some of its exciting features, we present a numerical example for the s_{14}-dominance limit.

Consider the following up-sector mass matrix in a WB where the 3×3 down sector mass matrix is diagonal[2]

$$\mathcal{M}_u = \begin{pmatrix} 0 & 0 & 0 & 56.9745 \\ 0 & 0 & 7.27005 & 12.9489\, e^{1.93232i} \\ 0 & 18.9053 & 172.766 & 4.52335\, e^{-1.57428i} \\ 0.0428697 & 1.66448 & 36.4393\, e^{-1.52453i} & 1390.29 \end{pmatrix}, \tag{5.35}$$

given in GeV at the M_Z scale. The up-type quark masses are then, at this scale,

$$m_u = 0.0018 \text{ GeV}, \quad m_c = 0.77 \text{ GeV}, \quad m_t = 174 \text{ GeV}, \quad m_T = 1392 \text{ GeV}. \tag{5.36}$$

which are deviate from the values in [66] by less than 1.6σ.

In the basis where the down sector mass matrix is diagonal, the matrix $\mathcal{V}^\dagger$ which diagonalizes $\mathcal{M}_u$ on the left will have absolute value

[2]Note that in this WB, the 4×4 up-sector mass matrix can always be written in this form, i.e. with 6 null entries and only three complex entries. This is achieved with rephasings of the quark fields and appropriate orthogonal transformations of the RH quark fields.

$$|\mathcal{V}^\dagger| \simeq \begin{pmatrix} 0.973615 & 0.224271 & 0.00369673 & 0.0419877 \\ 0.224338 & 0.97367 & 0.0404887 & 0 \\ 0.00853055 & 0.0397524 & 0.999173 & 0 \\ 0.0409159 & 0.00942494 & 0.000155354 & 0.999118 \end{pmatrix}. \tag{5.37}$$

Recall that $\mathcal{V}_{\text{CKM}}$ is given by a 4×3 matrix of the first three columns of this matrix.

We obtain also for the rephasing invariant phases relevant for CP violation

$$\sin(2\beta) = 0.7279, \quad \gamma = 69.58^\circ, \quad \chi = 0.01960, \quad \chi' = 0.00064236, \tag{5.38}$$

and the CP-violation invariant, defined as

$$J \equiv \text{Im}\left(V_{us} V_{cb} V_{ub}^* V_{cs}^*\right), \tag{5.39}$$

has absolute value $|J| = 3.064 \times 10^{-5}$.

One can check that these values for the mixings, the rephasing invariant phases and the CP violation invariant are recovered if one plugs $s_{14} = 0.042$ and the values (5.14) in (5.2). One can also verify that this results are compatible, at $\lesssim 2\sigma$, with the current experimental values for these quantities provided in [33][3]. This then justifies why we have chosen to use the fixed values in (5.14) for the SM parameters.

For the EWPMs related quantities discussed above, we obtain the following NP contributions

$$\begin{aligned} \Delta m_{B_d}^{\text{NP}} &\simeq 1.453 \times 10^{-12}\ \text{MeV}, \\ \Delta m_{B_s}^{\text{NP}} &\simeq 2.419 \times 10^{-12}\ \text{MeV}, \\ \Delta m_K^{\text{NP}} &\simeq 7.522 \times 10^{-13}\ \text{MeV}, \\ |\varepsilon_K^{\text{NP}}| &\simeq 4.959 \times 10^{-3}, \\ \frac{\text{Br}\left(K^+ \to \pi^+ \overline{\nu}\nu\right)}{\text{Br}(K^+ \to \pi^+ \overline{\nu}\nu)_{\text{SM}}} &\simeq 0.281, \end{aligned} \tag{5.40}$$

which, as stated, clearly emphasises the problem with the limit $s_{24} = s_{34} = 0$ and the value for the parameter $|\varepsilon_K^{\text{NP}}|$ as its value is about 20 times larger than $\delta\varepsilon_K$.

[3]One should compare the magnitudes of the mixings in (5.37) with their current best-fit values without imposing CKM unitarity. Then, it should be noted that, given the very low uncertainty associated to $|V_{ud}| = 0.97370 \pm 0.00014$ not all values of $s_{14} \in [0.03, 0.05]$ allow for deviations smaller than 3σ, but this is the only quantity studied here that is affected by that problem.

Chapter 6

The limit of realistic s_{14}-dominance: solving the ε_K problem

Even if one overlooks the intrinsic problem with ε_K, the limit of strict s_{14}-dominance is somewhat unnatural. In a more realistic scenario one would have $s_{24}, s_{34} \neq 0$ and could reasonably expect $|\varepsilon_K^{\mathsf{NP}}| < \delta\varepsilon_K$ to be achievable. However, in order to keep the simplicity and other interesting features of s_{14}-dominance one might have to require $s_{24}, s_{34} \ll s_{14}$, which amounts to replacing the strict s_{14}-dominance limit by a more realistic version. Nonetheless, a priori, it is not obvious that a small deviation from $s_{24}, s_{34} = 0$ would lead to $|\varepsilon_K^{\mathsf{NP}}| < \delta\varepsilon_K$ and thus the framework of s_{14}-dominance could be entirely incompatible with the resolution of the ε_K problem.

We will now show that this is not the case. More concretely, we will show that it is possible to achieve $|\varepsilon_K^{\mathsf{NP}}| < \delta\varepsilon_K$ in the allowed range for m_T, while having $s_{14} = 0.04 \pm 0.01 \sim \lambda^2$ and

$$s_{24}, s_{34} \lesssim \lambda^5, \tag{6.1}$$

with the most important features of strict s_{14}-dominance being effectively preserved.

Firstly, we will show how small NP contributions to ε_K can be obtained in this more realistic limit. Later, possible modifications to the observables analysed in section 5.2.2 are discussed. To conclude, we study the NP that emerges with $s_{24}, s_{34} \neq 0$ in processes that remained unaffected in the strict s_{14}-dominance limit.

The ultimate goal is once again to find allowed regions of the parameter space, where the model is able to overcome the NP constraints studied in chapter 4, but now within this slightly different framework.

6.1 Solving the ε_K problem with $s_{24}, s_{34} \ll s_{14}$

Using the BC parametrization, with the approximation

$$c_{13}, c_{23}, c_{24}, c_{34} \simeq 1 \tag{6.2}$$

which we shall use throughout this chapter and rephasing the left-handed heavy top quark field as $T_L \to e^{i\delta_{14}} T_L$, we parametrize the CKM matrix, in leading order, as

$$\mathcal{V}_{\text{CKM}} = \begin{pmatrix} V_{11} & V_{12} & V_{13} \\ V_{21} - c_{12}s_{14}s_{24}e^{-i\delta'} & V_{22} - s_{12}s_{14}s_{24}e^{-i\delta'} & V_{23} \\ V_{31} - c_{12}s_{14}s_{34}e^{i\delta_{14}} & V_{32} & V_{33} \\ V_{41} + s_{12}s_{24}e^{i\delta'} & V_{42} - c_{12}s_{24}e^{i\delta'} - c_{12}s_{23}s_{34}e^{-i\delta_{14}} & V_{43} - s_{23}s_{24}e^{i\delta'} - s_{34}e^{-i\delta_{14}} \end{pmatrix} + \mathcal{O}(\lambda^8), \tag{6.3}$$

where now we employ an important change of notation: $V_{\alpha\beta}$ with $\alpha = u, c, t$ and $\beta = d, s, b$ will henceforth refer to the entries of (6.3), the mixing matrix in the realistic limit; V_{ij} with $i, j = 1, 2, 3, 4$ will refer to the entries of (5.11) the mixing matrix in the strict s_{14}-dominance limit. Also, in (6.3), we relax one of the upper-bounds in (6.1) and assume even that $s_{24} \lesssim \lambda^4$. As done in (5.7), we introduced the phase difference $\delta' \equiv \delta_{24} - \delta_{14}$, which plays a role further on.

The new correction to the mixings will not meaningfully affect the magnitudes or the phases of the SM mixings, but, most important, will introduce new terms in the expression of $|\varepsilon_K^{\text{NP}}|$. One now obtains,

$$|\varepsilon_K^{\text{NP}}| \simeq \frac{G_F^2 M_W^2 m_K f_K^2 B_K \kappa_\varepsilon}{6\sqrt{2}\pi^2 \Delta m_K} \left| \mathcal{F} - \mathcal{F}' \right|, \tag{6.4}$$

Apart from physical constants, $\mathcal{F}$ corresponds to the NP piece that arises from having $s_{14} \neq 0$ and $s_{24}, s_{34} = 0$ as before in (5.33), while now $\mathcal{F}'$ corresponds to the corrections to the NP piece arising from relaxing this limit and allowing $s_{24}, s_{34} \neq 0$ too. This new factor $\mathcal{F}'$ is, in a very good approximation, given by

$$\mathcal{F}' \simeq \mathcal{F}'_1 \sin\delta' + \mathcal{F}'_2 \sin(\delta - \delta') + \mathcal{F}'_3 \sin 2\delta', \tag{6.5}$$

where

$$\begin{aligned} \mathcal{F}'_1 &= (\tilde{S}_{TT} s_{14}^2 - \tilde{S}_{tT} s_{23}^2 - \tilde{S}_{cT}) s_{12} c_{12} s_{14} s_{24}, \\ \mathcal{F}'_2 &= \tilde{S}_{tT} s_{13} s_{23} s_{14} s_{24}, \\ \mathcal{F}'_3 &= \tfrac{1}{2} \tilde{S}_{TT} s_{14}^2 s_{24}^2, \end{aligned} \tag{6.6}$$

and $\tilde{S}_{iT} \equiv S_{iT} \eta_{iT}^K$ with $i = c, t, T$. Using (5.33), (6.1) and (6.2) and keeping only the leading order terms, one obtains

$$\mathcal{F} - \mathcal{F}' \simeq s_{12} c_{12} s_{14}^2 \left(\tilde{S}_{tT} s_{13} s_{23} \sin\delta - \tilde{S}_{TT} s_{14} s_{24} \sin\delta' \right), \tag{6.7}$$

which suggests that having $\sin\delta' > 0$ may allow one to obtain smaller $|\varepsilon_K^{\text{NP}}|$. Note that in the PDG (and hence in the BC) parametrization $\sin\delta > 0$). In figure 6.1, a plot of $|\varepsilon_K^{\text{NP}}|$ as a function of m_T using the exact expression (6.4) is presented with (5.14) as input parameters as well as

$$s_{14} = 0.04, \qquad \delta' = \frac{\pi}{2}, \tag{6.8}$$

for various values of $s_{24} \lesssim \lambda^5$. This plot clearly illustrates how the new terms in (6.5) can effectively cancel the original terms (5.33) allowing one to achieve $|\varepsilon_K^{\text{NP}}| < \delta\varepsilon_K$ for a large range of heavy-top masses.

It is important to note, however, that this cancellation is not achieved through a fine-tuning of the new parameters s_{24} and δ'. In fact, it turns out that there exists a considerable range for these parameters where this results can be achieved, as will be demonstrated in section 6.5, where a global analysis is carried out that simultaneously takes into account the constraints associated with other relevant EWPMs quantities.

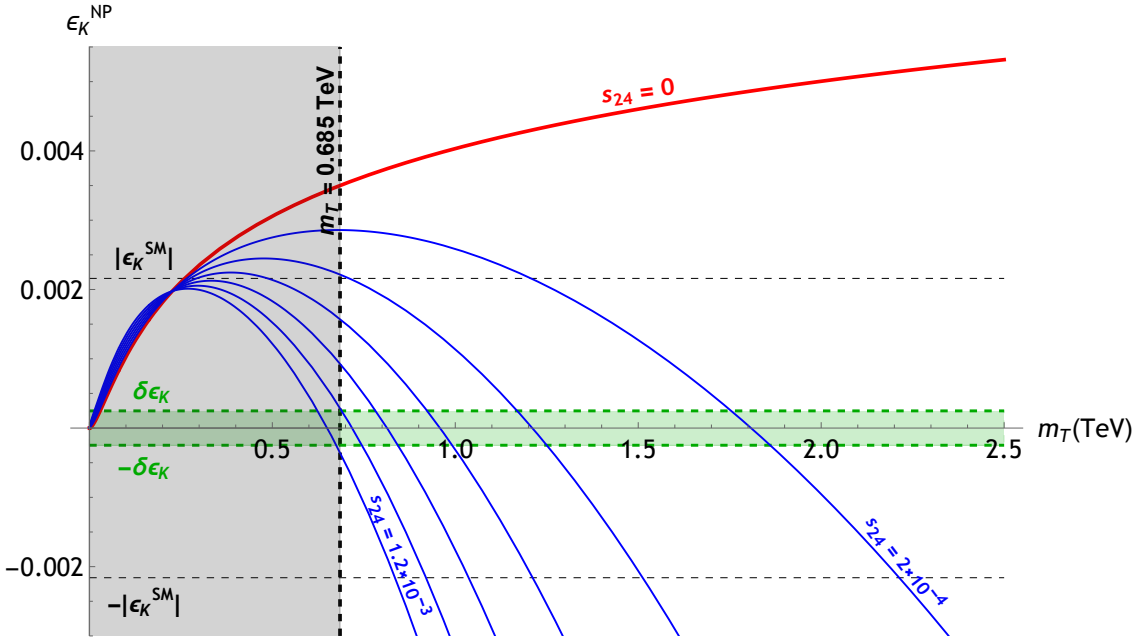

Figure 6.1: Analogous plot to that of figure 5.7 but for realistic dominance with $\theta_{14} = 0.04$ and $\delta' = \pi/2$. Various values of s_{24} are spanned in steps of 2×10^{-4} for $s_{24} \in [0, 1.2 \times 10^{-3}]$. The curve for $s_{24} = 0$ (in red) corresponds to the solid line in figure 5.7. The region $|\epsilon_K^{\text{NP}}| < \delta\varepsilon_K$ is highlighted.

Interestingly, the leading order and next to leading order terms of the corrections to NP contributions in (6.5) and (6.6) depend only on two new parameters, s_{24} and the phase difference δ'. Furthermore, notice that for $s_{14}, s_{24} \neq 0$ and $s_{34} = 0$, after the appropriate rephasing of the quark fields, (5.2) can be written as

$$\mathcal{V}^\dagger = \begin{pmatrix} 1 & 0 & 0 & 0 \\ 0 & c_{24} & 0 & s_{24} \\ 0 & 0 & 1 & 0 \\ 0 & -s_{24} & 0 & c_{24} \end{pmatrix} \begin{pmatrix} c_{14} & 0 & 0 & s_{14}e^{i\delta'} \\ 0 & 1 & 0 & 0 \\ 0 & 0 & 1 & 0 \\ -s_{14}e^{-i\delta'} & 0 & 0 & c_{14} \end{pmatrix} \cdot$$

$$\cdot \begin{pmatrix} 1 & 0 & 0 & 0 \\ 0 & c_{23} & s_{23} & 0 \\ 0 & -s_{23} & c_{23} & 0 \\ 0 & 0 & 0 & 1 \end{pmatrix} \begin{pmatrix} c_{13} & 0 & s_{13}e^{-i\delta} & 0 \\ 0 & 1 & 0 & 0 \\ -s_{13}e^{i\delta} & 0 & c_{13} & 0 \\ 0 & 0 & 0 & 1 \end{pmatrix} \begin{pmatrix} c_{12} & s_{12} & 0 & 0 \\ -s_{12} & c_{12} & 0 & 0 \\ 0 & 0 & 1 & 0 \\ 0 & 0 & 0 & 1 \end{pmatrix}, \tag{6.9}$$

δ' is the effective NP phase corresponding to the "two angle limit" where s_{14} and s_{24} are the only NP mixing angles, not δ_{14} as one could have assumed. This seems to indicate that having $s_{34} \neq 0$ is not really necessary to obtain $|\varepsilon_K^{\text{NP}}| \lesssim \delta\varepsilon_K$ and that this "two angle limit" with dominant s_{14} and small s_{24} may correspond to a minimal solution to the CKM-UP, the minimal solution that circumvents the ε_K problem. Nonetheless, in a more realistic scenario where $s_{34} \neq 0$, one can still have $s_{34} \sim \lambda^5$, without it affecting ε_K in any meaningful way. In fact only for $s_{34} \gtrsim \lambda^3$, do the leading order terms in (6.7) start depending on s_{34} and explicitly on δ_{14}. Still, it is not yet clear whether the implications of realistic s_{14}-dominance on other processes allow this "two angle limit" with vanishing s_{34}. These modifications will be the focus of the following section.

6.2 Modifications to $K^0 - \overline{K}^0$, $B^0_{d,s} - \overline{B}^0_{d,s}$ and $K^+ \to \pi^+ \overline{\nu}\nu$

When considering a realistic dominance case, many entries of V_{CKM} are modified as seen in (6.3). As shown in the previous section, these changes can lead to significant changes to $|\varepsilon_K^{\text{NP}}|$ and therefore, could potentially lead to important modifications to Δm_K^{NP}, $\text{Br}\,(K^+ \to \pi^+ \overline{\nu}\nu)$ or even $\Delta m_{B_{d,s}}^{\text{NP}}$. That is what we will check now, using (6.1). We shall skip a detailed study of the modifications to the heavy-top decays, but by analysing (6.3) and (5.7) it is easy to verify that with the prescription in (6.1) no meaningful changes will occur. The only result of relative significance is that the widths in (5.16) will no longer be strictly zero, but still very small.

All the changes to Δm_N^{NP} come essentially from modifications to λ_i^N with $i = c, t, T$. In the case of Δm_K^{NP} one has

$$\begin{aligned} \lambda_c^K &\simeq V_{21}V_{22}^* + \mathcal{O}(\lambda^7), \\ \lambda_t^K &\simeq V_{31}V_{32}^* + \mathcal{O}(\lambda^9), \\ \lambda_T^K &\simeq V_{41}V_{42}^* \left(1 - c_{12}s_{24}e^{-i\delta'}/V_{42}^*\right) + \mathcal{O}(\lambda^9), \end{aligned} \tag{6.10}$$

and given that $c_{12}s_{24}/V_{42}^* \sim \lambda^2 \simeq 5\%$, one can expect Δm_K^{NP} not to change significantly.

In the case of $\Delta m_{B_d}^{\text{NP}}$, one has

$$\begin{aligned}
\lambda_c^{B_d} &\simeq V_{21}V_{23}^* + \mathcal{O}(\lambda^9), \\
\lambda_t^{B_d} &\simeq V_{31}V_{33}^* + \mathcal{O}(\lambda^7), \\
\lambda_T^{B_d} &\simeq V_{41}V_{43}^* \left(1 - s_{34}e^{-i\delta_{14}}/V_{43}^*\right) + \mathcal{O}(\lambda^9),
\end{aligned} \tag{6.11}$$

and, since $V_{43}^* \sim \lambda^5$, $\Delta m_{B_d}^{\text{NP}}$ can change noticeably for $s_{34} \sim \lambda^5$. However, given how small δm_{B_d} is in the strict limit $(s_{24}, s_{34} = 0)$, it is safe to assume that these changes are not large enough to compromise the safety of the realistic limit with regard to the $B_d^0 - \overline{B}_d^0$ mixing. Moreover, the smaller s_{34} is, the smaller these changes will be and in the "two angle limit" ($s_{34} = 0$) discussed in the previous section, changes of around 5% or smaller can be expected, recovering essentially the value of $\Delta m_{B_d}^{\text{NP}}$ in the absolute s_{14}-dominance limit.

Similarly, for $\Delta m_{B_s}^{\text{NP}}$ one has

$$\begin{aligned}
\lambda_c^{B_s} &\simeq V_{22}V_{23}^* + \mathcal{O}(\lambda^{10}), \\
\lambda_t^{B_s} &\simeq V_{32}V_{33}^* + \mathcal{O}(\lambda^{10}), \\
\lambda_T^{B_s} &\simeq V_{41}V_{43}^* \left(1 - s_{34}e^{-i\delta_{14}}/V_{43}^*\right) + \mathcal{O}(\lambda^{10}),
\end{aligned} \tag{6.12}$$

and for $s_{34} \sim \lambda^5$ no dangerous changes can occur. For even smaller s_{34}, the result of strict s_{14}-dominance is essentially recovered.

To study the modifications to $\text{Br}\,(K^+ \to \pi^+ \overline{\nu}\nu)$, it is instructive to compute the factor A_{ds} again, now in this limit of realistic s_{14}-dominance. In general it is given by

$$\begin{aligned}
A_{ds} = {} & \lambda_c^K (F^u - \mathbb{1})_{22} N(x_c) + \lambda_t^K (F^u - \mathbb{1})_{33} N(x_t) + \lambda_T^K (F^u - \mathbb{1})_{44} N(x_T) \\
& + V_{cs}^* V_{td} (F^u - \mathbb{1})_{23} N(x_c, x_t) + V_{ts}^* V_{cd} (F^u - \mathbb{1})_{32} N(x_t, x_c) \\
& + V_{cs}^* V_{Td} (F^u - \mathbb{1})_{24} N(x_c, x_T) + V_{Ts}^* V_{cd} (F^u - \mathbb{1})_{42} N(x_T, x_c) \\
& + V_{ts}^* V_{Td} (F^u - \mathbb{1})_{34} N(x_t, x_T) + V_{Ts}^* V_{td} (F^u - \mathbb{1})_{43} N(x_T, x_t).
\end{aligned} \tag{6.13}$$

From (5.7) it is obvious that, for $s_{14} \sim \lambda^2$ and $s_{24}, s_{34} \lesssim \lambda^5$, the entry $(F^u - \mathbb{1})_{44} \approx 1$ is by far the largest of all the entries involved in (6.13), a result that somewhat resembles the decoupling limit in (4.47). This, coupled with the fact that

$$N(x_c) \ll N(x_t) \lesssim \frac{N(x_T)}{15} \tag{6.14}$$

within the mass range $m_T \in [0.685, 2.5]$ TeV and the fact that $|\lambda_t^K| \sim |\lambda_T^K|$, means that the first line of (6.13) is completely dominated by the heavy-top contribution. Similarly, it is straightforward to conclude that all the remaining terms in (6.13) are very small, so that, to a very good approximation, one has

$$A_{ds} \simeq -\lambda_T^K \frac{x_T}{8}. \tag{6.15}$$

Once more, this expression is the same as the one encountered in (4.48) for the approximate decoupling limit. Comparing this with the result in (5.29), one concludes that there are no meaningful changes to A_{ds} when deviating from $s_{24}, s_{34} = 0$.

Therefore the main modifications to the ratio

$$\frac{\text{Br}\,(K^+ \to \pi^+ \overline{\nu}\nu)}{\text{Br}\,(K^+ \to \pi^+ \overline{\nu}\nu)_{\text{SM}}} \simeq \left| 1 + \frac{\lambda_T^K \tilde{X}_0(x_T)}{\lambda_c^K X_0^{\text{NNL}}(x_c) + \lambda_t^K X_0(x_t)} \right|^2, \tag{6.16}$$

will essentially come from modifications to λ_T^K which as was shown in (6.10) are expected to be small. Therefore, one can expect the results from strict s_{14}-dominance limit to be recovered. Nonetheless, the NLO correction to λ_T^K which depends on both s_{24} and δ' allows for a bit more tweaking, so that the range of values for s_{14} that allows for the conditions in (4.47) to be achieved might be slightly larger. Varying s_{34} will not yield any noticeable changes, so that this in this limit, this quantity is effectively independent of s_{34}.

6.3 Numerical Example II: Realistic s_{14}-dominance with very small s_{24}, s_{34}

To exemplify our more realistic case near to our exact s_{14}-dominance, now with very small s_{24}, s_{34}, we consider the slightly different up-mass matrix (from the previous numerical example) given in GeV at the M_Z scale:

$$\mathcal{M}_u = \begin{pmatrix} 0 & 0 & 0 & 56.8458 \\ 0 & 0 & 7.28841 & 13.5107\, e^{1.90426i} \\ 0 & 18.9003 & 172.766 & 4.5632\, e^{-1.57415i} \\ 0.0428698 & 1.66405 & 36.522\, e^{-1.52607i} & 1390.29 \end{pmatrix}, \tag{6.17}$$

which leads to the same mass spectrum as the one in Eq. (5.36) and to

$$|\mathcal{V}^\dagger| \simeq \begin{pmatrix} 0.973615 & 0.224271 & 0.00369673 & 0.0419877 \\ 0.224355 & 0.973666 & 0.0404887 & 0.000499559 \\ 0.00853049 & 0.0397524 & 0.999173 & 1.4987 \times 10^{-6} \\ 0.0408234 & 0.00983053 & 0.000152441 & 0.999118 \end{pmatrix}, \tag{6.18}$$

which is extremely similar to (5.37). In this case, one can check that (6.18) corresponds to having

$$s_{14} = 0.042, \qquad s_{24} = 5 \times 10^{-4}, \qquad s_{34} = 1.5 \times 10^{-6}, \qquad \delta_{14} = 0, \qquad \delta_{24} = 0.6, \tag{6.19}$$

as well as (5.14), so that, although non-zero, s_{24} and especially s_{34} are still very small.

The rephasing invariant phases area also very similar to before, now being

$$\sin(2\beta) = 0.7278, \quad \gamma = 69.58°, \quad \chi = 0.01960, \quad \chi' = 0.000588093. \tag{6.20}$$

The same happens for the CP violation invariant which in this case is $|J| = 3.064 \times 10^{-5}$.

The following EWPMs observables, now have the following NP contributions

$$\begin{aligned}
\Delta m_{Bd}^{\text{NP}} &\simeq 1.423 \times 10^{-12}\ \text{MeV}, \\
\Delta m_{Bs}^{\text{NP}} &\simeq 2.475 \times 10^{-12}\ \text{MeV}, \\
\Delta m_{K}^{\text{NP}} &\simeq 8.188 \times 10^{-13}\ \text{MeV}, \\
|\varepsilon_K^{\text{NP}}| \ &\simeq 2.324 \times 10^{-4}, \\
\frac{\text{Br}\left(K^+ \to \pi^+ \overline{\nu}\nu\right)}{\text{Br}(K^+ \to \pi^+ \overline{\nu}\nu)_{\text{SM}}} &\simeq 0.311.
\end{aligned} \tag{6.21}$$

As it is clear, the problem with ε_K is now successfully solved. Comparing (5.40) and (6.21) one also sees that although noticeable changes to $\Delta m_{Bd}^{\text{NP}}$ and $\Delta m_{Bs}^{\text{NP}}$ took place, these are still small and in no way compromise the safety of the model. Therefore, this realistic scenario is successful in solving the ε_K problem while preserving the most relevant and interesting features of s_{14}-dominance and by employing only very small deviations to the strict s_{14}-dominance limit.

Nonetheless, given that now Imλ_T^K and F_{12}^u are not strictly zero, some processes that in the previous limit received no NP contribution, now might be significantly modified. We will focus on this in the following section.

6.4 Emergence of extra New Physics

One of the most important features of the strict s_{14}-dominance is that many of the processes discussed in chapter 4 receive extremely small or even no NP contribution at all. When adopting the more realistic limit even the processes originally unaffected by having $s_{14} \neq 0$ will now have non-zero NP contributions and it is crucial to verify whether those contributions can compromise the validity of the realistic limit.

6.4.1 $D^0 - \overline{D}^0$ mixing

For $s_{34}, s_{24} \neq 0$, in the BC parametrization, one has

$$x_D^{\mathsf{NP}} \simeq \frac{\sqrt{2} m_D}{3\Gamma_D} G_F f_D^2 B_D r(m_c, M_Z) c_{14}^2 s_{14}^2 s_{24}^2, \tag{6.22}$$

which in fact is the general formula for the NP contribution of this parameter in a model with an heavy-top. Hence, despite the fact that once more we have a quantity independent of s_{34}, this time this independence is unrelated to the mixing limit we chose. Thus with this parameter, one will only be able to impose constraints on s_{24}.

Then, for any value of s_{14} in the range $s_{14} \in [0.03, 0.05]$ one can achieve the condition introduced in (4.37)

$$x_D^{\mathsf{NP}} < x_D^{\mathsf{exp}} = 0.39^{+0.11}_{-0.12}\%, \tag{6.23}$$

provided that $s_{24} \lesssim 0.002 \sim \lambda^4$, which is a somewhat larger upper-bound than our assumption in (6.1). Hence, this limit is safe with regard to D^0 oscillations.

On the flip side this result means that, within this context no meaningful enhancement to this parameter can be achieved. For instance, for $s_{14} \simeq 0.05$ and $s_{24} \simeq 0.001$ one obtains $x_D^{\mathsf{NP}} \simeq 0.066\%$, which is around 2.7σ away from the experimental value, but still better than the strict s_{14}-dominance case, where no enhancement is found.

6.4.2 The $K_L \to \pi^0 \overline{\nu}\nu$ decay

In general with $s_{24}, s_{34} \neq 0$ one has $\mathsf{Im}\lambda_T^K \neq 0$ leading to a non-zero NP contribution to the branching ratio of $K_L \to \pi^0 \overline{\nu}\nu$. Using (6.1) one has

$$\begin{aligned} \mathsf{Im}\lambda_t^K &\simeq s_{13} s_{23} \sin\delta, \\ \mathsf{Im}\lambda_T^K &\simeq -c_{12}^2 s_{14} s_{24} \sin\delta', \end{aligned} \tag{6.24}$$

so that using the expressions in (4.42), one can write

$$\frac{\mathsf{Br}\left(K_L \to \pi^0 \overline{\nu}\nu\right)}{\mathsf{Br}\left(K_L \to \pi^0 \overline{\nu}\nu\right)_{\mathsf{SM}}} \simeq \left| 1 + \frac{\mathsf{Im}\lambda_T^K \tilde{X}_0(x_T)}{\mathsf{Im}\lambda_t^K X_0(x_t)} \right|^2 \simeq \left| 1 - \frac{c_{12}^2 s_{14} s_{24} \sin\delta'}{s_{13} s_{23} \sin\delta} \frac{\tilde{X}_0(x_T)}{X_0(x_t)} \right|^2, \tag{6.25}$$

where within our range of interest for m_T, one has to a very good approximation

$$\tilde{X}_0(x_T) \simeq \frac{3}{8}\left(1 + \log x_T\right) \lesssim 2 X_0(x_t). \tag{6.26}$$

With this in mind, it is easy to check that for $s_{24} \lesssim 0.001$, one obtains

$$\frac{c_{12}^2 s_{14} s_{24}}{s_{13} s_{23} \sin\delta} \lesssim \frac{1}{4} \tag{6.27}$$

and since $\sin\delta' > 0$ is needed to solve the ε_K problem, one should have

$$\frac{1}{4} \lesssim \frac{\text{Br}\left(K_L \to \pi^0 \overline{\nu}\nu\right)}{\text{Br}\left(K_L \to \pi^0 \overline{\nu}\nu\right)_{\text{SM}}} \leq 1, \tag{6.28}$$

so that a reduction of the branching ratio is expected when compared with the SM prediction. This seems to suggest that the KOTO experimental upper-bound for this quantity (see the discussion in 4.4.1) may possibly still be too high. If nothing, it is clear that any NP contribution coming from a model with an heavy-top in the s_{14}-dominance limit cannot bridge the gap between theory and experiment. Nonetheless, combining this type of model with some other New Physics beyond the SM, particularly in the neutrino sector may perhaps be able to significantly enhance the theoretical prediction.

Again, note that s_{34} does not play a role in this limit, at leading order.

6.4.3 The parameter ε'/ε

Recall from (4.63) that the NP contribution to this parameter is given by

$$\left(\frac{\varepsilon'}{\varepsilon}\right)_{\text{NP}} \simeq \tilde{F}(x_i)\text{Im}\lambda_T^K. \tag{6.29}$$

As mentioned previously, in the strict s_{14}-dominance limit there is no NP contribution to ε'/ε given that $\text{Im}\lambda_T^K = 0$, and the condition

$$-4 \times 10^{-4} \lesssim \left(\frac{\varepsilon'}{\varepsilon}\right)_{\text{NP}} \lesssim 10 \times 10^{-4}, \tag{6.30}$$

is trivially verified. For $s_{24}, s_{34} \neq 0$ one obtains

$$\left(\frac{\varepsilon'}{\varepsilon}\right)_{\text{NP}} \simeq -\tilde{F}(x_i) c_{12}^2 s_{14} s_{24} \sin\delta', \tag{6.31}$$

by using (6.24). Once more, note that within the framework of s_{14}-dominance, this NP contribution is independent of s_{34} at leading order.

We now take the decoupling limit, which as we have seen earlier is a good approximation in both s_{14}-dominance scenarios. Therefore, we shall use

$$\tilde{F}(x_T) = F(x_T) - \frac{x_T}{8}\left(P_X + P_Y + P_Z\right). \tag{6.32}$$

In the region of interest $m_T \in [0.685, 2.5]$ TeV, from Appendix A one can write

$$\tilde{F}(x_T) \simeq P_0 + P_X \tilde{X}_0(x_T) + P_Y \tilde{Y}_0(x_T) + P_Z \tilde{Z}_0(x_T), \tag{6.33}$$

where, similarly to (6.26), one has

$$\tilde{Y}_0(x_T) \equiv Y_0(x_T) - \frac{x_T}{8} \simeq -\frac{3}{8}\left(1 - \log x_T\right), \tag{6.34}$$

$$\tilde{Z}_0(x_T) \equiv Z_0(x_T) - \frac{x_T}{8} \simeq -\frac{109}{144} + \frac{\log x_T}{3},$$

as well as

$$P_E E(x_T) \ll P_0, P_W \tilde{W}_0(x_T), \tag{6.35}$$

where $W = X, Y, Z$. In the end, one can approximate

$$\tilde{F}(x_T) \approx P_1 + P_2 \log x_T, \tag{6.36}$$

with

$$P_1 = P_0 + \tfrac{3}{8}P_X - \tfrac{3}{8}P_Y - \tfrac{109}{144}P_Z \simeq 21.67, \tag{6.37}$$

$$P_2 = \tfrac{3}{8}P_X + \tfrac{3}{8}P_Y + \tfrac{1}{3}P_Z \simeq -2.54.$$

Within the range $m_T \in [0.685, 2.5]$ TeV, this approximation[1] yields an error no bigger than 6% while providing a much simpler form when compared to (6.32) and (4.58), allowing for a quick analysis of this NP contribution. For instance, given that $\log x_T \lesssim 7$ for $m_T \leq 2.5$ TeV, one can immediately conclude that $\tilde{F}(x_T) > 0$ and $(\varepsilon'/\varepsilon)_{\text{NP}} < 0$ in this mass range, so that the upper-bound of (6.30) is never achieved within the framework of s_{14}-dominance.

Moreover, it is now clear that the NP contribution is an increasing function of m_T in our range of interest. Therefore, for any given set of parameters s_{14}, s_{24} and δ', one has

$$-\left[\tilde{F}(x_T)|_{m_T=0.685\ \text{TeV}}\right] c_{12}^2 s_{14} s_{24} \sin\delta' \leq \left(\frac{\varepsilon'}{\varepsilon}\right)_{\text{NP}} \leq 0, \tag{6.38}$$

and the problem reduces to finding the regions in $(s_{14}, s_{24}, \delta')$ space where

$$-4 \times 10^{-4} \leq -\left[\tilde{F}(x_T)|_{m_T=0.685\ \text{TeV}}\right] c_{12}^2 s_{14} s_{24} \sin\delta'. \tag{6.39}$$

In terms of s_{24} one has

$$s_{24} \lesssim \frac{4 \times 10^{-4} \cdot \left(P_1 + P_2 \log x_T\right)|_{m_T=0.685\ \text{TeV}}}{c_{12}^2 s_{14} \sin\delta'}, \tag{6.40}$$

with the RHS being the lowest within $s_{14} \in [0.03, 0.05]$, for $s_{14} = 0.05$ and $\delta' = \pi/2$, where one has $s_{24} \lesssim 7.8 \times 10^{-4}$. Within our parameter regions of interest, this is the most stringent constraint to s_{24} originating from the condition (6.30). Nonetheless, for other values of s_{14} and δ', important constraints

[1] Note that in this mass range this is a good approximation for any model with an heavy-top, provided that the decoupling limit offers a good approximation to A_{ds}, i.e not necessarily just in the s_{14}-dominance limits.

on s_{24} might still be imposed by (6.30), i.e. one might still achieve upper-bounds for s_{24} compatible with the $s_{24} \sim \lambda^5$ prescription.

All in all, there seems to exist a considerably large region of parameters where values as large as $s_{24} \sim \lambda^5$ are allowed, although larger values of s_{14} and $\sin\delta'$ seem to slightly be disfavoured. This means that, contrary to the strict s_{14}-dominance limit, the realistic limit is safe with regard to all the processes and EWPM-parameters we proposed to study. However, our understanding of the parameter space based on the individual analyses presented throughout this chapter for each process, would substantially benefit from a global analysis .

6.5 Global Analysis

It is then instructive to present a global analysis of the parameter space of our realistic s_{14}-dominance case, subject to all the phenomenological constraints we just discussed. In particular, we look for the allowed ranges for s_{14}, s_{24}, δ' and m_T .

In figure 6.2 we present the result of a simulation of 10^6 points (see Appendix C), with $s_{14}, s_{24}, s_{34}, \delta_{14}, \delta_{24}$ and m_T as the free parameters. These span values of s_{14} that allow for the CKM unitarity problem to be solved and values of s_{24}, s_{34} compatible with the realistic case of s_{14}-dominance. More concretely the ranges used for the free parameters are

$$\delta_{14}, \delta_{24} \in [0, 2\pi], \qquad s_{14} \in [0.03, 0.05], \qquad s_{24}, s_{34} \in [0, 0.001], \qquad m_T \in [0.685, 2.5]\,\text{TeV}, \tag{6.41}$$

where the range for s_{24} and s_{34} are compatible with our assumption that $s_{24}, s_{34} \lesssim \lambda^5$.

The points displayed in figure 6.2 verify

$$\begin{gathered} |\varepsilon_K^{\text{NP}}| < \delta\varepsilon_K = 2.48 \times 10^{-4}, \\ \Delta m_K^{\text{NP}} < \Delta m_K^{\text{exp}} = 3.484 \times 10^{-12}\ \text{MeV}, \\ (\varepsilon'/\varepsilon)_{\text{NP}} \in [-4, 10] \times 10^{-4}, \\ \frac{\text{Br}(K^+ \to \pi^+ \overline{\nu}\nu)}{\text{Br}(K^+ \to \pi^+ \overline{\nu}\nu)_{\text{SM}}} \in [0.24, 2.28]. \end{gathered} \tag{6.42}$$

We do not impose any constraint associated to other observables such as $\Delta m_{B_{d,s}}$ and x_D, because as shown before their NP contributions are extremely suppressed in both limits of s_{14}-dominance. We also omit plots involving s_{34}, as this parameter, within the chosen range $s_{34} \in [0, 0.001]$, has no noticeable influence of importance on the outcome of the allowed parameter region. This gives strength to the notion that the "two angle limit" discussed in (6.1), might be the ultimate minimal solution to the CKM-UP.

Interestingly from the top panel of figure 6.2, one has $s_{24} \gtrsim 1 \times 10^{-4}$ as an approximate lower-bound

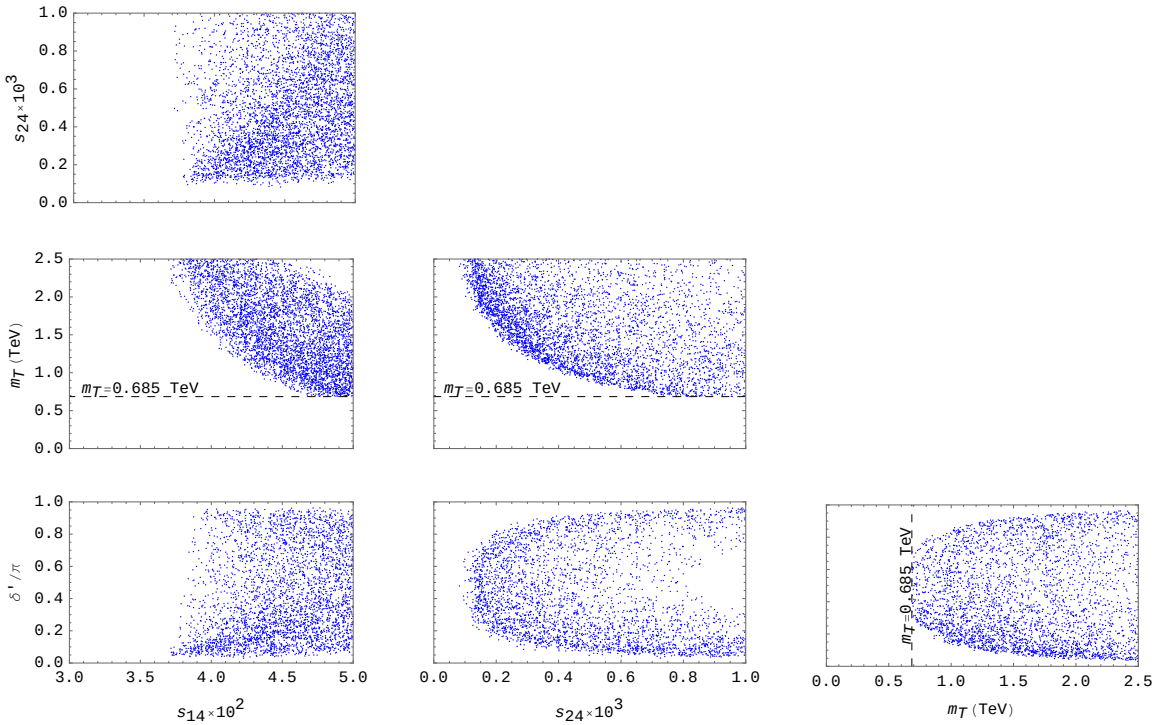

Figure 6.2: Results for the allowed parameter regions of our model verifying the conditions in (6.41, 6.42) and using (5.14).

for s_{24}. Nonetheless, one should keep in mind that this minimal-bound depends on the maximal heavy-top mass associated to the range we have chosen, in this case $m_T = 2.5$ TeV, as its clear from the central panel.

Overall, the results shown in these panels suggest that there exists a considerably large region in parameter space subject to the ranges given in (6.41), where the conditions (6.42) are fulfilled. It is important to note, however, that values around $s_{14} \lesssim 0.037$ seem to be extremely disfavoured. This is not surprising considering the results displayed in figure 5.6.

Chapter 7

Conclusions

Motivated by the success and simplicity of VLQ extensions in addressing the CKM-UP, we discussed, in this thesis, the main features and phenomenological implications of extensions of the SM with an heavy-top to processes such as neutral meson mixings and kaon decays. We chose to focus on models with just one up-type VLQ isosinglet as they provided the most simple of frameworks which succesfully address the CKM-UP, and which at the same time prove to be more "natural" than extensions with down-type VLQs.

Then, based on current experimental results and improved theoretical predictions, we established criteria for the safety of such models, i.e. conditions for the sizes of NP contributions of experimentally measurable quantities such as Δm_K, ε'/ε and ε_K that, for now, guarantee that the combination of SM and NP contributions do not deviate significantly from the experimental results. Most noteworthily, we have shown how, given the results of recent theoretical calculations for the SM prediction of ε_K which are very similar to the experimental value, the typical upper-bound for the NP contribution of this parameter $|\varepsilon_K^{\text{NP}}| \lesssim |\varepsilon_K^{\text{exp}}|$, should be replaced by the much more stringent condition $|\varepsilon_K^{\text{NP}}| \lesssim \delta\varepsilon_K$.

Having established these criteria, we then explored the possibility of having a minimal extension of the SM involving the sole introduction of an heavy-top quark T. This was implemented within the limit of s_{14}-dominance, where the introduction of $s_{14} \sim \lambda^2$ alone is sufficient to solve the CKM-UP, allowing the remaining mixing angles s_{24} and s_{34} to either be zero or much smaller.

In a first attempt, we explored the limit of strict s_{14}-dominance, where $s_{24} = s_{34} = 0$ and the NP phases δ_{14} and δ_{24} of the BC parametrization are unphysical. Within this limit, some extremely interesting features were encountered such as the dominant heavy-top decays to light quarks while decays to the bottom or top quark are very suppressed, which is a result that defies the usual assumption. In fact, this salient feature means that heavy-top masses as low as $m_T = 0.685$ TeV cannot be excluded, which is a value potentially accessible to the next generation of accelerators. Moreover, in this limit, not only does the 3×3 block of V_{CKM} containing the SM mixings remain essentially unchanged, but also the NP contributions to processes such as $D^0 - \overline{D}^0$, $K_L \to \pi^0\overline{\nu}\nu$ and to the parameter ε'/ε are automatically zero, while for $B^0_{d,s} - \overline{B}^0_{d,s}$, although non-zero, are still exceedingly small. These results demonstrated that this limit can, to a very significant extent, recover many of the SM predictions. Even processes

that may receive significant NP contributions like $K^0 - \overline{K}^0$ and $K^+ \to \pi^+ \overline{\nu}\nu$ do not strictly restrict the relatively small parameter space formed by the only two free parameters of the model: s_{14} and m_T. However, in the end, this limit failed to accommodate the new more stringent constraint we had set for the NP contribution of ε_K, leaving the whole parameter space for this limit completely excluded.

This result then lead us to explore a slightly modified version of this limit, the limit of realistic s_{14}-dominance, where the prescription for s_{14} was maintained as a means to solve the CKM-UP, but the assumption of vanishing s_{24} and s_{34} was relaxed and instead $s_{24}, s_{34} \sim \lambda^5$ was used, so that now δ_{14} and δ_{24} have to be considered. It was then shown that, in this limit, the problem previously encountered for ε_K could be satisfyingly solved leading to a reasonably large allowed region of parameters. Moreover, the results for the SM mixings, the heavy-top decays and the NP contributions to $K^0 - \overline{K}^0$, $B^0_{ds} - \overline{B}^0_{ds}$ and $K^+ \to \pi^+ \overline{\nu}\nu$, that where encountered in the strict limit where essentially recovered. The remaining processes which previously received no contribution, now do, but in this limit they are still very small and do not comprise the safety of the model. Interestingly, in this analysis the leading order expressions for all the NP contributions of the studied processes/parameters depend solely on three of the five new mixing parameters, the mixing angles s_{14} and s_{24}, as well as the phase difference $\delta' = \delta_{24} - \delta_{14}$. This means that the addition of s_{34} might be superfluous and the "two angle limit" defined by having $s_{14} \sim \lambda^2$, $s_{24} \sim \lambda^5$ and $s_{34} = 0$ and consequently δ' as the only relevant NP phase, should constitute the true minimal solution to the CKM-UP for one heavy-top models.

Finally, we conclude. Here, we have proposed an extremely useful minimal framework beyond the SM, that, while providing a solution to the CKM unitarity problem, has, in addition, exceptionally striking and intriguing new features which make it also a possible candidate model for finding New Physics.

Bibliography

[1] R. Davis, Jr., D. S. Harmer, and K. C. Hoffman. Search for neutrinos from the sun. *Phys. Rev. Lett.*, 20:1205–1209, 1968. doi: 10.1103/PhysRevLett.20.1205.

[2] Y. Fukuda et al. Evidence for oscillation of atmospheric neutrinos. *Phys. Rev. Lett.*, 81:1562–1567, 1998. doi: 10.1103/PhysRevLett.81.1562.

[3] J. K. Ahn et al. Observation of Reactor Electron Antineutrino Disappearance in the RENO Experiment. *Phys. Rev. Lett.*, 108:191802, 2012. doi: 10.1103/PhysRevLett.108.191802.

[4] G. C. Branco, H. R. C. Ferreira, A. G. Hessler, and J. I. Silva-Marcos. Universality of Strength of Yukawa Couplings, Quark Singlets and Strength of CP Violation. *JHEP*, 05:001, 2012. doi: 10.1007/JHEP05(2012)001.

[5] F. F. Deppisch. Lepton Flavour Violation and Flavour Symmetries. *Fortsch. Phys.*, 61:622–644, 2013. doi: 10.1002/prop.201200126.

[6] G. C. Branco, N. R. Ribeiro, and J. I. Silva-Marcos. Universal Democracy Instead of Anarchy. 4 2013.

[7] F. J. Botella, G. C. Branco, M. N. Rebelo, and J. I. Silva-Marcos. What if the masses of the first two quark families are not generated by the standard model Higgs boson? *Phys. Rev. D*, 94(11): 115031, 2016. doi: 10.1103/PhysRevD.94.115031.

[8] G. C. Branco, W. Grimus, and L. Lavoura. Relating the scalar flavor changing neutral couplings to the CKM matrix. *Phys. Lett. B*, 380:119–126, 1996. doi: 10.1016/0370-2693(96)00494-7.

[9] F. del Aguila, J. A. Aguilar-Saavedra, and G. C. Branco. CP violation from new quarks in the chiral limit. *Nucl. Phys. B*, 510:39–60, 1998. doi: 10.1016/S0550-3213(97)00708-6.

[10] G. C. Branco, R. G. Felipe, and F. R. Joaquim. Leptonic CP Violation. *Rev. Mod. Phys.*, 84:515–565, 2012. doi: 10.1103/RevModPhys.84.515.

[11] C.-Y. Seng, M. Gorchtein, H. H. Patel, and M. J. Ramsey-Musolf. Reduced Hadronic Uncertainty in the Determination of V_{ud}. *Phys. Rev. Lett.*, 121(24):241804, 2018. doi: 10.1103/PhysRevLett.121.241804.

[12] C. Y. Seng, M. Gorchtein, and M. J. Ramsey-Musolf. Dispersive evaluation of the inner radiative correction in neutron and nuclear β decay. *Phys. Rev. D*, 100(1):013001, 2019. doi: 10.1103/PhysRevD.100.013001.

[13] A. Czarnecki, W. J. Marciano, and A. Sirlin. Radiative Corrections to Neutron and Nuclear Beta Decays Revisited. *Phys. Rev. D*, 100(7):073008, 2019. doi: 10.1103/PhysRevD.100.073008.

[14] C.-Y. Seng, X. Feng, M. Gorchtein, and L.-C. Jin. Joint lattice QCD–dispersion theory analysis confirms the quark-mixing top-row unitarity deficit. *Phys. Rev. D*, 101(11):111301, 2020. doi: 10.1103/PhysRevD.101.111301.

[15] L. Hayen. Standard model $\mathcal{O}(\alpha)$ renormalization of g_A and its impact on new physics searches. *Phys. Rev. D*, 103(11):113001, 2021. doi: 10.1103/PhysRevD.103.113001.

[16] K. Shiells, P. G. Blunden, and W. Melnitchouk. Electroweak axial structure functions and improved extraction of the Vud CKM matrix element. *Phys. Rev. D*, 104(3):033003, 2021. doi: 10.1103/PhysRevD.104.033003.

[17] A. Czarnecki, W. J. Marciano, and A. Sirlin. Precision measurements and CKM unitarity. *Phys. Rev. D*, 70:093006, 2004. doi: 10.1103/PhysRevD.70.093006.

[18] Y. Aoki et al. FLAG Review 2021. 11 2021.

[19] D. A. Bryman and R. Shrock. Constraints on Sterile Neutrinos in the MeV to GeV Mass Range. *Phys. Rev. D*, 100:073011, 2019. doi: 10.1103/PhysRevD.100.073011.

[20] A. M. Coutinho, A. Crivellin, and C. A. Manzari. Global Fit to Modified Neutrino Couplings and the Cabibbo-Angle Anomaly. *Phys. Rev. Lett.*, 125(7):071802, 2020. doi: 10.1103/PhysRevLett.125.071802.

[21] A. Crivellin, F. Kirk, C. A. Manzari, and M. Montull. Global Electroweak Fit and Vector-Like Leptons in Light of the Cabibbo Angle Anomaly. *JHEP*, 12:166, 2020. doi: 10.1007/JHEP12(2020)166.

[22] B. Capdevila, A. Crivellin, C. A. Manzari, and M. Montull. Explaining $b \to s\ell^+\ell^-$ and the Cabibbo angle anomaly with a vector triplet. *Phys. Rev. D*, 103(1):015032, 2021. doi: 10.1103/PhysRevD.103.015032.

[23] L. Bento, G. C. Branco, and P. A. Parada. A Minimal model with natural suppression of strong CP violation. *Phys. Lett. B*, 267:95–99, 1991. doi: 10.1016/0370-2693(91)90530-4.

[24] F. del Aguila and M. J. Bowick. The Possibility of New Fermions With Δ I = 0 Mass. *Nucl. Phys. B*, 224:107, 1983. doi: 10.1016/0550-3213(83)90316-4.

[25] G. C. Branco and L. Lavoura. On the Addition of Vector Like Quarks to the Standard Model. *Nucl. Phys. B*, 278:738–754, 1986. doi: 10.1016/0550-3213(86)90060-X.

[26] G. Barenboim and F. J. Botella. Delta F=2 effective Lagrangian in theories with vector - like fermions. *Phys. Lett. B*, 433:385–395, 1998. doi: 10.1016/S0370-2693(98)00695-9.

[27] F. del Aguila, M. Perez-Victoria, and J. Santiago. Observable contributions of new exotic quarks to quark mixing. *JHEP*, 09:011, 2000. doi: 10.1088/1126-6708/2000/09/011.

[28] B. Belfatto, R. Beradze, and Z. Berezhiani. The CKM unitarity problem: A trace of new physics at the TeV scale? *Eur. Phys. J. C*, 80(2):149, 2020. doi: 10.1140/epjc/s10052-020-7691-6.

[29] G. C. Branco, J. T. Penedo, P. M. F. Pereira, M. N. Rebelo, and J. I. Silva-Marcos. Addressing the CKM unitarity problem with a vector-like up quark. *JHEP*, 07:099, 2021. doi: 10.1007/JHEP07(2021)099.

[30] B. Belfatto and Z. Berezhiani. Are the CKM anomalies induced by vector-like quarks? Limits from flavor changing and Standard Model precision tests. *JHEP*, 10:079, 2021. doi: 10.1007/JHEP10(2021)079.

[31] G. C. Branco, L. Lavoura, and J. P. Silva. *CP Violation*, volume 103. 1999.

[32] C. Giunti and C. W. Kim. *Fundamentals of Neutrino Physics and Astrophysics*. 2007. ISBN 978-0-19-850871-7.

[33] P. A. Zyla et al. Review of Particle Physics. *PTEP*, 2020(8):083C01, 2020. doi: 10.1093/ptep/ptaa104.

[34] F. J. Botella, G. C. Branco, M. Nebot, and M. N. Rebelo. Unitarity triangles and the search for new physics. *Nucl. Phys. B*, 651:174–190, 2003. doi: 10.1016/S0550-3213(02)01089-1.

[35] L. Wolfenstein. Parametrization of the Kobayashi-Maskawa Matrix. *Phys. Rev. Lett.*, 51:1945, 1983. doi: 10.1103/PhysRevLett.51.1945.

[36] D. Decamp et al. Determination of the Number of Light Neutrino Species. *Phys. Lett. B*, 231:519–529, 1989. doi: 10.1016/0370-2693(89)90704-1.

[37] L. M. Carpenter and A. Rajaraman. Revisiting Constraints on Fourth Generation Neutrino Masses. *Phys. Rev. D*, 82:114019, 2010. doi: 10.1103/PhysRevD.82.114019.

[38] V. Barger, J. Jiang, P. Langacker, and T. Li. String scale gauge coupling unification with vector-like exotics and non-canonical U(1)(Y) normalization. *Int. J. Mod. Phys. A*, 22:6203–6218, 2007. doi: 10.1142/S0217751X07038128.

[39] K. Kowalska and D. Kumar. Road map through the desert: unification with vector-like fermions. *JHEP*, 12:094, 2019. doi: 10.1007/JHEP12(2019)094.

[40] S. Zheng. Minimal Vectorlike Model in Supersymmetric Unification. *Eur. Phys. J. C*, 80(3):273, 2020. doi: 10.1140/epjc/s10052-020-7843-8.

[41] A. E. Nelson. Naturally Weak CP Violation. *Phys. Lett. B*, 136:387–391, 1984. doi: 10.1016/0370-2693(84)92025-2.

[42] S. M. Barr. Solving the Strong CP Problem Without the Peccei-Quinn Symmetry. *Phys. Rev. Lett.*, 53:329, 1984. doi: 10.1103/PhysRevLett.53.329.

[43] J. A. Aguilar-Saavedra. Effects of mixing with quark singlets. *Phys. Rev. D*, 67:035003, 2003. doi: 10.1103/PhysRevD.69.099901. [Erratum: Phys.Rev.D 69, 099901 (2004)].

[44] T. Inami and C. S. Lim. Effects of Superheavy Quarks and Leptons in Low-Energy Weak Processes k(L) —> mu anti-mu, K+ —> pi+ Neutrino anti-neutrino and K0 <—> anti-K0. *Prog. Theor. Phys.*, 65:297, 1981. doi: 10.1143/PTP.65.297. [Erratum: Prog.Theor.Phys. 65, 1772 (1981)].

[45] A. J. Buras and R. Fleischer. Quark mixing, CP violation and rare decays after the top quark discovery. *Adv. Ser. Direct. High Energy Phys.*, 15:65–238, 1998. doi: 10.1142/9789812812667_0002.

[46] G. Buchalla, A. J. Buras, and M. E. Lautenbacher. Weak decays beyond leading logarithms. *Rev. Mod. Phys.*, 68:1125–1144, 1996. doi: 10.1103/RevModPhys.68.1125.

[47] G. Cacciapaglia, A. Deandrea, L. Panizzi, N. Gaur, D. Harada, and Y. Okada. Heavy Vector-like Top Partners at the LHC and flavour constraints. *JHEP*, 03:070, 2012. doi: 10.1007/JHEP03(2012)070.

[48] J. Brod, M. Gorbahn, and E. Stamou. Standard-Model Prediction of ϵ_K with Manifest Quark-Mixing Unitarity. *Phys. Rev. Lett.*, 125(17):171803, 2020. doi: 10.1103/PhysRevLett.125.171803.

[49] G. C. Branco, P. A. Parada, and M. N. Rebelo. D0 - anti-D0 mixing in the presence of isosinglet quarks. *Phys. Rev. D*, 52:4217–4222, 1995. doi: 10.1103/PhysRevD.52.4217.

[50] E. Golowich, J. Hewett, S. Pakvasa, and A. A. Petrov. Relating D0-anti-D0 Mixing and D0 —> l+ l- with New Physics. *Phys. Rev. D*, 79:114030, 2009. doi: 10.1103/PhysRevD.79.114030.

[51] Y. S. Amhis et al. Averages of b-hadron, c-hadron, and τ-lepton properties as of 2018. *Eur. Phys. J. C*, 81(3):226, 2021. doi: 10.1140/epjc/s10052-020-8156-7.

[52] F. J. Botella, G. C. Branco, and M. Nebot. Singlet Heavy Fermions as the Origin of B Anomalies in Flavour Changing Neutral Currents. 12 2017.

[53] E. Nardi. Top - charm flavor changing contributions to the effective b s Z vertex. *Phys. Lett. B*, 365: 327–333, 1996. doi: 10.1016/0370-2693(95)01308-3.

[54] P. N. Kopnin and M. I. Vysotsky. Manifestation of a singlet heavy up-type quark in the branching ratios of rare decays K —> pi nu anti-nu, B —> pi nu anti-nu and B —> K nu anti-nu. *JETP Lett.*, 87:517–523, 2008. doi: 10.1134/S0021364008100019.

[55] I. Picek and B. Radovcic. Nondecoupling of terascale isosinglet quark and rare K- and B-decays. *Phys. Rev. D*, 78:015014, 2008. doi: 10.1103/PhysRevD.78.015014.

[56] G. Buchalla, A. J. Buras, and M. K. Harlander. Penguin box expansion: Flavor changing neutral current processes and a heavy top quark. *Nucl. Phys. B*, 349:1–47, 1991. doi: 10.1016/0550-3213(91)90186-2.

[57] A. J. Buras, D. Buttazzo, J. Girrbach-Noe, and R. Knegjens. $K^+ \to \pi^+\nu\overline{\nu}$ and $K_L \to \pi^0\nu\overline{\nu}$ in the Standard Model: status and perspectives. *JHEP*, 11:033, 2015. doi: 10.1007/JHEP11(2015)033.

[58] E. Cortina Gil et al. Measurement of the very rare $K^+ \to \pi^+\nu\overline{\nu}$ decay. *JHEP*, 06:093, 2021. doi: 10.1007/JHEP06(2021)093.

[59] A. J. Buras, M. Gorbahn, S. Jäger, and M. Jamin. Improved anatomy of ε'/ε in the Standard Model. *JHEP*, 11:202, 2015. doi: 10.1007/JHEP11(2015)202.

[60] J. Aebischer, C. Bobeth, and A. J. Buras. ε'/ε in the Standard Model at the Dawn of the 2020s. *Eur. Phys. J. C*, 80(8):705, 2020. doi: 10.1140/epjc/s10052-020-8267-1.

[61] F. J. Botella, G. C. Branco, M. Nebot, M. N. Rebelo, and J. I. Silva-Marcos. Vector-like Quarks at the Origin of Light Quark Masses and Mixing. *Eur. Phys. J. C*, 77(6):408, 2017. doi: 10.1140/epjc/s10052-017-4933-3.

[62] A. M. Sirunyan et al. Search for pair production of vectorlike quarks in the fully hadronic final state. *Phys. Rev. D*, 100(7):072001, 2019. doi: 10.1103/PhysRevD.100.072001.

[63] M. Aaboud et al. Combination of the searches for pair-produced vector-like partners of the third-generation quarks at $\sqrt{s} = 13$ TeV with the ATLAS detector. *Phys. Rev. Lett.*, 121(21):211801, 2018. doi: 10.1103/PhysRevLett.121.211801.

[64] F. J. Botella and L.-L. Chau. Anticipating the Higher Generations of Quarks from Rephasing Invariance of the Mixing Matrix. *Phys. Lett. B*, 168:97–104, 1986. doi: 10.1016/0370-2693(86)91468-1.

[65] A. M. Sirunyan et al. Search for vectorlike light-flavor quark partners in proton-proton collisions at $\sqrt{s}$ =8 TeV. *Phys. Rev. D*, 97:072008, 2018. doi: 10.1103/PhysRevD.97.072008.

[66] A. E. Cárcamo Hernández, Y. Hidalgo Velásquez, S. Kovalenko, H. N. Long, N. A. Pérez-Julve, and V. V. Vien. Fermion spectrum and $g-2$ anomalies in a low scale 3-3-1 model. *Eur. Phys. J. C*, 81 (2):191, 2021. doi: 10.1140/epjc/s10052-021-08974-4.

[67] K. G. Chetyrkin, J. H. Kuhn, A. Maier, P. Maierhofer, P. Marquard, M. Steinhauser, and C. Sturm. Charm and Bottom Quark Masses: An Update. *Phys. Rev. D*, 80:074010, 2009. doi: 10.1103/PhysRevD.80.074010.

[68] X.-D. Huang, X.-G. Wu, J. Zeng, Q. Yu, X.-C. Zheng, and S. Xu. Determination of the top-quark $\overline{MS}$ running mass via its perturbative relation to the on-shell mass with the help of the principle of maximum conformality. *Phys. Rev. D*, 101(11):114024, 2020. doi: 10.1103/PhysRevD.101.114024.

[69] J. Brod and M. Gorbahn. Next-to-Next-to-Leading-Order Charm-Quark Contribution to the CP Violation Parameter ϵ_K and ΔM_K. *Phys. Rev. Lett.*, 108:121801, 2012. doi: 10.1103/PhysRevLett.108.121801.

[70] A. J. Buras, B. Duling, T. Feldmann, T. Heidsieck, C. Promberger, and S. Recksiegel. Patterns of Flavour Violation in the Presence of a Fourth Generation of Quarks and Leptons. *JHEP*, 09:106, 2010. doi: 10.1007/JHEP09(2010)106.

[71] J. Brod and M. Gorbahn. $_K$ at Next-to-Next-to-Leading Order: The Charm-Top-Quark Contribution. *Phys. Rev. D*, 82:094026, 2010. doi: 10.1103/PhysRevD.82.094026.

[72] C. Bobeth, A. J. Buras, A. Celis, and M. Jung. Patterns of Flavour Violation in Models with Vector-Like Quarks. *JHEP*, 04:079, 2017. doi: 10.1007/JHEP04(2017)079.

[73] A. J. Buras, B. Duling, T. Feldmann, T. Heidsieck, C. Promberger, and S. Recksiegel. The Impact of a 4th Generation on Mixing and CP Violation in the Charm System. *JHEP*, 07:094, 2010. doi: 10.1007/JHEP07(2010)094.

[74] S. Aoki et al. FLAG Review 2019: Flavour Lattice Averaging Group (FLAG). *Eur. Phys. J. C*, 80(2): 113, 2020. doi: 10.1140/epjc/s10052-019-7354-7.

[75] A. J. Buras and D. Guadagnoli. Correlations among new CP violating effects in $\triangle$ F = 2 observables. *Phys. Rev. D*, 78:033005, 2008. doi: 10.1103/PhysRevD.78.033005.

Appendix A

Numerical values and Inami-Lim functions

Here we present the numerical values of the input parameters used throughout this work, as well as the explicit expressions for the Inami-Lim functions.

The values used for the Fermi constant G_F and the masses of the Z and W bosons are [33]

$$\begin{aligned} G_F &= 1.1664 \times 10^{-5}\ \text{GeV}^{-2}, \\ M_W &= 80.3791\ \text{GeV}, \\ M_Z &= 91.1876\ \text{GeV}. \end{aligned} \tag{A.1}$$

The masses of the quarks m_i which enter the Inami-Lim functions are the $\overline{\text{MS}}$ masses $m_i(\mu = m_i)$. We use the central values of [67, 68]

$$\begin{aligned} m_c(m_c) &= 1.279 \pm 0.013\text{GeV}, \\ m_t(m_t) &= 162.6 \pm 0.4\text{GeV}. \end{aligned} \tag{A.2}$$

For the factors η_{ij}^N we use the central values of [69–72]

$$\begin{aligned} \eta_{cc}^K &= 1.87 \pm 0.76, \\ \eta_{tt}^K &= 0.5765 \pm 0.0065, \\ \eta_{ct}^K &= 0.496 \pm 0.04, \\ \eta_{tt}^B &= 0.55 \pm 0.01. \end{aligned} \tag{A.3}$$

For the remaining correction factors associated to the $B^0_{d,s}$ systems we simply use $\eta^B_{ij} \simeq 1$, which should not be problematic, given that the terms involving the charm quark are not relevant in calculations. Following [70], the QCD corrections involving T are approximated as

$$\eta^K_{cT} \simeq \eta^K_{ct},$$

$$\eta^K_{tT} \simeq \eta^K_{TT} \simeq \eta^K_{tt}, \tag{A.4}$$

$$\eta^B_{tT} \simeq \eta^B_{TT} \simeq \eta^B_{tt}.$$

In table A.1 we present the values used in this work for quantities relevant to the neutral meson systems. For the D^0 system we also use $\Gamma_D = 1/\tau_D$ for the total decay width of D^0, with mean life-time $\tau_D = (410.1 \pm 1.5) \times 10^{-15}$ s [33] and we use $r(m_c, M_Z) \approx 0.778$, where [50]

$$r(\mu, M) = \left(\frac{\alpha_s(M)}{\alpha_s(m_t)}\right)^{2/7} \left(\frac{\alpha_s(m_t)}{\alpha_s(m_b)}\right)^{6/23} \left(\frac{\alpha_s(m_b)}{\alpha_s(\mu)}\right)^{6/25} \tag{A.5}$$

and $\alpha_s \equiv g_s^2/4\pi$ is the strong coupling constant.

N^0	m_N [MeV]	Δm_N^{exp} [MeV]	f_N [MeV]	B_N
K^0	497.611 ± 0.013	$(3.484 \pm 0.006) \times 10^{-12}$	155.7 ± 0.3	0.717 ± 0.024
B^0_d	5279.65 ± 0.12	$(3.334 \pm 0.013) \times 10^{-10}$	190.0 ± 1.3	1.30 ± 0.10
B^0_s	5366.88 ± 0.14	$(1.1683 \pm 0.0013) \times 10^{-8}$	230.3 ± 1.3	1.35 ± 0.06
D^0	1864.83 ± 0.05	$\left(6.25^{+2.70}_{-2.90}\right) \times 10^{-12}$	$f_D = 212 \pm 0.7$	≈ 1.18 [73]

Table A.1: Mass and mixing parameters [33] and decay constants and bag parameters [74] for the neutral meson systems. In computations use the central values.

Also, when computing the ε_K parameter, we use the central value of $\kappa_\varepsilon = 0.92 \pm 0.02$ [75].

The Inami-Lim functions used throughout this paper are given by [44, 56]

$$S_{ij} \equiv S_0(x_i, x_j) = x_i x_j \left[\frac{\log x_i}{(x_i - x_j)(1 - x_i)^2}\left(1 - 2x_i + \frac{x_i^2}{4}\right) + (x_i \leftrightarrow x_j) - \frac{3}{4(1 - x_i)(1 - x_j)}\right], \tag{A.6}$$

$$S_{ii} \equiv S_0(x_i) \equiv \lim_{x_j \to x_i} S(x_i, x_j) = \frac{x_i}{(1 - x_i)^2}\left(1 - \frac{11}{4}x_i + \frac{x_i^2}{4}\right) - \frac{3}{2}\frac{x_i^3 \log x_i}{(1 - x_i)^3}, \tag{A.7}$$

$$X_0(x_i) = \frac{x_i}{8(x_i - 1)}\left(x_i + 2 + \frac{3x_i - 6}{x_i - 1}\log x_i\right), \tag{A.8}$$

$$Y_0(x_i) = \frac{x_i}{8(x_i - 1)}\left(x_i - 4 + \frac{3x}{x_i - 1}\log x_i\right), \tag{A.9}$$

$$Z_0(x_i) = -\frac{\log x_i}{9} + \frac{18x_i^4 - 163x_i^3 + 259x_i^2 - 108x_i}{144(x_i-1)^3} + \frac{32x_i^4 - 38x_i^3 - 15x_i^2 + 18x_i}{72(x_i-1)^4}\log x_i, \tag{A.10}$$

$$E_0(x_i) = -\frac{2\log x_i}{3} + \frac{x_i(18 - 11x_i - x_i^2)}{12(1-x_i)^3} + \frac{x_i^2(15 - 16x_i + 4x_i^2)}{6(1-x_i)^4}\log x_i. \tag{A.11}$$

All these functions are gauge invariant, however, $X_0(x_i), Y_0(x_i)$ and $Z_0(x_i)$ correspond to linear combinations of gauge-dependent functions as discussed in 4.4. The expressions for $X_0(x_i)$ and $Y_0(x_i)$ are obtained by combining a $\Delta F = 1$ box-diagram function with a Z-penguin function. These are $B_0(x_i)$ and $C_0(x_i)$, respectively, in the t' Hooft-Feynamn gauge. On the other hand, $Z_0(x_i)$ is obtained by combining the electromagnetic-penguin function, $D_0(x_i)$ in this same gauge, with the Z-penguin function. Moreover, $S_0(x_i, x_j)$ is a $\Delta F = 2$ box diagram function that is relevant in meson mixings and $E_0(x_i)$ is associated to gluon penguins. Here ΔF refers to the changes to the flavour quantum numbers in a given process. For instance, the $K^+ \to \pi^+\nu\overline{\nu}$ decay ($\overline{d} \to \overline{s}\nu\overline{\nu}$ in terms of quark content) corresponds to a $\Delta F = 1$ process, whereas the $K^0 - \overline{K}^0$ mixing ($d\overline{s} \leftrightarrow \overline{d}s$ in terms of quark content) is a $\Delta F = 2$ process.

At first glance there seems to exist an incompatibility between the gauge independent expressions in (4.46) and (4.59). How can both $X_0 \equiv C_0(x_i) - B_0(x_i)$ and $Y_0 \equiv C_0(x_i) - 4B_0(x_i)$ be gauge independent? Following [56], we will now answer this question.

In a general R_ξ-gauge one has

$$\begin{aligned} X_0(x_i) &\equiv C_0(x_i,\xi) - 4B_0\left(x_i,\xi,\tfrac{1}{2}\right), \\ Y_0(x_i) &\equiv C_0(x_i,\xi) - B_0\left(x_i,\xi,-\tfrac{1}{2}\right), \\ Z_0(x_i) &\equiv C_0(x_i,\xi) - \tfrac{1}{4}D_0(x_i,\xi), \end{aligned} \tag{A.12}$$

where

$$\begin{aligned} B_0(x_i,\xi,I_3) &\equiv B_0(x_i) + f(I_3)\overline{\rho}(x_i,\xi), \\ C_0(x_i,\xi) &\equiv C_0(x_i) + \tfrac{1}{2}\overline{\rho}(x_i,\xi), \\ D_0(x_i,\xi) &= D_0(x_i) - 2\overline{\rho}(x_i,\xi), \end{aligned} \tag{A.13}$$

with I_3 being the third component of weak isospin associated to the outgoing fermions in box diagrams and $f\left(-\frac{1}{2}\right) = \frac{1}{8}$ and $f\left(\frac{1}{2}\right) = \frac{1}{2}$. The gauge dependence of all these functions is contained in the factor

$$\overline{\rho}(x_i,\xi) = \rho(x_i,\xi) - \frac{7}{2}B_0(x_i), \tag{A.14}$$

where

$$\rho(x_i,\xi) = \frac{\xi}{x-\xi}\left(\frac{3}{4}\frac{1}{x-1}+\frac{1}{8}\frac{\xi}{x-\xi}\right)x\log x - \frac{\xi}{8}\left[\frac{6}{1-\xi}\log\xi - 1\right] + \frac{1}{8}\frac{\xi^2}{x-\xi}\left[\left(\frac{5+\xi}{1-\xi}-\frac{\xi}{x-\xi}\right)\log\xi - 1\right]. \tag{A.15}$$

Plugging (A.13) in (A.12), one recovers

$$\begin{aligned} X_0(x_i) &= C_0(x_i) - 4B_0(x_i), \\ Y_0(x_i) &= C_0(x_i) - B_0(x_i), \\ Z_0(x_i) &= C_0(x_i) - \tfrac{1}{4}D_0(x_i), \end{aligned} \tag{A.16}$$

i.e. the expressions in (4.46) and (4.59).

The t' Hooft-Feynman gauge ($\xi = 1$) is particularly useful because one has $\overline{\rho}(x,1) = 0$, so that

$$B_0(x_i,1,I_3) = B_0(x_i) = \frac{1}{4}\left(\frac{x_i}{1-x_i}+\frac{x_i\log x_i}{(x_i-1)^2}\right) \tag{A.17}$$

$$C_0(x_i,1) = C_0(x_i) = \frac{x_i}{8}\left(\frac{x_i-6}{x_i-1}+\frac{3x_i+2}{(x_i-1)^2}\log x_i\right) \tag{A.18}$$

$$D_0(x_i,1) = D_0(x_i) = -\frac{4\log x_i}{9}+\frac{-19x_i^3+25x_i^2}{36(x_i-1)^3}+\frac{x_i^2(5x_i^2-2x_i-6)}{18(x_i-1)^4}\log x_i, \tag{A.19}$$

and the functions associated to $\Delta F = 1$ box diagrams, Z-penguin diagrams and electromagnetic penguin diagrams acquire the simplest forms.

The function $F(x_i)$ in Eq. (4.58), relevant to the study of ε'/ε, is a linear combination of $X_0(x_i), Y_0(x_i), Z_0(x_i)$ and $E_0(x_i)$. We use the following values for the constants entering this expression [59]

$$\begin{aligned} P_0 &\simeq -3.392 + 15.3037\ B_6^{(1/2)} + 1.7111\ B_8^{(3/2)}, \\ P_X &\simeq 0.655 + 0.02902\ B_6^{(1/2)}, \\ P_Y &\simeq 0.451 + 0.1141\ B_6^{(1/2)}, \\ P_Z &\simeq 0.406 - 0.0220\ B_6^{(1/2)} - 13.4434\ B_8^{(3/2)}, \\ P_E &\simeq 0.229 - 1.7612\ B_6^{(1/2)} + 0.6525\ B_8^{(3/2)}, \end{aligned} \tag{A.20}$$

as well as the central values of $B_6^{(1/2)} = 1.11 \pm 0.20$ and $B_8^{(3/2)} = 0.70 \pm 0.04$ [60].

Appendix B

Effective low energy Lagrangians

In (3.4) and throughout much of chapter 4 we presented low energy effective Lagrangians. These correspond to convenient ways of parametrizing the low energy effects of the full theory [31, 32]. To understand this, consider the CC interaction presented in figure B.1(a). In momentum space, the Feynman rule for the W-boson line is given by

$$G^W_{\mu\nu}(k) = i\frac{-g_{\mu\nu} + \frac{k_\mu k_\nu}{M_W^2}}{k^2 - M_W^2 + i\varepsilon}, \tag{B.1}$$

which in the limit of low energies, i.e. $|k|^2/M_W^2 \ll 1$ leads to

$$G^W_{\mu\nu}(k) \to i\frac{g_{\mu\nu}}{M_W^2}. \tag{B.2}$$

This results means that the W-boson internal line in this limit is contracted into a point as illustrated in figure B.1(b), so that the W-boson degree of freedom is effectively removed.

Figure B.1: (a) Tree level Feynman diagram describing the neutron beta decay; (b) Feynman diagram describing the effective interaction in the limit of low energies $|k|^2/M_W^2 \ll 1$.

The effective Lagrangian describing this process is typically written as

$$\mathscr{L}_{\text{eff}} = -\frac{4G_F}{\sqrt{2}}\left(\overline{u}_L\gamma_\mu V_{ud} d_L\right)\left(\overline{e}_L\gamma^\mu\nu_e\right). \tag{B.3}$$

However, building the same Lagrangian using (B.2) and the vertices arising from the Lagrangian in (2.40), one obtains

$$\mathscr{L}_{\text{eff}} = -\frac{g^2}{2M_W^2}\left(\overline{u}_L\gamma_\mu d_L\right)\left(\overline{e}_L\gamma^\mu\nu_e\right), \tag{B.4}$$

so that one can establish the important relation

$$\frac{G_F}{\sqrt{2}} = \frac{g^2}{8M_W^2}. \tag{B.5}$$

For other processes involving the Z gauge boson, the Higgs boson or heavy quarks internal lines, similar considerations apply and these heavy degrees of freedom can be effectively removed in the limit of low energies. In fact, it is by applying these considerations to the quark internal lines present in the one-loop contributions to neutral meson mixings and meson decays, that the expressions for the IL functions and the effective Lagrangians in chapter 4 are obtained.

Appendix C

Software Code

Here we present the Wolfram Mathematica notebook used to generate the 10^6 points displayed in figure 6.2.

```
(*--------Input Values--------------*)


(*SM mixing parameters*)
sol = {theta12 -> 0.2264, theta13 -> 0.0037, theta23 ->
    0.0405, delta -> 1.215};

(*Quark masses*)
mu = 0.00127;
mc = 1.279;
mt = 162.6;

(*Physical constants*)
GF = 1.1663787*10^-5(*GeV^-2*);
MW = 80.37912; (*GeV*)
MZ = 91.1876; (*GeV*)

(*Values relevant for neutral kaon mixing and kaon decays*)
ke = 0.92;
mK = 0.497611 (*GeV*);
BK = 0.717;
fK = 0.1557(*GeV*);
```

```
DmKexp = 3.484*10^-15(*GeV*);

(*Values relevant for epsilon'/epsilon*)
msmc = 109.1;
mdmc = 5.4;
u = (114.54/(msmc + mdmc))^2 ;
B6 = 1.11; B8 = 0.7;
R6 = B6 u; R8 = B8 u;
ro0 = -3.392; ro6 = 15.293; ro8 = 1.71;
rX0 = 0.655; rX6 = 0.029; rX8 = 0;
rY0 = 0.451; rY6 = 0.114; rY8 = 0;
rZ0 = 0.406; rZ6 = -0.022; rZ8 = -13.434;
rE0 = 0.229; rE6 = -1.760; rE8 = 0.652;
P0 = ro0 + ro6 R6 + ro8 R8;
PX = rX0 + rX6 R6 + rX8 R8;
PY = rY0 + rY6 R6 + rY8 R8;
PZ = rZ0 + rZ6 R6 + rZ8 R8;
PE = rE0 + rE6 R6 + rE8 R8;
Co = PX + PY + PZ;

(*-------------CKM--------------*)


(*Building the CKM matrix*)

O12 = {{Cos[theta12], Sin[theta12], 0, 0}, {-Sin[theta12],Cos[theta12], 0, 0},
{0, 0, 1, 0}, {0, 0, 0, 1}};

O23 = {{1, 0, 0, 0}, {0, Cos[theta23], Sin[theta23], 0},
{0, -Sin[theta23], Cos[theta23], 0}, {0, 0, 0,1}};

O13 = {{Cos[theta13], 0, Sin[theta13] Exp[-I delta], 0},
{0, 1, 0, 0},{-Sin[theta13] Exp[I delta], 0, Cos[theta13], 0}, {0, 0, 0, 1}};

O14 = {{Cos[theta14], 0, 0, Sin[theta14] Exp[-I delta14]},
{0, 1, 0, 0},{0, 0, 1, 0}, {-Sin[theta14] Exp[I delta14], 0, 0, Cos[theta14]}};

O24 = {{1, 0, 0, 0}, {0, Cos[theta24], 0, Sin[theta24],Exp[-I delta24]},
```

```
{0, 0, 1, 0}, {0, -Sin[theta24] Exp[I delta24], 0, Cos[theta24]}};

O34 = {{1, 0, 0, 0}, {0, 1, 0, 0}, {0, 0, Cos[theta34],
Sin[theta34]}, {0, 0, -Sin[theta34], Cos[theta34]}};

V = O34 . O24 . O14 . O23 . O13 . O12 . DiagonalMatrix[{1, 1, 1, 0}];
Vc = O34 . O24 . O14 . O23 . O13 . O12 . DiagonalMatrix[{1, 1, 1, 0}]
/. {delta -> -delta, delta14 -> -delta14, delta24-> -delta24};
U = O34 . O24 . O14 . O23 . O13 . O12;

(*CKM lambdaN factors*)
lambdaK = {{Conjugate[V[[1, 2]]] V[[1, 1]],
Conjugate[V[[2, 2]]] V[[2, 1]], Conjugate[V[[3, 2]]] V[[3, 1]], Conjugate[V[[4, 2]]] V[[4, 1]]}};

lambdaB = {{Conjugate[V[[1, 3]]] V[[1, 1]],
Conjugate[V[[2, 3]]] V[[2, 1]], Conjugate[V[[3, 3]]] V[[3, 1]], Conjugate[V[[4, 3]]] V[[4, 1]]}};

lambdaBs = {{Conjugate[V[[1, 3]]] V[[1, 2]],
Conjugate[V[[2, 3]]] V[[2, 2]], Conjugate[V[[3, 3]]] V[[3, 2]], Conjugate[V[[4, 3]]] V[[4, 2]]}};


(*------Inami-Lim functions----------*)


x[a_] := a^2/MW^2;

s[a_, b_] :=
  a b ((Log[a]/((a - b) (1 - a)^2)) (1 - 2 a +
        a^2/4) + (Log[b]/((b - a) (1 - b)^2)) (1 - 2 b + b^2/4) -
      3/(4 (1 - a) (1 - b)));

s0[a_] := (a/(1 - a)^2) (1 - (11/4) a + a^2/4) - (3/
       2) ((a^3 Log[a])/(1 - a)^3);

zero = {{0, 0, 0}};

S = {{s0[x[mu]], s[x[mu], x[mc]], s[x[mu],x[mt]], s[x[mu], x[mT]]}, {s[x[mc], x[mu]], 1.87 s0[x[mc]],
     0.496 s[x[mc], x[mt]], 0.496 s[x[mc], x[mT]]}, {s[x[mt], x[mu]],
```

```
    0.496 s[x[mt], x[mc]], 0.5765 s0[x[mt]],
    0.5765 s[x[mt], x[mT]]}, {s[x[mT], x[mu]], 0.496 s[x[mT], x[mc]],
    0.5765 s[x[mT], x[mt]], 0.5765 s0[x[mT]]}};

S3 = ArrayFlatten[{{Delete[Transpose[Delete[Transpose[S], 4]], 4],
     Transpose[zero]}, {zero, 0}}];

X0[z_] = (z/(8 (z – 1))) (z + 2 + ((3 z – 6)/(z – 1)) Log[z]);
Y0[z_] = (z/(8 (z – 1))) (z – 4 + ((3 z)/(z – 1)) Log[z]);
Z0[z_] = ((–1)/9) Log[z] + (18 z^4 – 163 z^3 + 259 z^2 – 108 z)/(144 (z – 1)^3) +
((32 z^4 – 38 z^3 – 15 z^2 + 18 z)/(72 (z – 1)^4)) Log[z];
E0[z_] = ((–2)/3) Log[z] + (z (18 – 11 z – z^2))/(12 (1 – z)^3) +
((z^2 (15 – 16 z + 4 z^2))/(6 (1 – z)^4)) Log[z];
F[z_] = P0 + PX*X0[z] + PY*Y0[z] + PZ*Z0[z] + PE*E0[z];


(*––––––––Calculating Ads––––––––*)


N0[z1_, z2_] = ((z1 z2)/(8 (z1 – z2))) (Log[z1] – Log[z2]);

X = V . Transpose[Conjugate[V]]; (*matrix controlling FCNCs*)

W = X – IdentityMatrix[4];

Vcis = {Transpose[Conjugate[V]][[2]]};
Vjd = {Transpose[V][[1]]};

n = {{(x[mu]/8) W[[1, 1]], N0[x[mu], x[mc]] W[[1, 2]],
     N0[x[mu], x[mt]] W[[1, 3]], N0[x[mu], x[mT]] W[[1, 4]]},
     {N0[x[mu], x[mc]] W[[2, 1]], (x[mc]/8) W[[2, 2]],
     N0[x[mc], x[mt]] W[[3, 4]], N0[x[mc], x[mT]] W[[2, 4]]},
     {N0[x[mu], x[mt]] W[[3, 1]], N0[x[mc], x[mt]] W[[3, 2]],
     (x[mt]/8) W[[3, 3]], N0[x[mt], x[mT]] W[[3, 4]]},
     {N0[x[mu], x[mT]] W[[4, 1]], N0[x[mc], x[mT]] W[[4, 2]],
     N0[x[mt], x[mT]] W[[4, 3]], (x[mT]/8) W[[4, 4]]}};

Ads = Vcis . n . Transpose[Vjd];
```

```
(*----Calculating NP contributions----------*)

epsilonK =  Tr [(( GFˆ2 MWˆ2 mK fKˆ2 BK ke)/(12 Sqrt[2 Piˆ2DmKexp)])
            Im[lambdaK . (S – S3) . Transpose[lambdaK]]] /. sol;

DeltamK = ((GFˆ2 MWˆ2 mK fKˆ2 BK)/(6 Piˆ2)) Abs[lambdaK . (S – S3) .
Transpose[lambdaK]] 10ˆ3 /. sol//Tr;  (*MeV*)

epsilonp = Im[F[x[mT]] Transpose[lambdaK][[4]] + Ads Co]
            /.  sol  //  Tr;  (* epsilon'/epsilon *)

(* Kˆ+–>Piˆ+nub nu *)
KlSM = Transpose[lambdaK][[2]] Pc 0.2252ˆ4 +
      Transpose[lambdaK][[3]] (X0[x[mt]]) /.  sol  /.  Pc –> 0.404;

KlNP = Transpose[lambdaK][[2]] Pc 0.2252ˆ4 +
       Transpose[lambdaK][[3]] (X0[x[mt]]) +
       Transpose[lambdaK][[4]] X0[x[mT]] + Ads /. sol /.  Pc –> 0.404;

k = Abs[KlNP/KlSM]ˆ2 // Tr;


(*-----Generating 10ˆ6 points-----------*)


t14 = {};
t24 = {};
deltap = {};
MT = {};

For[i = 0,  i  < 1000000, i++;

 {theta14 = RandomReal[{0.03, 0.05}],
  theta24 = RandomReal[{0, 0.001}],
  delta14 = RandomReal[{0, 2 Pi}],
  theta34 = RandomReal[{0, 0.001}],
  delta24 = RandomReal[{0, 2 Pi}],
```

```
 mT = RandomReal[{685, 2500}]};

If [k > 0.24 && k < 2.28 &&
   Abs[epsilonK] < 0.000248 &&
   Abs[Delta_mK] < 3.484*10^-12 &&
   epsilonp > -0.0004 && epsilonp < 0.001,
   {AppendTo[t14, theta14];
   AppendTo[t24, theta24];
   AppendTo[MT, mT];
   AppendTo[deltap, delta24 - delta14]}];

 Clear[theta14, theta24, theta34, delta14, delta24, mT]
 ]

data1 = Transpose@{Sin[t14]*100, Sin[t24]*1000};
data2 = Transpose@{Sin[t14]*100, MT/1000};
data3 = Transpose@{Sin[t24]*1000, MT/1000};
data4 = Transpose@{Sin[t14]*100, deltap/Pi};
data5 = Transpose@{Sin[t24]*1000, deltap/Pi};
data6 = Transpose@{MT/1000, deltap/Pi};
```